AD-A110 642 RENSSELAER POLYTECHNIC INST TROY N Y DEPT OF MECHANI--ETC F/G 11/8
ANALYSIS OF LUBRICANT FILMS IN BEARINGS UNDER INCIPIENT FAILURE--ETC(U)
1981 J L LAUER AFOSR-78-3473

UNCLASSIFIED AFOSR-TR-82-0010 NL

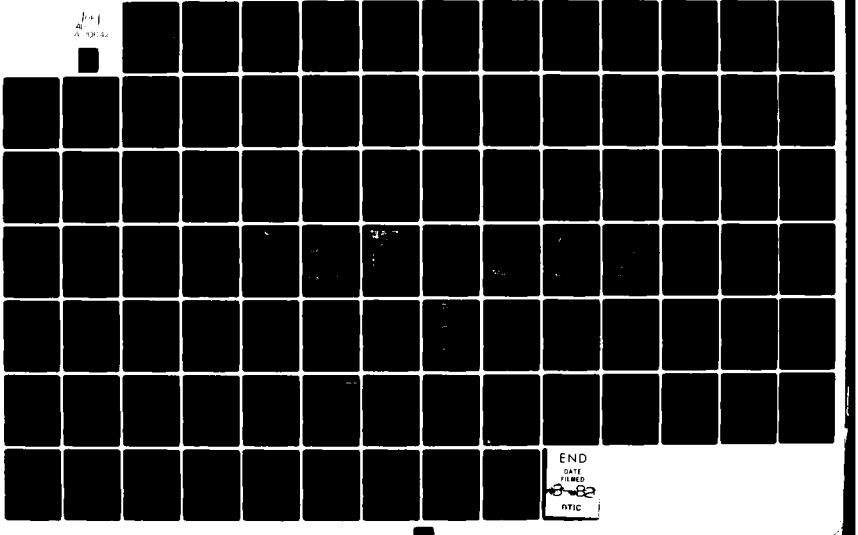

END
DATE FILMED
4-82
DTIC

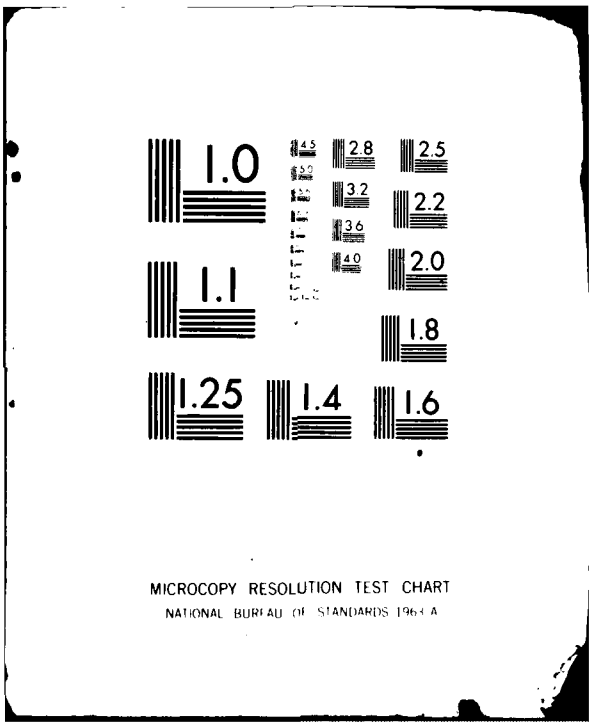
1.0
1.1
1.25
1.4
1.6
1.8
2.0
2.2
2.5
2.8
3.2
3.6
4.0
4.5
5.0
MICROCOPY RESOLUTION TEST CHART
NATIONAL BUREAU OF STANDARDS 1963 A

Unclassified

SECURITY CLASSIFICATION OF THIS PAGE (When Data Entered)

13 JAN 1982

REPORT DOCUMENTATION PAGE		READ INSTRUCTIONS BEFORE COMPLETING FORM
1. REPORT NUMBER AFOSR-TR- 82-0010	2. GOVT ACCESSION NO. AD-A110 642	3. RECIPIENT'S CATALOG NUMBER
4. TITLE (and Subtitle) "Analysis of Lubricant Films in Bearings Under Incipient Failure Conditions"		5. TYPE OF REPORT & PERIOD COVERED Final
		6. PERFORMING ORG. REPORT NUMBER
7. AUTHOR(s) James L. Lauer		8. CONTRACT OR GRANT NUMBER(s) AFOSR-78-3473
9. PERFORMING ORGANIZATION NAME AND ADDRESS Department of Mechanical Engineering Rensselaer Polytechnic Institute Troy, NY 12181		10. PROGRAM ELEMENT, PROJECT, TASK AREA & WORK UNIT NUMBERS 61102F 2303/A2
11. CONTROLLING OFFICE NAME AND ADDRESS Directorate of Chemical Science/NC Air Force Office of Scientific Research Building 410, BAFB, Washington, D.C. 20032		12. REPORT DATE 1981
		13. NUMBER OF PAGES 113
14. MONITORING AGENCY NAME & ADDRESS(if different from Controlling Office) LEVEL II		15. SECURITY CLASS. (of this report) Unclassified
		15a. DECLASSIFICATION/DOWNGRADING SCHEDULE
16. DISTRIBUTION STATEMENT (of this Report) 71		
17. DISTRIBUTION STATEMENT (of the abstract entered in Block 20, if different from Report)		
18. SUPPLEMENTARY NOTES		
19. KEY WORDS (Continue on reverse side if necessary and identify by block number) Elastohydrodynamic Lubrications, Traction Fluids, Trichloroethane, Fourier Emission Spectrometry, Surface Analysis, Polarized Infrared Spectra.		

DTIC ELECTE FEB 9 1982 S D H

82 02 0 [illegible]

20. ABSTRACT (Continue on reverse side if necessary and identify by block number)

Infrared emission spectra have been obtained from operating elastohydrodynamic bearings through a diamond window. Failure modes were observed in two instances, with a cycloparaffinic and an aromatic lubricant, both in the presence of an organic chloride. The mechanism of carbonization and polymerization appeared to be ionic in each case.

All the infrared spectra were polarized to a degree depending on the shear rate and more so in presence of an organic chloride. In at least one

(over)

DD FORM 1 JAN 73 1473

Unclassified

SECURITY CLASSIFICATION OF THIS PAGE (When Data Entered)

AD A110642

DTIC FILE COPY

case the chloride came out of solution and two phase flow occurred.

The instrumentation developed is so discriminating and sensitive that spectra from layers as thin as one molecular thickness would seem to be obtainable. It can therefore be useful for surface analysis in different situations.

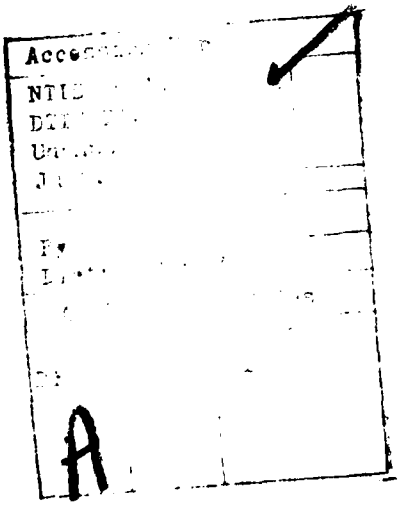

AFOSR-TR- 82 -0010

ANALYSIS OF LUBRICANT FILMS IN BEARINGS UNDER INCIPIENT FAILURE CONDITIONS

FINAL SCIENTIFIC PROJECT REPORT

for the period
1 January 1978 - 30 June 1981

Grant No. AFOSR-78-3473
to the
Air Force Office Of Scientific Research

by

James L. Lauer
Research Professor
Department of Mechanical Engineering
Aeronautical Engineering & Mechanics
Rensselaer Polytechnic Institute
Troy, NY 12181

TABLE OF CONTENTS

ABSTRACT

Infrared emission spectra have been obtained from operating elasto-hydrodynamic bearings through a diamond window. Failure modes were observed in two instances, with a cycloparaffinic and an aromatic lubricant, both in the presence of an organic chloride. The mechanism of carbonization and polymerization appeared to be ionic in each case.

All the infrared spectra were polarized to a degree depending on the shear rate and more so in presence of an organic chloride. In at least one case the chloride came out of solution and two phase flow occurred.

The instrumentation developed is so discriminating and sensitive that spectra from layers as thin as one molecular thickness would seem to be obtainable. It can therefore be useful for surface analysis in different situations.

TABLE OF CONTENTS

1. INTRODUCTION

Infrared emission spectrophotometry is one of the very few procedures capable of analyzing the events leading to bearing failure. It can be used on an operating bearing by examining the radiation emanating through a window and it can yield information regarding the situation in the very thin film of lubricant which separates the solid moving surfaces--the micro-reactor where the action is. This film, in a typical ball bearing under very heavy load, may be less than a hundred molecules thick and perhaps a hundred micrometers in diameter. Under operating conditions it heats up, perhaps up to 100°C, but usually only to 40°-50°C. A fraction of the thermal energy, which is generated by internal friction, can be allowed to pass through a diamond window--diamond for transparency and hardness--and analyzed.

It is obvious that the instrumentation is not simple. It must be free from excessive vibrations or the sample is removed from the range of the instrumentation. The sensitivity and, above all, the spectral discrimination, must be extremely high. We were able to attain sufficiently high levels by various differential techniques so that we believe to be well able to analyze monomolecular layers.

An important difference between a stationary sample and a lubricating film of an operating bearing is, of course, the motion itself. It leads to some rather unusual spectral features caused by polarization phenomena. Then the temperature is likely to be nonuniform through the film and that can lead to partial--or complete--reabsorption of the emitted radiation. Hence the analysis of the spectra is not a simple matter either and requires many redundancies.

Nevertheless we attained much of what we set out to do. Despite the rapidity of the failure reactions we were able to follow two of them

in some detail, we were able to prove viscosity loss through flow polarization, we discovered the possibility of two-phase flow by losing a component from solution under operating conditions and we were able to state some principles which may be helpful in avoiding failures. A simple result is this: When chlorinated solvents are used in an overhaul, care should be taken to remove them all before introducing the lubricant.

2. APPARATUS

The basic measuring instrument was a slow-scanning Michelson interferometer, originally purchased from Beckman-RIIC (Model FS-720). This instrument was designed for the far infrared spectral region (40-400 cm^{-1}) and for absorption spectroscopy only. All but the central optics of this instrument was changed; a new beamsplitter was provided, the scanning mirror drive was automated, the electronics was entirely replaced and, most importantly, an inlet system for emission spectroscopy was designed and built. The last-named apparatus portion was, of course, what made this work possible. It underwent a series of changes as improvements suggested themselves. As a result we now have what we believe to be the most discriminating and sensitive infrared emission spectrophotometer anywhere, an instrument capable of obtaining an infrared spectrum from a surface layer less than 100 μm in diameter and perhaps only one molecular layer thick (at this time the limiting dimensions are not yet known). Because such thin layers turned out to be oriented on a molecular scale, the orientation was itself used to increase the apparatus sensitivity and, conversely, to provide information on the nature of the sample volume.

In the following subsections particular portions of the apparatus and accessories will be discussed, with emphasis on recent achievements.

2.1 Ball/Plate Sliding Lubricating Contact

Most of the work was concerned with emission spectroscopy of the lubricant in operating heavily loaded bearings under so-called elastohydrodynamic lubricating conditions. In this type of operation the two surfaces, which are in relative motion with respect to each other, are of non-conforming geometries and are elastically deformed. Examples of

elastohydrodynamic lubrication are gears, cams, and above all, ball bearings. Failure of ball bearings, in particular, is often caused by scuffing, a mechanism of catastropic failure, which was one of the main objectives of this study.

Figure 1 shows the mockup bearing assembly used for most of our work. The mechanical setup is basically a ball-on-plate sliding contact. A loaded (generally) steel ball (diameter 0.0572 m) is rotated in a cup containing the test fluid and made to slide over a diamond window at the bottom. The contact region is formed in the fluid layer between the elastically flattened ball and the diamond surface. Typical layer thicknesses are 0.2 μm for customary fluid viscosities and fluid temperatures under typical loads and linear sliding velocities. It is possible to measure these thicknesses by photographing the interference pattern (distorted Newton rings) through a microscope while the system is in operation.

The loading of the ball is accomplished by locating a roller-supported platform on the upper ball surface and hanging different weights on this platform. Two rollers (outer races of roller bearings) run over the steel ball along the same perimeter as the diamond contact. The friction of these rollers is negligible compared to that of the ball/diamond sliding contact. The rollers are lubricated with the fluid under study. The contact points of the rollers on the ball are at about $\pm$ 30° degrees with the vertical.

The ball itself is rotated about a horizontal axis by a flexible shaft. Connection between ball and shaft is made by a cup ground hollow by a similar bearing ball and by cyanoacrylate "super-" glue. The shaft is held in place at the rim of the cup by a sloppy bearing. On the opposing side of the rim is a set-screw (Figure 2) to maintain the ball's position over the diamond window; the shaft is flexible and transfers torque only.

The shaft is driven by an electric motor mounted on a separate table. The ball/plate assembly is located on a steel table for rigidity which itself straddles the interferometer on its optical table. The optical table is of commercial construction, a one-ton granite slab on an air-cushioned pedestal to isolate room vibrations. The heavy steel table with the mock bearing becomes, in effect, part of the stone table. However, motor vibrations could still transfer to the optics by way of the shaft. To prevent this calamity from arising, the outer housing of the shaft is clamped to the steel table at a carefully determined position and thus "tuned" in a manner similar to that used by musicians playing the cello. In other words, frequencies in the range detected by the radiation detector are tuned out. The solution of the vibration problem was of crucial importance to this project; typically the contact area analyzed by infrared emission is 50-100 μm in diameter and two meters away from the detector (sensitive area of 1000 μm diameter). Any small vibrations could activate a substantial optical lever. This circumstance alone would be serious enough, but the sensitivity of the Golay pneumatic detector (a small gas volume partly contained by a deformable membrane) to microphonics aggravated the problems. Indeed, some solid state detectors are less prone to microphonics but also less sensitive to weak infrared vibration and require cooling; we opted for the Golay.

The test fluid in the cup (about 75 ml) is thermostatted by a coil of circulated water. Temperatures are noted at various stations by thermocouples. The rotational velocity of the shaft is measured by a frequency counter.

2.2 Interferometer Modifications

Although we were donated two Beckman-RIIC Model FS-720 Far Infrared Interferometers--one by the Sun Company and a later model by the du Pont Company--we rebuilt them to such an extent that, in effect, only the housing and the optical parts remained. As a matter of fact, even the beamsplitter, the central part of a Michelson interferometer, was replaced. Thus our instrumentation can truly be called unique and the question might be asked whether, in view of reasonably priced infrared interferometers available now, our reconstruction work was justified. Aside from the high cost of the commercial instrumentation when this work was started, our construction was justified because ours is the only truly infrared emission interferometer built for exceedingly weak signals, having 10 cm diameter optics throughout, an exceedingly sensitive detector, phase-locked electronics, and slow mirror drives, in addition to a unique emission inlet system adapted to microscopy. Indeed the original design for the far infrared proved to be highly adaptable for emission in the mid-infrared because in either case the source signals are weak.

Our modifications can be grouped into (a) optical, i.e. beamsplitter, mirror drive, and polarized emission microscope, and (b) electronic and computational.

2.2.1 Optical Interferometer Modifications

2.2.1.1 Beamsplitter

The key optical element of any Michelson interferometer is the beamsplitter. For the far-infrared a stretched film of Mylar (polyethylene terephthalate) is the usual materal. Because of absorption Mylar is not usable in the mid-infrared and germanium-coated salt (potassium chloride or bromide)

plates have become standard commercial practice. A holder was built to accommodate three-inch diameter, one-quarter to one-half inch thick plates in the Mylar film holder of the instrument. The beamsplitter is a sandwich of two plates, one of them coated with a 0.55 μm thick layer of germanium by evaporation. The diameter of these plates is therefore larger than usual, our requirement for large radiation throughput, but also a source of continuous concern. Figure 3 shows a photograph of the beamsplitter in essentially monochromatic light. The fringes arise from the air wedge between the germanium-coated plate and the uncoated plate in close contact with it. Most of the fringes are near the edge where the clamping takes place. The central region--at least two inches out of three--is basically fringeless, showing that the plates were parallel at that time and making good contact with each other.

A few months later the same beamsplitter was removed and photographed (Figure 4). The quality of the spectra had deteriorated (broader bands, a general frequency shift) and the central fringe of the interferogram had become inverted. Since one of the two split beams is reflected at the salt/germanium interface while the other is reflected at the air/germanium interface--when there is an airspace between the germanium coating and the uncoated salt face next to it--the recombined beams are about 180° degrees out of phase on recombination. This condition would be tolerable were it uniform across the entire area of the beamsplitter, but, of course, it never is. The height and direction of the central fringe is therefore a measure of beamsplitter quality. Almost perfect interferogram symmetry could be obtained when the beamsplitter was in the condition of Figure 3.

To reduce the sagging of the beamsplitter, which caused this deterioration, a new holder was designed and built, which could accommodate one-

half inch thick plates and the laboratory was placed under much stricter humidity control than before.

Our high sensitivity of spectral measurements is, to a very large extent, a result of our emphasis on bemsplitter quality (flatness to one fringe per three inches has become our standard specification). Commercial interferometers, having smaller optics, are less subject to beamsplitter deformation. A note to a journal on the relationship between beamsplitter flatness and central fringe intensity in interferograms is in preparation.

2.2.1.2 Mirror Drive

Two standard FS-720 interferometer mirror drives were available at the time of sale: a continuous one and a step drive with a micrometer screw calibrated in micrometers. In either case the shortest mirror displacement between readings was 4 μm, corresponding to a phase difference of 8 μm. (It will be recalled that digitized signal readings are necessary in infrared interferometry because Fourier transforms and other computational procedures are required in order to compute spectra). Information theory limits the highest wavenumber obtainable with such a spacing to 625 cm^{-1} or, in other words, only the far infrared frequency region is accessible. To change the instrumentation to the midinfrared, it was necessary to reduce the displacement interval eight-fold to 0.5 μm. This task was done at the start of the project for the continuous drive (our Sun Co. interferometer) by dividing a Moiré photocell waveform electronically. Special circuits were built for this purpose, basically consisting of a smoothing filter and a differentiator. This system has been working reasonably well, as long as the fine tuning was checked at frequent intervals and the Moiré gratings were in good condition. A much better system was built in the final project year for the stepdrive (the du Pont) instrument. Since the same idea was also applied later to the

polarized emission inlet system it will be discussed in some detail below.

A new stepping motor and control unit were incorporated into the drive mechanism for the movable Michelson interferometer mirror in the step-drive instrument since the original equipment was poor and, in any case, no longer operational. Our second interferometer system, which uses Moiré gratings to monitor the Michelson mirror displacment, will soon be transformed to step-drive as well. Since an optical measurement system (Moiré gratings) does not require--at least in principle--the same rigidity of construction as a mechanical one, it was cheaper to purchase originally. It was also believed originally, erroneously so, that the optical system would be faster since photocell pulses transmitted when the two Moiré gratings were aligned in parallel did not necessitate a change of drive speed. In actual fact the Moiré gratings system is speed-limited since the effective intensity of the light passed through parallel Moiré slits is greatly reduced when the gratings are in fast relative motion and the trigger signals asking the digital voltmeter to take readings become unreliable. Indeed the fringe-counting laser interferometric system used in most commercial infrared interferometers today provides very fast triggering, but such fast triggering is not necessary for the Golay detector we have been using.

It should be mentioned that stepping motors are electromagnetic actuators which convert electric pulses into discrete incremental output shaft motion. The output shaft of a stepping motor rotates through a number of incremental positions determined by the number of pulses it has received and the speed of the rotating shaft is determined by the period between pulses. The positional error in a stepping motor is non-cumulative; accurate angular position and speed control can be readily achieved and triggering pulses are readily available.

We have been using M-series stepping motors made by the Superior Electric Company of Bristol, CT, consisting of a Model M062FD-09 Slo-syn motor, an MPS-3000 power supply, an STM 103 translator module, and two 133832-006 dropping resistors. Figure 5 gives the wiring diagram of the stepping motor control system. The translator module is the heart of the stepping motor system. It provides all the triggering signals to each winding in the motor to assure stable and smooth running. The motor can also be single-stepped and is bidirectional.

The stepping motor is so controlled that it causes the mirror to move 0.4 μm per step, corresponding to an optical path difference of 1.0 μm. Theoretically, therefore, the smallest measureable wavelength is 2.0 μm or the highest frequency is 5000 cm^{-1}, which means that the entire mid-infrared region is available to us (the low frequency or high wavelength limit is about 15 μm or 600 cm^{-1}, determined by absorption of the germanium bemasplitter).

2.2.1.3 Chopper and Blackbody Reference

Both interferometers are equipped with choppers of the tuning fork type shown in Fig. 6. The tines are located in front of the opening in the mirror housing where the source radiation is transferred from the vertical direction to the horizontal direction, which is the plane of incidence of the interferometer. This location is not the best theoretically since potential radiation upstream from the chopper blades would still be accepted by the detector. Ideally the chopper should be immediately behind the source. Our choice was dictated by the need for a blackbody reference whose radiation is introduced into the optical path by reflection of the chopper blades and is detected alternatingly with the source radiation. Whenever the chopper blades have come together to block the source radiation

blackbody radiation is introduced. The phase-locked amplifier will then amplify only the difference between source and reference radiation.

The chopper frequency can be varied about 20 Hz. This slow rate is dictated by the nature of the detector. However, it must be fast compared to the reading rate, which is about two per second. Hence it takes somewhat less than ten minutes to collect 1000 data points, which has been our operating standard. Indeed, we found that a 10:1 ratio of chopper to reading rate can be considered fast in this context. Commercial infrared interferometers do not use choppers but instead displace the interferometer mirror for an entire spectrum in about a second and accumulate many spectra for averaging. Since about 1000 spectra would be required to match our singal/noise ratio, the data accumulation time would be about the same as ours. For an operation comparable to ours, a blackbody emission spectrum would have to alternate with a source emission spectrum every second. The question then arises whether enough energy per data point (1000 data points, i.e. one reading per millisecond) would impinge on the detector to produce valid data. It would seem possible to me to achieve it, but our system would still have greater radiation-gathering power because of the larger optics and is simpler, as we can use a room-temperature detector. We did some exploratory work with a liquid nitrogen-cooled mercury-cadmium-telluride detector--in the hope of increasing our sensitivity even more--but found the resulting shielding problem difficult to handle. All the instrumentation ahead of the detector and chopper would be at a temperature above that of the detector and radiate strongly.

Our present blackbody reference source is shown in Fig. 7. It was designed and built entirely during the last year of the project and is very much superior to what we had before. Commercial sources could not be used since they could not meet our space limitations. We require independent temperature and flux control and fast changes of either. We also require

very constant operation, once set, a high degree of flux directionality, and remote controls, since the unit is built into the interferometer. Temperature control alone is unsatisfactory since then the slopes of the blackbody curves (intensity versus wavelength) of source and reference can differ and our difference spectra can have sloping backgrounds and inverted spectral bands. In our unit the radiation emerges from the hole in front. The flux can be controlled by the spring loaded adjustable wedge in front of the hole. The temperature is controlled by circulating water from a thermostatted reservoir. The same water can also be circulated around a stationary sample, thus maintaining sample and reference at very nearly the same temperatures. The outer shell of the blackbody is always maintained at ambient temperature.

Figure 8 shows the blackbody schematically. The emerging flux is so aligned and focused as to impinge on the chopper blades when they are closed. Temperatures up to 200°C can be maintained with the outer steel remaining at room temperature.

2.2.1.4 Polarized Emission Microscope System

The original reason for the use of a microscope objective to pick up radiation from a lubricating contact was simple: The contact area between a bearing ball and a plate--diamond window in our case--is small, typically less than one-half millimeter in diameter--and if sufficient radiation is to be gathered from the thin lubricant film in this region, it must be done over a reasonably large solid angle. A lens of large numerical aperture and a working distance consistent with the geometry was therefore postulated. Fortunately Beck Ltd of England makes Cassegrainian lenses of all-reflecting elements, which can be aligned by eye and still work over the entire infrared region without chromatic aberration. For our work we used two lenses, 15X and 36X, having numerical apertures of 0.28 and 0.50, and working distances of 24 and 8 mm respectively.

Most of the work reported here was done with the 15X lens. Later we applied the same procedure to emission spectroscopy from stationary surface deposits. Then it became evident (Figure 9) that the lnes of the higher numerical aperture provided spectra of higher resolution as well as of somewhat higher intensity than that of the lower numerical aperture. A lens of 54X magnification and a numerical aperture of 0.65 turned out to be still better in this respect but its working distance of only 3.5 mm made its use for lubricant spectroscopy impractical. Since all these lenses accept the same radiant flux--the greater numerical aperture is compensated by a smaller field of view--the increased intensity must be ascribed to the relatively reduced obstruction of the convex mirror support in the Cassegrainian design at greater numerical aperture. This seems to be precisely the case; for example, the percent of the central area obstructed by the 15X lens is 17.5%, while it is only 12.5% for the 36X lens. However, the higher resolution attained with objectives of higher numerical aperture would seem to be caused by the higher effective angle of incidence--the thickness of the emitting layer is increased as is the contribution of components of the transition moment vector giving rise to the infrared emission in the first place. The latter effect would be large for transition moments oriented perpendicular to the surface and much smaller or non-existent for others. Figure 9 shows no differences between bands, but differences did come up in other work.

The microscope objective also turned out to be of great advantage in infrared Fourier emission spectroscopy whenever surface deposits to be analyzed were granular. The radiation emitted from a larger area would be dominated by blackbody radiation from the interstices between grains. The microscope lens could be trained on a single grain or on only a few grains and thus bring out discrete spectral features. Since the standard focal length of all microscope lenses is large; 160 mm nowadays (it used to be 170 mm 30 years ago), the

radiation impinging on the collimator of the interferometer has a narrow spread--another factor improving the resolution.

The small convergence and axial symmetry of the radiation flux emerging from the microscope objective makes it possible to check it for polarization. Fortunately the entire optical path through the instrumentation is axially symmetric and not sensitive to the polarization plane with the sole--but important--exception of the beamsplitter. As Bell [1] points out, however, a germanium beamsplitter differentiates between s and p polarization only slightly, favoring the former by about 10% and this is the value we confirmed experimentally.

It therefore occurred to us that the discrimination of the instrumentation for polarized emission bands could be greatly improved by substituting a rotating polarizing disc for the chopper. At successive 90° degrees of rotation of the disc about the optical axis the radiation transmitted through the disc would be polarized in mutually perpendicular planes. Reference signals would be sent to the amplifier at exactly every quarter turn of the disk from an arbitrary reference position (or phase angle $\Delta\phi$) and only the difference between detector readings for these positions would be amplified. Randomly polarized graybody radiation would be subtracted out.

This mode of operation, which we have been calling Mode 2 (Mode 1 is the normal operation with the chopper), works very well, even though the interferogram produced in this difference mode can be very weak. Two conditions must be met--in addition, of course to the requirement that the source radiation be polarized--, (i) the radiation beam must be collimated or be at least of small angular spread, and (ii) the rotational speed must be exactly constant. As already mentioned, the first condition is satisfactorily met on the downstream side of the collecting lens. Constancy of rotational speed is obtained by another stepping motor/control unit system, which is essentially identical with that used on interferometer mirror drive (except for speed).

Figure 10 shows the setup, containing a cog-belt drive, a timing plate, and an optical sensor over it. The motor drive assembly is mounted on a plate above but separated from the collimator box cover. It rides on two nylon sliders. Correct tension can be applied to the belt by thumb-wheels. The timing plate containing black and white sensors can be rotated with respect to the geared disc, on which it sits. This rotation is equivalent to turning the sample and thereby changing the reference direction with respect to which the polarized radiation is recorded. By setting the reference plane in such a way as to maximize the signal (the difference between the radiation detected which is polarized parallel and perpendicular to the reference plane) for a wavenumber region limited by a appropriate optical filter, the direction of the average transition moments producing the infrared radiation in this region can be located. Some of the most interesting results of this work came from this method of analysis. In ball/plate experiments it is advantageous to make the reference coincident with the Hertzian conjunction plane, i.e. the plane containing the center of the ball and the center line through the Hertzian contact, in order to detect flow polarization.

Polarized infrared radiation is indicated whenever appreciable output is recorded in Mode 2 operation. However, the signal is often weak. In those cases, a Mode 3 method, where the polarizer is placed at a given known angle but procedure is otherwise, the same as Mode 1 is sometimes useful.

Figures 11 a,b,c are schematic diagrams of the three modes of operation. The sensitivity and discrimination of the combination of a high numerical aperture lens and Mode 2 operation makes this instrumentation superior to any other infrared instrumentation I know of. We have been able to detect dimethylpyrrole in the deposit formed on a piece of

aluminum foil when a drop of a micromolar chloroform solution was allowed to spread and then evaporate. In fact, this procedure would seem to be adaptable to the analysis of liquid chromatography fractions. Work is now in progress to determine detectability limits; they could well be of the order of a monomolecular layer for some materials.

2.2.2 Electronic and Computational Modifications

2.2.2.1 Amplifiers and Detectors

An Ithaco Model 191A Lock-In amplifier was used for both interferometers to substitute for the original amplifiers of both interferometers. For much of this work the reference signal was still provided by the photocells of the Moiré grating device used to determine the interferometer mirror displacement. Since the gratings were ruled at 2.0 μm intervals and a 0.5 μm displacement was necessary to cover the complete mid-infrared, our original system required an electronic divider, consisting essentially of a smoothing filter to eliminate glitches caused by scratches and dust on the Moiré gratings, two differentiators, and a zero-crossing detector. In other words, the "sine-wave" output produced by the photocell as a result of the partial blocking of the radiation from a lamp by the relative motion of two combs is used to provide triggering signals at the peak, valley, and the two zero crossings; differentiation converts peaks and valleys to zero crossing. While this arrangement is designed to measure distance rather than time--the rate of mirror displacement cannot be assumed to be sufficiently uniform--it is nevertheless not independent of displacement rate because of the relatively long electronic and detector time constants. Furthermore the smoothing filter, which is absolutely necessary to permit differentiation, lengthens the time constant. Hence although originally considered faster

than a stepping motor drive, the Moiré system is actually slower and less accurate. For this reason, it was replaced by stepping motors as described in the preceding sections.

The lock-in amplifier is, of course, essential not only to reduce the random noise and increase the weak signal/noise ratio but to provide the differential signal amplification, i.e. source emission minus blackbody at nearly the same temperature for Mode 1 operation, source emission polarized in a plane parallel minus source emission polarized in a plane perpendicular to the reference plane (all planes containing the optical axis of the objective lens) in Mode 2 and source emission polarized at a known angle with respect to the reference plane minus unpolarized blackbody radiation in Mode 3.

One lock-in amplifier in inadequate to furnish the ratio between two signals, e.g. the source and the blackbody signal in Mode 1 or the two polarized signals in Mode 2 so as to provide a running record of the emissivity or the dichroic ratio. Two lock-in amplifiers would be necessary for this purpose, one of them operated one-half cycle behind the other and yielding the sum of the two signals instead of their difference (with a phase inverter). Two separate interferograms would then be recorded and stored for every spectral run. They would then have to be transformed separately by computer to yield two spectra and the spectra ratioed. (NOTE: It is not possible to take running ratios and to carry out only one Fourier transformation to get the ratio spectrum because the Fourier transform of a ratio is not the ratio of the spectra of numerator and denominator but a convolution of them. Instead of two separate lock-in amplifiers it is possible (from Ithaco Inc.) to use only one but with a chopper providing two different frequencies which can then be amplified separately). Since our work required mostly only comparisons rather than exact determinations of emissivities,

we did not construct emissivity spectra. In a few cases we recorded source and blackbody spectra in succession and ratioed them later. This procedure did not work out, however, because of excessive noise. We did, however, purchase parts for two lock-in amplifiers at reasonable cost but could not proceed with the construction of the ratioing system because of the memory limitations of our minicomputer. This situation will change soon, however, as described in the following section.

2.2.2.2 Minicomputer

All the interferometer work for this project was carried out with a Texas Instruments Model 990/4 Minicomputer, which was provided with a SLING interface for the plotting of spectra automatically on a Houston Instrument Model 2000 X/Y analog recorder. Because of severe memory limitations in the central processor our program package had to be cut down to its bare essentials. Even so, since overlays were required, the computation and plotting of one 1000-point spectrum would require almost an hour, while the data acquisition took only about 15 minutes. Only one spectrum could be drawn at a time, making comparisons of spectra a long and tedious operation. Furthermore, when data were acquired from one interferometer, the other could not be used and no calculations could be done.

Toward the end of this project, when it became apparent that one of its major results was the application of our highly sensitive methods to surface analysis, making it necessary to compare quite a number of polarized spectra for just one analysis, a trade-in of the Texas Instrument computer for a Digital Equipment Corporation PDP-11/24 with certain options could be effected. With about ten-times the capacity of our old machine, this unit will be able to calculate spectra while acquiring data and it will be able to calculate emissivity spectra. It will also plot a number of spectra on the same graph for comparison.

3. RESULTS

3.1 Trichloroethane Addition to a Traction Fluid

3.1.1 Polymer Formation

1,1,2-Trichloroethane is representative of a great many halogenated materials used in cleaning bearings, gear housings, and other parts of machinery used in modern aircraft. Chlorinated ethylenes have also been used as scavengers for tetraethyl lead and as carburetor cleanants. Since lubrication problems have been reported to occur often after extense overhauls, an examination of the effect of organic chlorides warranted our study. Since one paper on this subject was already published and another was presented and is in the process of publication* and since both of these papers are appended only the highlights will be stressed here. Our views on the interpretation of the results have changed over the time of the project; hence the following report is somewhat different from our earlier ideas.

The traction fluid used was of commercial origin, but did not contain the usual additive package of anti-wear and anti-corrosion materials. Essentially it was a mixture of polycyclohexyl derivatives. Such fluids are now well known to transmit torque in bearings, but without increasing wear. The mechanism of their action has been explained by Winer [2] and by Johnson [3] and coworkers, but a definitive theory is still lacking. Winer regards a traction fluid as a glassy-solid in the contact region, subject to shear deformation until its yield point, while Johnson regards it as a visco-elastic (rubbery) liquid. Our experiments showed periodic changes of infrared emission from the contact region at low load and low speed, which were accompanied by changes in the fluid flow pattern about the rotating ball.

---

* Appendices A and B

(It will be recalled that the ball/plate contact is at the bottom of the fluid reservior and that the rotating ball surface as it emerges from the cup carries adhering fluid along). At the ball circumference contacting the diamond more and more fluid would accumulate, forming a ridge or--looked at from the side--a dromedary-like hump. Then the hump would collapse. After a while, it would start growing again. Presumably lubricant would "pile up" at the EHD inlet, resulting in an unsymmetrical pressure distribution and hysteresis. Hysteresis is a bulk phenomenon implying visco-elastic properties and adhesion of the lubricant.

The infrared emission spectra from the operating contact region containing the traction fluid did not show many sharp and outstanding bands but when trichloroethane was added strong bands at 990 and at 1600 cm^{-1} soon appeared, which are characteristic of olefinic and/or aromatic structures. These same bands also appeared with the traction fluid alone after prolonged operation of the contact at high pressure and shear rates. It is likely that some chloride contamination was present at all times. When the contact was disassembled after these runs a polymeric material (friction polymers) was found on the diamond surface. Furthermore, chlorine was found on the ball surface and especially on the wear scar under the scanning electron microscope, using the surface X-ray analyzer.

Polarized infrared spectra of the traction fluid from the conjunction region showed the emergence of the new bands even more strongly, especially in the presence of the chloride.

The best way to explain the chemical changes in the lubricant appears to be by an ionic mechanism along the lines of Kovacic [4] for methylcylohexane polymerization in the presence of ferric chloride. Both

aromatics and olefins are formed. The formation of ferric chloride on the surface of our steel ball (440 C stainless) is certainly possible.

3.1.2 Changes of Film Thickness and Traction

In later work we were able to determine the thickness of the lubricant (traction fluid with and without trichloroethane) film by a Newton's ring method [5] and the traction (friction coefficient) with the same apparatus and obtained the results of Figures 12 and 13. The film thickness and the traction were lowered by the chloride addition, the film thickness more so, the traction less so,as the surface speed was increased. The decrease of traction by the addition of the chloride and the reduced influence of the chloride at higher surface speed--and therefore larger film thickness--would seem to point to a surface effect. In other words, as the film gets thicker the surface contribution becomes diluted and the effect of the chloride smaller. Indeed, this reasoning for a surface effect was stated by Rounds [6], who included polycyclohexyls in his study. However, the film thickness is reduced by the chloride addition, as we have shown, and this effect is increased with increasing surface velocities. Furthermore, in practically all instances, the film temperature--which corresponds to our overall emission spectral intensity--is decreased by the chloride addition.

We determined the viscosity of the fluid with and without chloride addition (3%) by the standard capillary U-tube method at ambient temperature and pressure and found no measureable difference. Polarized infrared spectra from the operating contact showed a higher degree of polarization when the chloride was present, but no detailed study was done for the traction fluid;it was for polyphenyl ether (reported in the next section).

The apparent discrepancies could be reconciled by assuming a viscosity greatly lowered by the chloride at the very high pressures occurring in the contact. A lower viscosity would reduce the film thickness especially when it is low and would reduce the traction and thereby also the film temperature. However, since already a one percent concentration of the chloride had rather large effects, it was difficult to explain the much lowered viscosity.

Two measurements were made which helped us explain the phenomenon, (i) a differential thermal analysis at ambient pressure on the traction fluid with and without chloride addition and (ii) a measurement of the glass transitions by the ruby fluorescence method at high pressures in the diamond anvil cell.

The DTA procedure showed one glass transition for the neat fluid but two for the mixture (Figures 14 and 15) as the temperature was reduced and the latter showed (alas it was done on a similar but not on exactly the same fluid) two glass transitions and a phase separation for the mixture. The latter work was done by a procedure we developed some years ago [7]. (The substitution of low temperature for high pressure is often, but not always, valid, hence the diamond cell work was undertaken). The results of these measurements then would seem to indicate that the fluid separated into two phases as the pressure was increased; in other words, two phase flow passed through the lubricated contact as shown in Fig. 16. Two phase flow could explain the large change of apparent viscosity at high shear rates and pressures.

The project was about to end when we began to look into such two-phase flow. Of course, this idea does not exclude adsorption of the chloride on the boundary surfaces--we had found such adsorption--, but it could explain all our observations, including the increased degree of polarization of the

emitted infrared radiation (increased shear rate). A survey of the literature turned out to be very fruitful. The work by Chin and Han [8] just published, contains photographs of droplets breaking up in a suspending medium under conditions resumbling those prevailing in our elastohydrodynamic lubricating contact (but at much lower shear rates). Figure 17 is taken from their work The subject of suspended droplets under shear flow is very complicated. It is important from an engineering point of view because of its role in polymer processing [9].

3.2 Trichloroethane Addition to a Polyphenyl Ether (5P4E)

3.2.1 Lubrication Failure and Scuffing

Polyphenyl ether (5P4E, an ether composed of five phenyl rings linked by four oxygens atoms) is an exceedingly high boiling fluid, very inert, which is in the lubricating oil range and has been proposed for and used in high temperature applications. Its room temperature viscosity (200 cs) is exceedingly high. From the spectroscopic point of view, 5P4E is ideal because it has sharp and strong bands whose corresponding vibrational modes are well understood.

In one experiment the bearing ball which had been exposed to the traction fluid containing 3% of trichloroethane (cf. Section 3.1) and failed, was used on 5P4E. This stainless steel ball had barely visible score marks which SEM had shown to be covered by chlorine. The result was rapid catastrophic failure. The ball became very much more scored and the fluid brown and then black. Analysis showed that metallic particles were dispersed with "carbon" in the lubricant. It should be noted that the operating conditions of load and speed had been rather severe. An infrared emission spectrum obtained from the contact just prior to failure showed many band inversions and very broad bands, which are indicative of very high temperatures. A possible

mechanism for similar failures had been proposed by Goldblatt[10], involving aromatic radical ions, acids, and resins. Some of the intermediate species are aromatics adsorbed on the metal surface. An argument against this mechanism can be made on the basis of non-anhydrous conditions. This argument can be countered by the high temperatures observed. The real cause of scuffing is still to be found.

In this connection it seems pertinent to point out that the reactivity of a wear scar on such a stainless steel ball toward alcoholic hydrochloric acid, for example, was found to be up to two orders of magnitude greater that that of the rest of the ball surface (as determined with an interference microscope). There seems to be little doubt that, once a surface reaction gets underway, it can rapidly lead to catastrophe. On the other hand, a wear scar on a titanium-nitride-coated steel ball does not seem to react and no scuffing failure has ever been observed by us with such balls.

3.2.2 Polarization and Molecular Alignment

Figure 18 shows typical EHD emission spectra obtained with the present apparatus. The Mode 1 operation spectrum shows the key bands at 680, 765, 965, and 1180 cm^{-1} representing different fundamental modes of vibration within the polyphenyl ether molecule. The linear sliding speed was 0.6 m/s and the average Hertzian pressure about 1.2 GPa. When the chloride was present the relative band intensities (Fig. 18) changed even though the operating conditions remained the same. Most noticeably the 680 cm^{-1} band is less intense than the 1180 cm^{-1} band when the chloride is absent (Fig. 18), but stronger when it is present (Fig. 18). While the average contact surface temperature was basically the same for chloride present and absent, the average EHD film temperature with the chloride present was somewhat lower (estimated at 100°C). This difference would not account for the spectral

differences, however. The main reason for the spectral differences is the different molecular orientation--polarization of the bands--produced by the presence and absence of the chloride. Even though no polarizer was used in Mode 1 operation, the emission bands are still influenced by orientation of the transition moment; a transition moment vibrating exactly in the direction of observation cannot give rise to electromagnetic radiation, such as infrared, observable in this direction. The relative intensities of the 680 and 765 cm^{-1} bands are particularly sensitive to this effect, since the latter band, representing an out-of-the-phenyl-ring-plane vibration should become unobservable to us when the ring is oriented parallel to the diamond window. It would seem that the presence of chloride is conducive to this orientation (all the spectra are plotted "normalized" so as to fill the available ordinate scale. However, relative band intensities are significant, of course). The reduction of the relative intensity of the 765 cm^{-1} band by pressure and shear was referred to in an earlier publication [6].

The Mode 2 spectra of Figure 18 were obtained for three different phase angles ϕ, i.e. angles between the reference plane and the Hertzian conjunction plane. Since they are all difference spectra--dichroic spectra representing the difference between infrared emissions polarized parallel and perpendicular to the reference plane--they contain rather sharp bands which can point up or down and can only be interpreted by comparison of series of spectra. The very fact that Mode 2 spectra could be recorded from operating contacts is proof of flow polarization and hence molecular orientation produced by shear flow. The velocity gradient in the EHD contact helps orient the lubricant molecules along preferred directions. Stationary liquid samples

gave no Mode 2 spectra; the difference between the infrared radiation intensities polarized in two mutually perpendicular planes did not depend significantly on frequency. (A small Mode 2 signal, which is nearly independent of frequency, is attributed to apparatus error). In other words, under shear flow the lubricant moelcules are oriented in the plane parallel to the diamond window with respect to the flow direction as well (i.e. in addition to being restricted to motion in this plane as described in the preceding paragraph). The variation of band intensity with phase angle allows deduction of the degree of alignment by the velocity gradient in the EHD contact. Clearly, the presence or absence of the chloride--one percent only--has a drastic effect on the degree of orientation.

This effect is more clearly seen by the schematic lines of Figure 19 for the 1180 cm^{-1} band of polyphenyl ether. Please not that these figures can be compared only relatively--only three experiments were run with and without the chloride (it takes about an hour under full constant operating conditions to obtain one spectrum). However, there can be no question that the fluid is more shear flow-aligned in the presence of chloride than without, for then the connecting lines are V-shaped already under less intense operating conditions. Without chloride only the most drastic operating condition produced the V-shaped intensity plot observed with chloride; with chloride all of the intensities follow a V-pattern.

The V-pattern is largely a result of the lack of more data points, i.e. more variation in the angle between the (arbitrary) reference plane and the conjunction plane. Many more points were therefore obtained for a few selected operating conditions. The plots of Figure 20 represent such a study. Note that different spectral bands--corresponding to differently directed transition moments--have maxima and minima at different angles, just

as expected. Indeed the precise direction of the molecules as a whole and the proportion so oriented can be calculated from these data--and is in progress. These data were, furthermore, obtained with a titanium nitride-coated bearing ball substituted for the usual uncoated (440C) stainless steel ball. This thin coating made the ball surface about 50% harder. (The coating was done in Dr. Hinterman's Laboratoire Suisse de Recherches Horlogerès at Neuchâtel, Switzerland.) There is no apparent difference between the spectra with and without chloride for coated and uncoated balls! This observation already constitutes a good indication that the polar chloride additive has a bulk as well as a surface, effect. Very likely there is a surface effect, but our spectral measurements are not sensitive enough to pick up thin surface layers but are sensitive enough to see differences in the bulk fluid. X-ray surface analysis in conjunction with scanning electron microscopy has shown the presence of adsorbed chloride with both coated and uncoated balls, perhaps more on stainless steel balls (no quantitative analysis has been made). Tractions with titanium nitride-coated balls were not different from tractions with uncoated steel balls.

To show the geometrical relationships more clearly, Figure 21 has been included. The optical axis of our instrumentation is along the X-direction. The shear plane, or conjunction plane, which is vertical in our experiments, is the X/Y plane. An arbitrary orientation of the transition moment giving rise to an infrared emission band is shown. In general, it would be inclined with respect to the major molecular axis by the angle α as shown. Angle θ and ϕ represent colatitude and longitude in the usual way.

The model of Figure 21 has been used to show that the intrinsic molecular dichrosim--measured by the angle α--is separable from the flow dichroism under these geometrical conditions [8]. Since we do observe changes of our

dichroic spectra with shear rates, flow dichroism must exist and, furthermore, be affected by the one percent (or less on occasion) of chloride present in the lubricant.

The explanation for this behavior must be similar to the two phase flow model proposed for the traction fluid in the presence of chloride.

3.3 Temperature Gradients Through EHD Films and Molecular Alignment Evidenced by Infrared Spectroscopy

Since the published paper is appended as Appendix C, only a few words will be said here. The shape of an infrared emission band is very sensitive to temperature gradients in the direction of observation. Partial and complete emission band reversals have been observed in the infrared emission spectra from portions of operating sliding contacts. An elementary analysis has been carried out to show that partial reversals are due to temperature gradients in the fluid film--the film acts both as a radiation-emitter and absorber, and that total reversals--an emission spectrum appears as an absorption spectrum--are likely to be due to a continuum source, such as hot solid asperities. The total energy radiated under the latter conditions exceeds that under the others. A decrease in gap width with increased load was accompanied by a dramatic spectral change in the case of 5P4E polyphenyl ether, which is indicative of molecular alignment.

4. DISCUSSION

Two instances of failure were studied spectroscopically, one with a cycloparaffinic lubricant, one with an aromatic lubricant. Apparently both were triggered by the presence of an organic chloride under very severe operating conditions: elastohydrodynamic regime, shear rates near 10^6 sec^{-1}, non-conforming bearing surfaces, very high loads. Ferric chloride could have catalyzed the reactions leading to polymerization and carbonization of the lubricant by ionic mechanisms well understood by catalytic workers. The temperatures accompanying the failure mechanism--which, of course, led to contact between moving surfaces with possible welding and contact breaking--were very much higher than even the high temperatures expected for this type of operation. It is therefore possible that water and oxygen, which were very likely present in the lubricant, though in small concentrations, were effectively squeezed out, thus making the ionic reactions possible.

Since we were able to follow there failures spectroscopically, at least to some extent, it does seem likely that metal/metal contact started the process. However, some metal/metal asperities contact has been shown to always be present under elastohydrodyanimic conditons. The key to the avoidance of failure is a healing process, by which the asperities making contact are worn off before they can rise to failure. When the chloride was present this mechanism was interfered with. Reasoning by an analogy with electrical contacts, where organic chlorides and other halides are deliberately sprayed on to <u>make</u> contact, the key to the mechanism could be the presence of a thin oxide layer on the metal surface. Interestingly, titanium nitride-coated bearings never scuffed in our experiences.

It would seem to be almost impossible to avoid the presence of chlorides entirely. However, their concentration could be kept low and other additives, e.g. the well-known anti-corrosive amines could be used to advantage in counteracting them. The observation that an organic chloride could come out of solution under elastohydrodynamic pressure and then accumulate in the contact region could mean that a "solubilizing" agent could be useful. The literature is full of "solubilizers" to keep oil in aqueous suspension, but almost blank for non-aqueous solvents. A study along these directions could be fruitful.

Related to this idea is the observation of flow dichroism resulting from molecular orientation undergone by every fluid we looked at. By this mechanism fluid viscosity can be significantly decreased. The lubricating gap is thereby reduced and failure made more likely. Since the orientation must occur in the inlet zone of the contact, fluids that would be expected to orient with difficulty would have an advantage. Indeed long chain molecular species seem to have an advantage.

In addition to the above conclusions the work has been most useful by helping in the development of apparatus for the study of thin layers on solid surfaces by infrared emission microspectrophotometry. By picking up the radiation emitted from a very small area (i) blackbody radiation and intergranular scattering is much reduced and (ii) radiation originating from transition moments normal to the surface can still be observed. All-reflecting objective lenses of high numerical aperture are required to introduce the radiation into an already very sensitive Fourier spectrometer of high optical speed. The spectral contrast can be enhanced further by differential point by point recording. In one mode of operation the source radiation is compared to a blackbody reference exactly controlled at the

sample temperature and flux level and in another mode use is made of the fact that most thin surface layers are oriented and therefore polarized and a continuous differencing process between signals in two mutally perpendicular polarization planes can be carried out. The latter procedure, as it discriminates against randomly polarized stray graybody radiation would seem to sensitive enough to allow the analysis of monomolecular layers. These procedures have already been used advantageously in the analysis of various Air Force problems.

5. PUBLICATIONS AND PRESENTATIONS

"Polarized Infrared Emission Spectra from Operating Bearings," James L. Lauer, Paper No.592. Invited paper presented at the Coblentz Symposium of the 29th Pittsburgh Conference at Cleveland, Ohio, March 1, 1978.

"Chemistry and Physics of Lubricants," James L. Lauer. One-hour invited lecture at Session III - Lubricants, Manufacturing of Wire III, Clinic, Society of Manufacturing Engineers, April 5, 1978, in Newark, New Jersey. Published in Wire World, 1978.

"Study of Polyphenyl Ether Fluid (5P4E) in Operating Elastohydrodynamic Contacts by Infrared Emission Spectroscopy," James L. Lauer. Presented at the ASLE/ASME Joint Lubrication Conference in Minneapolis on October 25, 1978 (Paper No.78 - Lub-21).

"High-Pressure Infrared Interferometry," James L. Lauer, in Fourier Transform Infrared Spectroscopy, Vol.1, Chapter 5, pp.169-213, Academic Press, New York, 1978.

"Traction and Lubricant Film Temperature as Related to the Glass Transition Temperature and Solidification," James L. Lauer, ASLE Transactions, 21, 250-256 (July 1978).

"Orientation of Lubricant Molecules in Operating Bearings by Polarized Infrared Fourier Microspectroscopy," James L. Lauer and Vincent W. King, Paper No.70. Presented at the 25th Canadian Spectroscopy Symposium, Mt. Gabriel, Quebec, Canada, September 28-29, 1978.

"Fourier Emission Infrared Microspectrometer for Surface Analysis," James L. Lauer and Vincent W. King, Paper No.17. Presented at the 25th Canadian Spectroscopy Symposium, Mt. Gabriel, Quebec, Canada, September 28-29, 1978.

"Study of Polyphenyl Ether Fluid (5P4E) in Operating Elastohydrodynamic Contacts by Infrared Emission Spectroscopy," James L. Lauer and Vincent W. King, J. Lubrication Technology, 101, 67-73 (1979).

Discussion of Paper by Bair, S.S. and Winer, W.O., "Shear Strength Measurements of Lubricants at High Pressure," James L. Lauer, J. Lubrication Technology, 101, 256 (1979).

"Conditions of Lubricants in Operating Elastohydrodynamic Bearing Contacts by Simultaneous Infrared Emission Spectrophotometry," James L. Lauer and Vincent W. King. Presented : the Second International Conference on Infrared Physics, EHD Zurich, Switzerland, March 5-9, 1979. Proceedings of the Second International Conference on Infrared Physics, pp.379-390, 1979.

"Fourier Emission Infrared Microspectrophotometer for Surface Analysis - I. Application to Lubrication Problems," James L. Lauer and Vincent W. King, Infrared Physics, 19, 395-412 (1979).

"Spectroscopic Study of the Effect of an EHD Contact of Trichloroethane Addition to a Traction Fluid," James L. Lauer and Vincent W. King. Paper presented at the Annual ASLE Meeting in Anaheim, May 1980. (Preprint No.80-AM-4D-2).

"Temperature Gradients through EHD Films and Molecular Alignment Evidenced by Infrared Spectroscopy," James L. Lauer and Vincent King. Paper presented at the ASLE Joint Lubrication Conference, San Francisco, August 1980. (Preprint No.80-C2/Lub-12).

"Analysis of Fourier Infrared Emission Spectra through Windows in Operating Contacts," James L. Lauer and Vincent W. King. Paper No.263, presented at the Pittsburgh Conference, March 10-14, 1980 in Atlantic City, New Jersey.

"Polarized Fluoroescence of Lubricants in Operating Bearings," James L. Lauer and Vincent W. King. Paper No.631, presented at the Pittsburgh Conference, March 10-14, 1980.

"Infrared Emission Spectroscopy from Operating Bearings--Apparatus and Interpretation, Meaning to Lubrication," James L. Lauer. Invited lecture on February 1, 1980 at NBS-Gaitherburg, Maryland, with NBS and NRL participations.

"Polarized Infrared Emission from Surface Layers," James L. Lauer and L.E. Keller. Presented at the 27th Canadian Spectroscopy Symposium, File No. 426-79, in Toronto, Canada, on October 6-8, 1980.

"Emission Spectra from Operating Bearings," James L. Lauer. Seminar lecture, Department of Mechanical Engineering, Aeronautical Engineering and Mechanics, RPI, December 3, 1980.

"Friction Polymers and Other Chemical and Physical Phenomena at Lubricant Boundaries," James L. Lauer. Critical Review Presented at the "Interdisciplinary Collaboration in Tribology (ICT)" Meeting, NASA/LeRC, Cleveland, Ohio, March 2, 1981.

"Analysis of Lubricants by Infrared Fourier Emission Spectrophotometry," James L. Lauer. Inorganic/Analytical Chemistry Seminar Lecture at RPI on February 26, 1981.

"Polarized Infrared Emission Spectra of Materials Adsorbed on Solid Surfaces," James L. Lauer and L.E. Keller. Paper No.145, presented at the 1981 Pittsburgh Conference on Analytical Chemistry and Applied Spectroscopy, Atlantic City, New Jersey, March 9, 1981 and published in the Proceedings.

"Temperature Gradients through EHD Films and Molecular Alignment Evidenced by Infrared Spectroscopy," James L. Lauer and Vincent W. King, ASME Trans., J. Lubr. Tech., 103, 65-73 (January 1981).

"Spectroscopic Study of the Effect on an EHD Contact of Trichloroethane Addition to a Traction Fluid," James L. Lauer and Vincent W. King, ASLE Transactions, 24, 3, 331-339 (1981).

"Alignment of Fluid Molecules in an EHD Contact," James L. Lauer, L.E. Keller and Vincent W. King. Presented at the ASME/ASLE Lubrication Conference, International Hotel, New Orleans, Louisianna, October 7, 1981. (ASLE Paper No.81-5C-1).

"Microscopic Contour Changes of Tribological Surfaces by Chemical and Mechanical Action," James L. Lauer, Simon Fung and P. Kwan. Offered for presentation at the ASME/ASLE Lubrication Conference, Washington, D.C., October 5-7, 1982.

"Infrared Emission Spectra, Traction and Thickness of EHD Films Bounded by TiN-Coated Steel," James L. Lauer, P. Vogel and L.E. Keller. Offered for presentation at the ASME/ASLE Lubrication Conference, Washington, D.C., October 5-7, 1982.

"Phenomena at Moving Phase Boundaries." Invited speaker (J.L. Lauer) at the 1982 Gordon Research Conference on Friction and Lubrication.

RPI Patent Case No.198, "Method for the Detection and Analysis of Oriented Material," L.E. Keller, J.L. Lauer and V.W. King. Assigned to the Secretary of the Air Force, October 1981.

RPI Patent Case No. 199, "Adjustable Compact Radiation Source with Controllable Outer Surface Temperature," L.E. Keller and J.L. Lauer. Assigned to the Secretary of the Air Force, October 1981.

6. REFERENCES

1. Bell, R.J., "Introductory Fourier Transform Spectroscopy." Academic Press, New York, 1972, p. 122.

2. Bair, S.S., and Winer, W.O., "Surface Temperatures and Glassy State Investigations in Tribology," NASA Contractor Report 3162. NASA Scientific and Technical Information Branch, 1979.

3. Johnson, K.L., and Roberts, A.D., "Observations of Visco-elastic Behavior of an Elastohydrodynamic Lubricant Film," *Proc. of the Royal Soc. of London, 337A,* pp. 217-242 (1974).

4. Kovacic, P., Morneweck, S.T., and Volz, H.A., "The Nature of the Methyleyclohexane--Ferric Chloride Reaction," *J. Am. Chem. Soc. 28,* 2551-4 (1963).

5. Lauer, J.L., "Determination of Physical and Chemical States of Lubricants in Concentrated Contacts - Part 2," NASA Contractor Report 3402, NASA Scientific and Technical Information Branch, 1981.

6. Rounds, F.G., "Effect of Aromatic Hydrocarbons on Friction and Surface Coating Formation with Three Additives," *ASLE Trans, 16,* pp. 141-149 (1973).

7. Lauer, J.L. and Peterkin, M.W., "Glass Transition and Fluid Pressure Determination from the Fluorescence Spectrum of Ruby," *Canadian J. of Spectroscopy, 21,* 153-158 (1976).

8. Chin, H.B., and Han, C.D., *J. Rheol, 24,* 1, (1980).

9. Han, C.D., "Multiphase Flow in Polymer Processing," pp. 459 , *ff* Academic Press, New York, 1981.

10. Goldblatt, I.L., "Model for Lubrication Behavior of Polynuclear Aromatics," *Ind. Eng. Chem. Prod. Res. Develop., 10,* 270-278 (1971).

LIST OF FIGURES

Figure 16 Model to explain the influence of trichloroethane (TCE) additive on flow dichroism.

Figure 17 a) Photographs of droplets describing the effect of initial droplet size on breakup patterns [11]: (a), (b), and (c) for a = 0.53 mm; (d), (e), and (f) for a 0.91 mm. The droplet phase is a 2% PIB solution, the suspending medium is a 2%Separan solution, and the apparent wall shear rate is 39.5 sec^{-1}.

b) Photographs of droplets describing the effect of shear rate on breakup patterns [11]: (a), (b), and (c) at γ = 13.7 sec^{-1} (d), (e), and (f) at γ = 102.4 sec^{-1}. The droplet phase is a 2% PIB solution, the suspending medium is a 2% Separan solution, and the initial droplet size is 0.68 mm.

c) Photographs of droplets describing the effect of suspending medium viscosity on breakup patterns [11]: (a), (b) and (c) with a 2% Separan solution γ = 102.4 sec^{-1}, a = 1.20 mm; (d), (e), and (f) with a 4% Separan solution, γ = 6.6 sec^{-1}, a = 0.53 mm. The droplet phases is a 10% PIB solution. (from Ref 9)

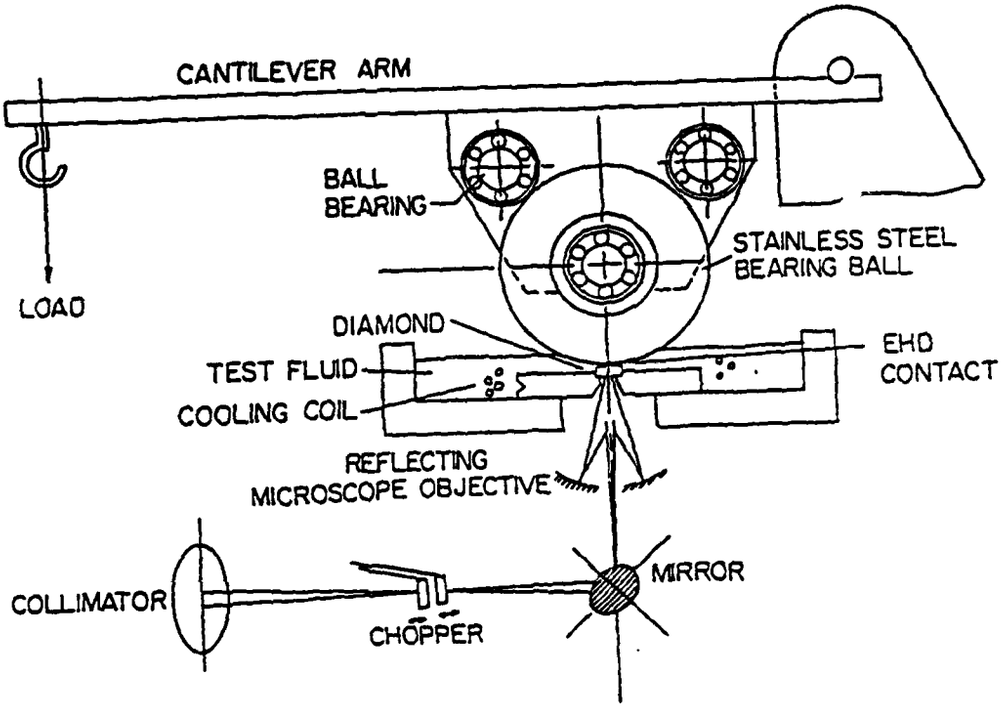

Figure 1 Mockup Bearing Assembly

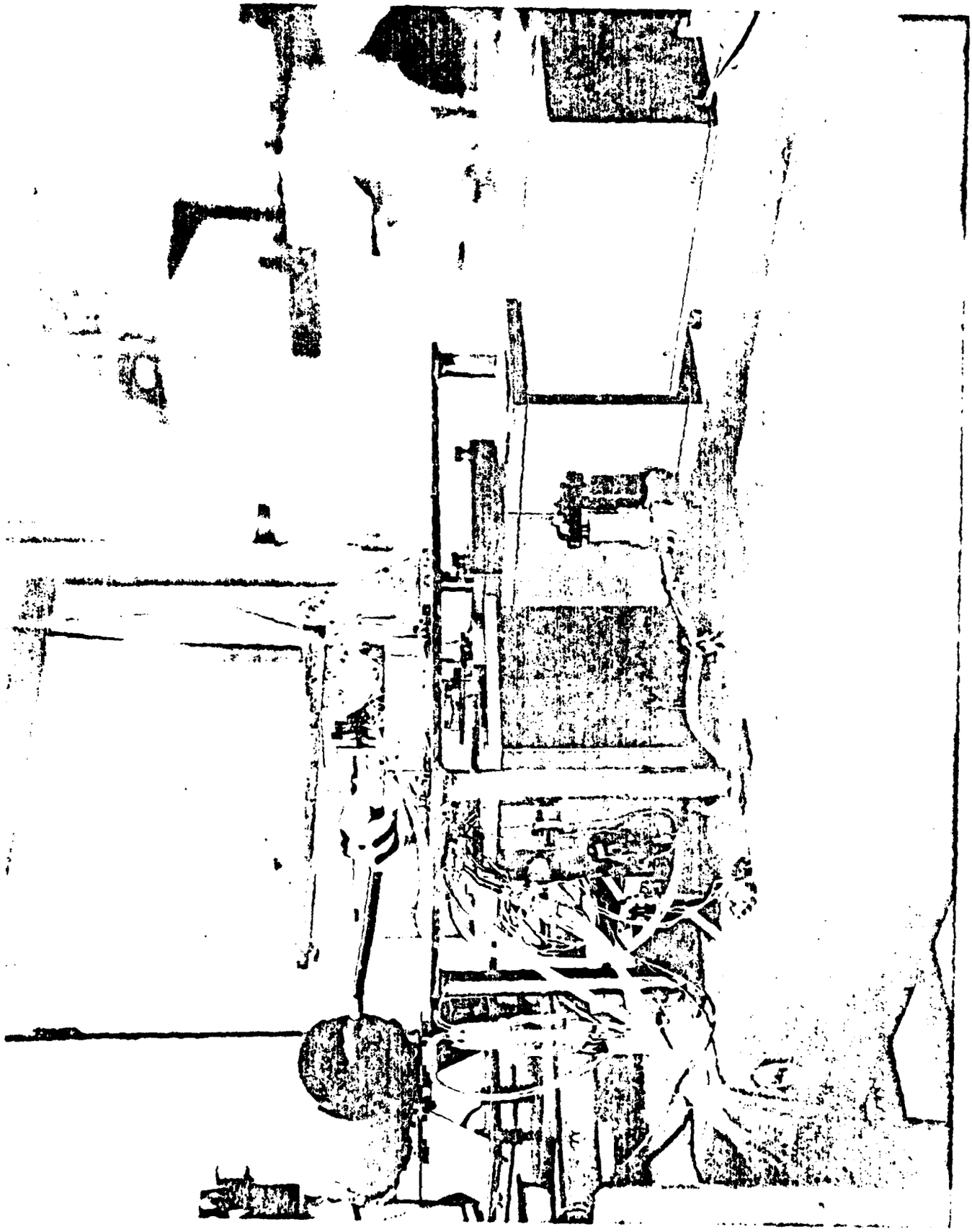

Figure 2 Photographs of Apparatus Assembly

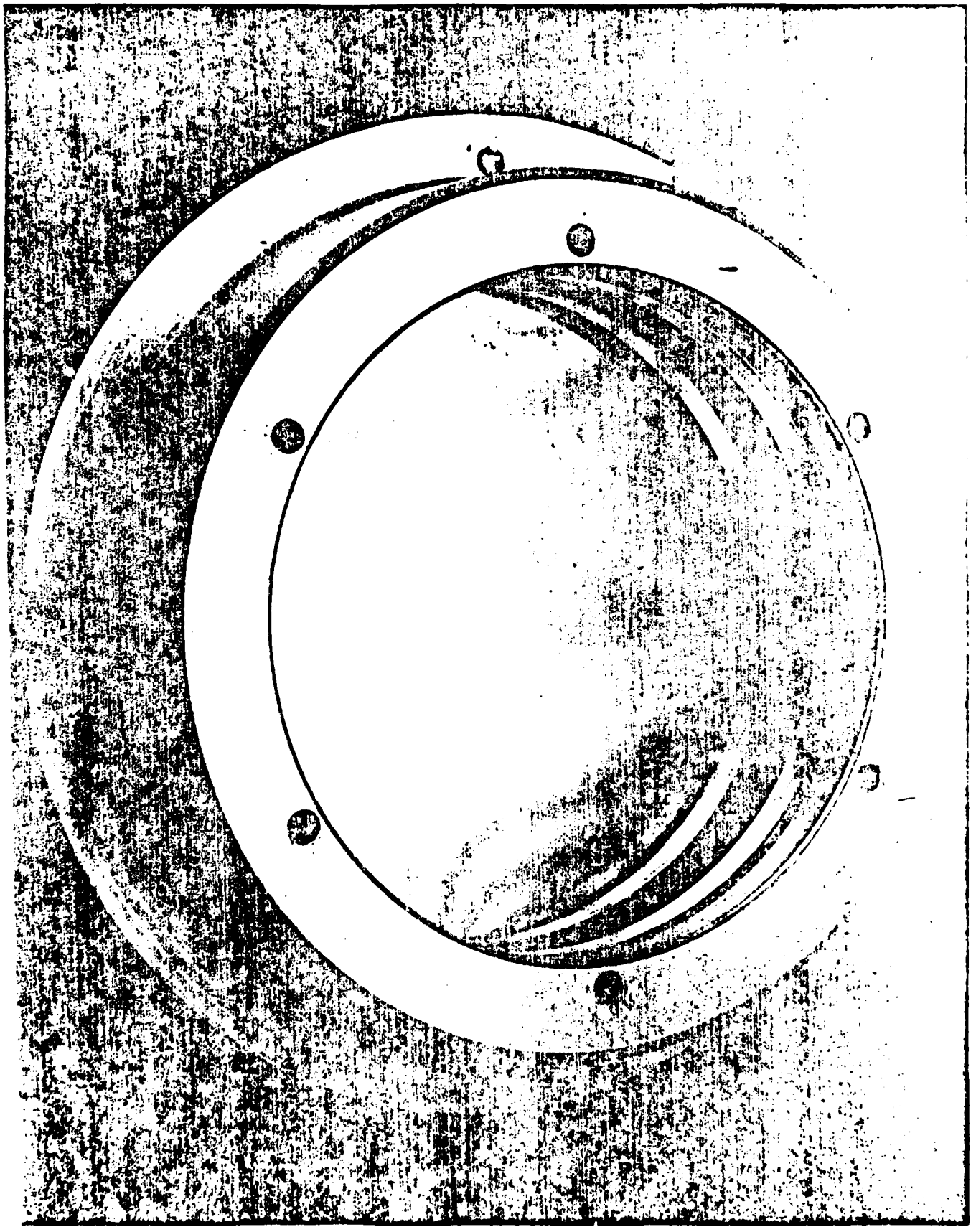

Figure 3 Beamsplitter under monochromatic light (new)

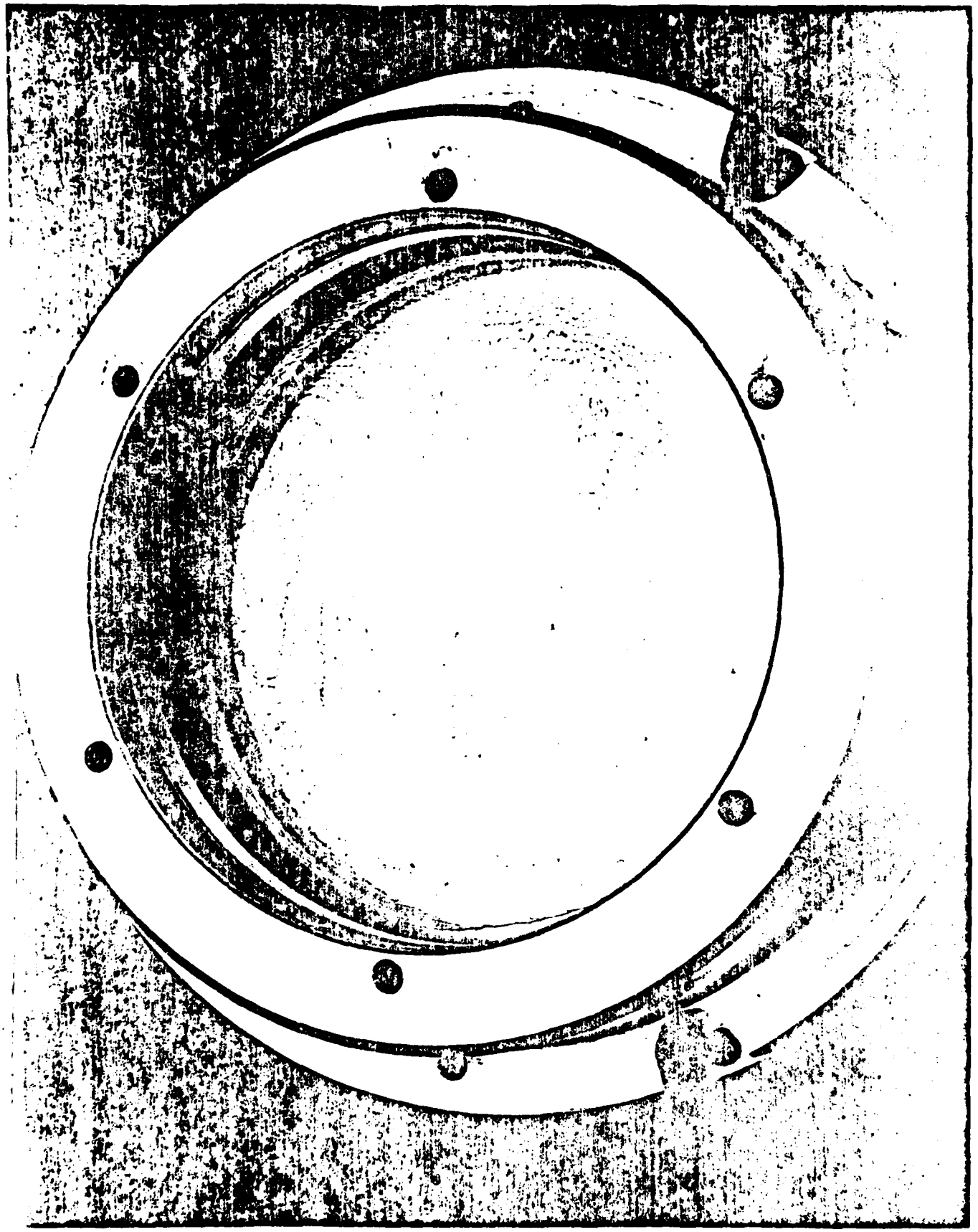

Figure 4 Beamsplitter under monochromatic light (old)

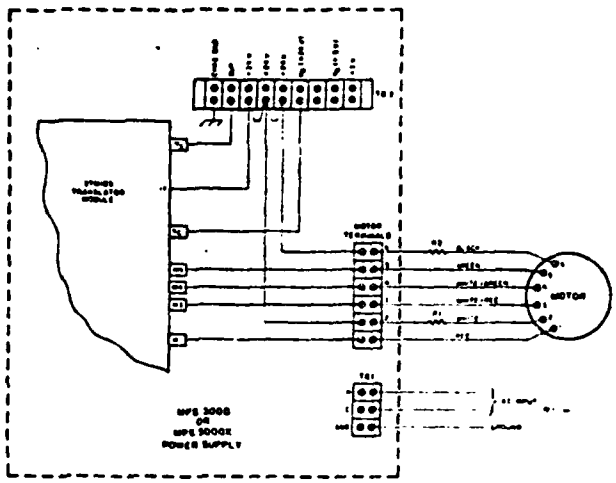

POWER SUPPLY CONNECTIONS TO
STM103 TRANSLATOR MODULE

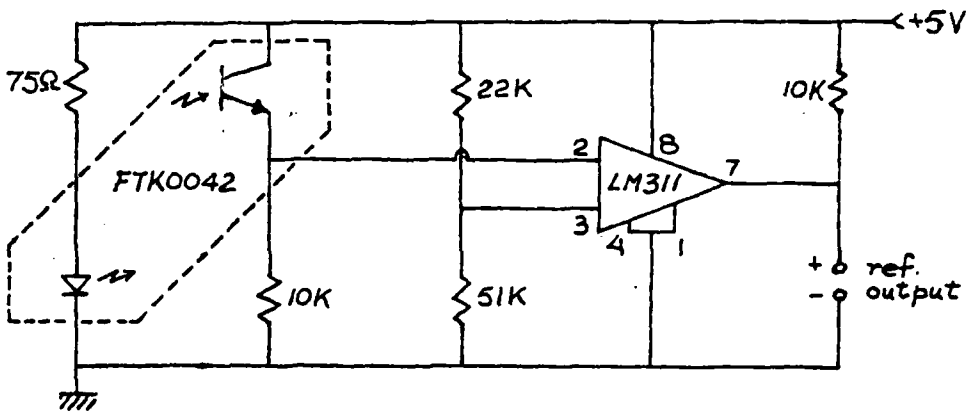

Figure 5 Wiring diagram of stepping motor control system

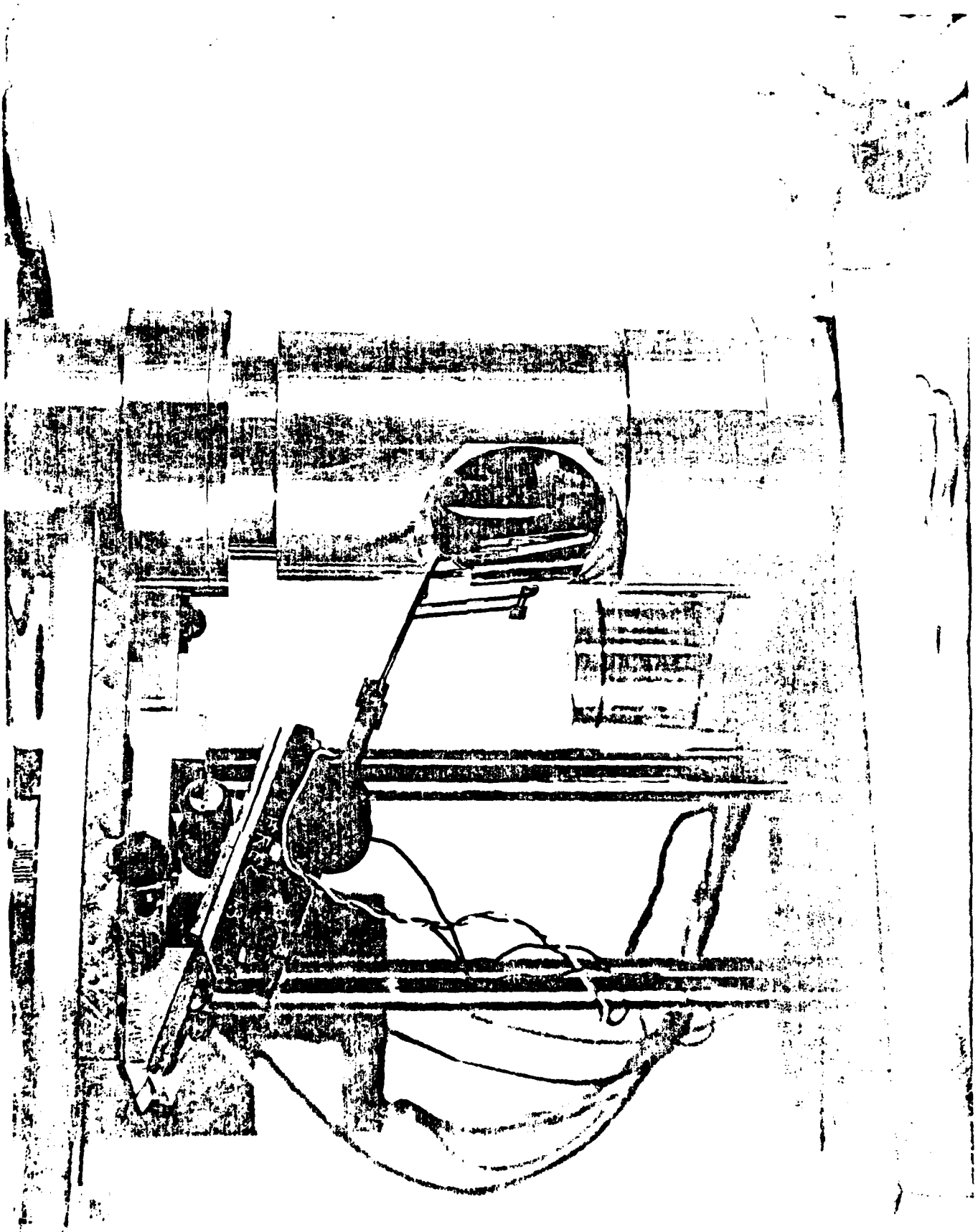

Figure 6 Chopper Assembly

Figure 7 Blackbody Reference Source

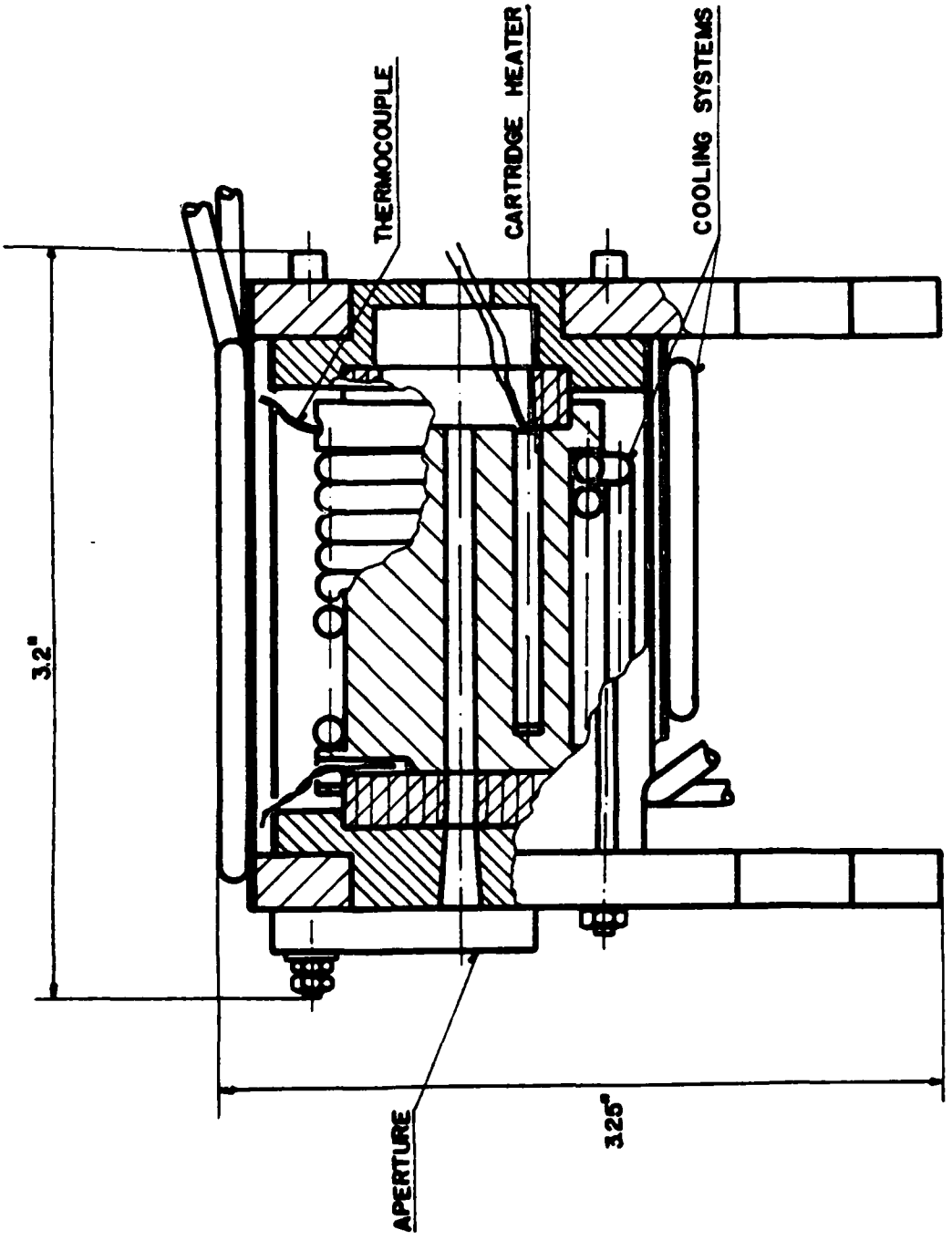

BLACKBODY REFERENCE

Figure 8 Blackbody Schematics

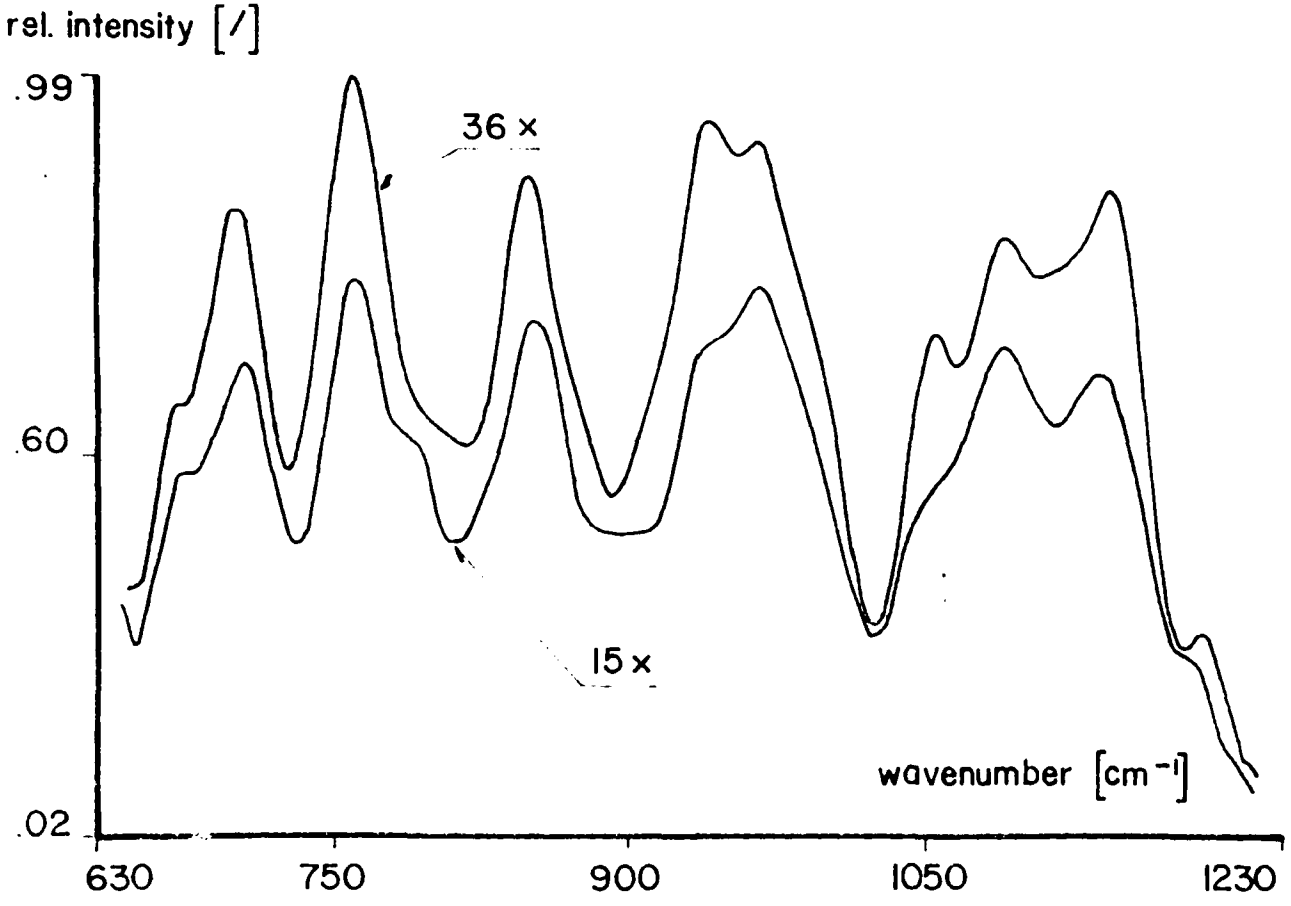

Figure 9 Comparison of Emission Spectra of A Polyphenyl Ether Coating Scanned with Microscope Objectives of Different Magnification and Numerical Aperture.

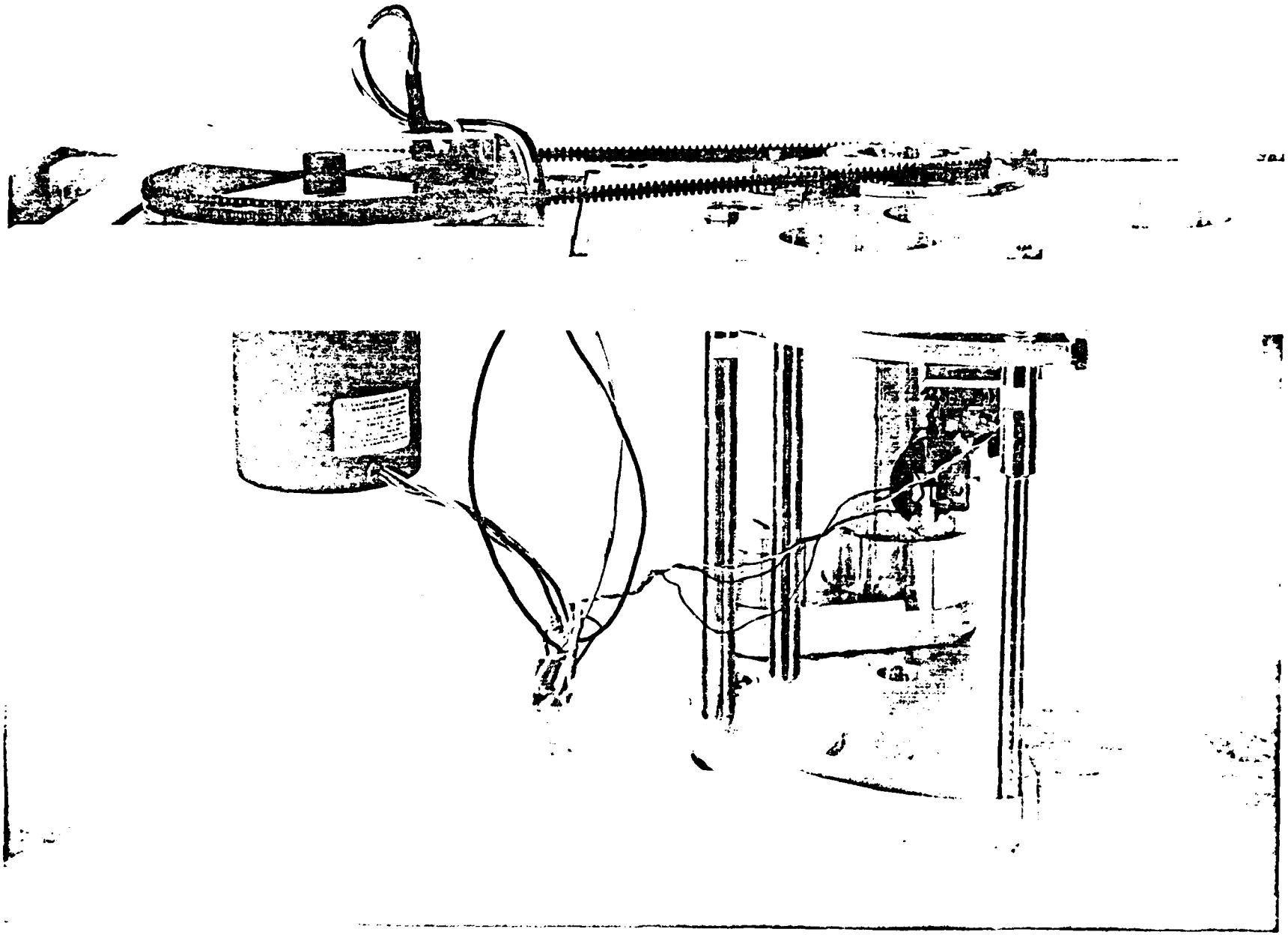

Figure 10 Rotating polarizer setup

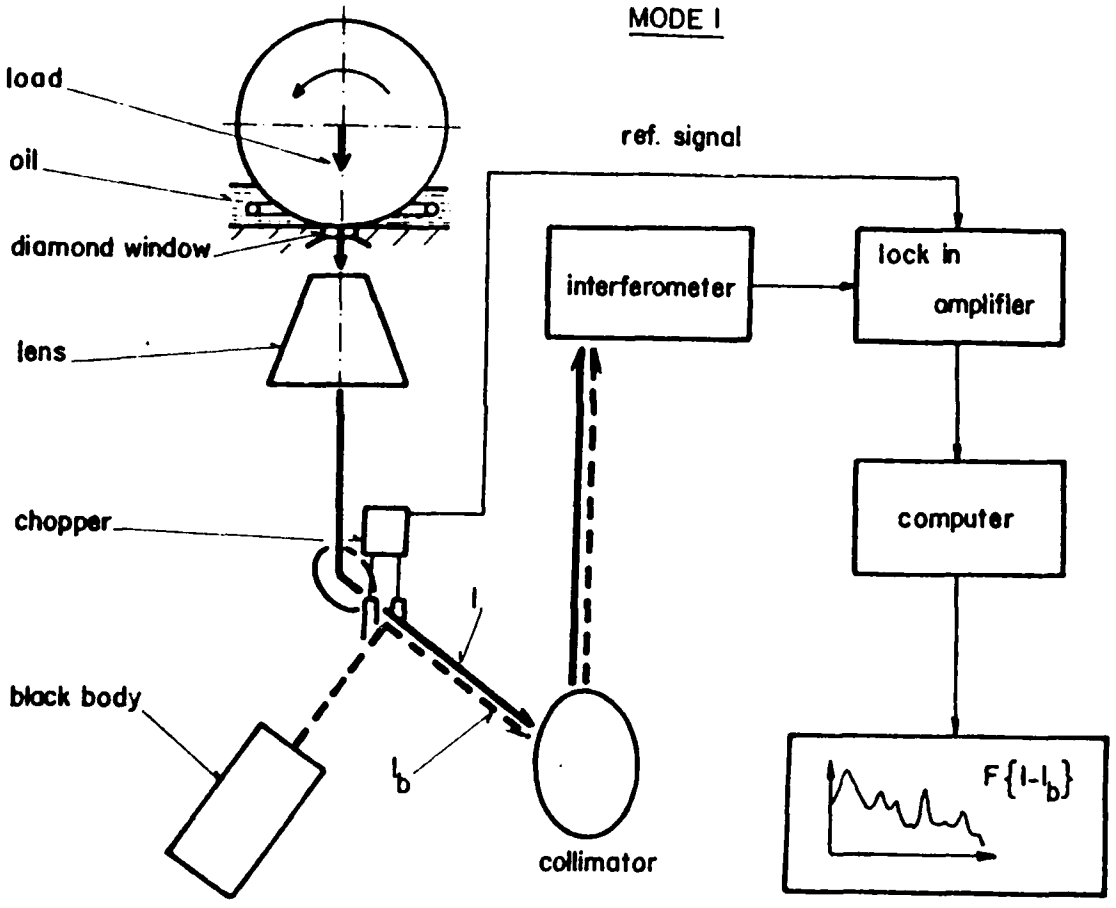

Figure 11 Emission Spectra Recording Attachment

a) Mode 1, no polarizer, blackbody radiation referenced to sample radiation by reflection off chopper blades.

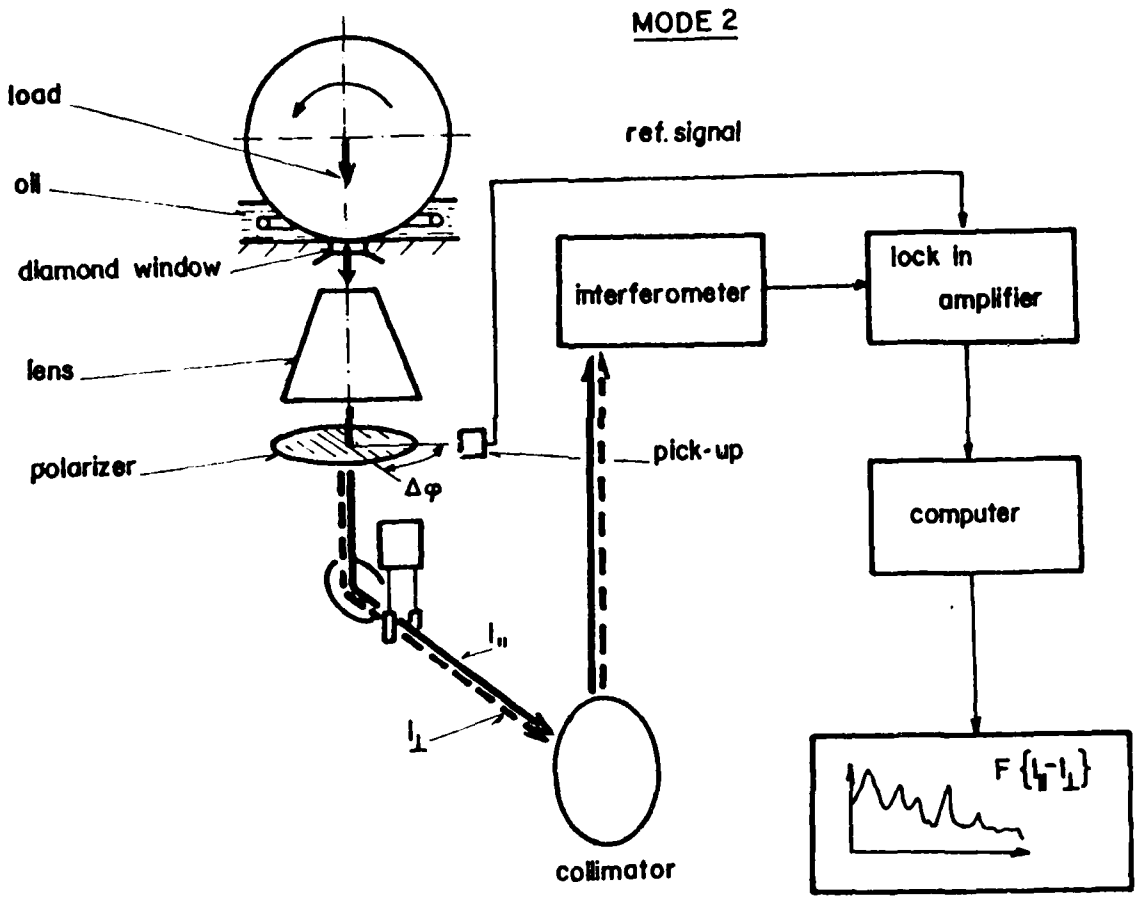

b) ROTATING POLARIZER

Figure 11 Emission Spectra Recording Attachment

b) Mode 2, rotating polarizer, mutually perpendicular planes of polarization referenced against each other, chopper kept open.

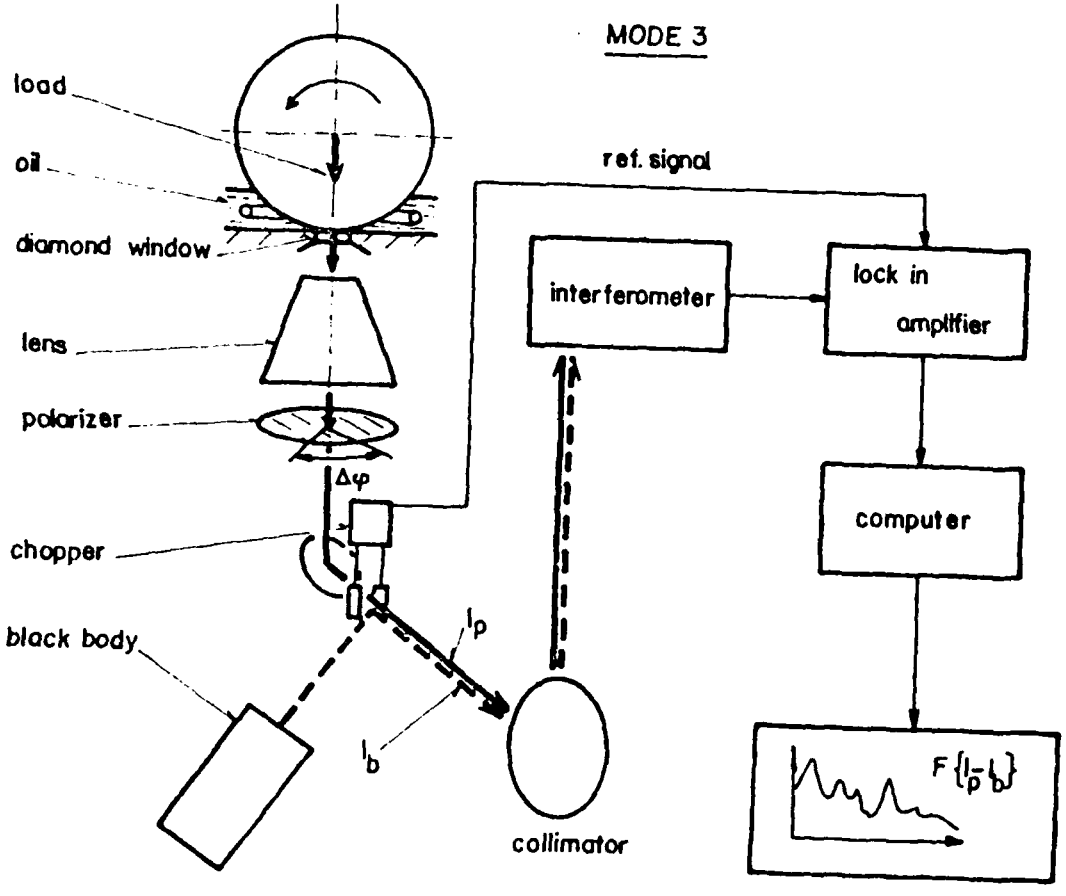

c) STATIONARY POLARIZER

Figure 11 Emission Spectra Recording Attachment

c) Mode 3, polarizer kept in one position, blackbody radiation referenced to polarized sample radiation by reflection off chopper blades.

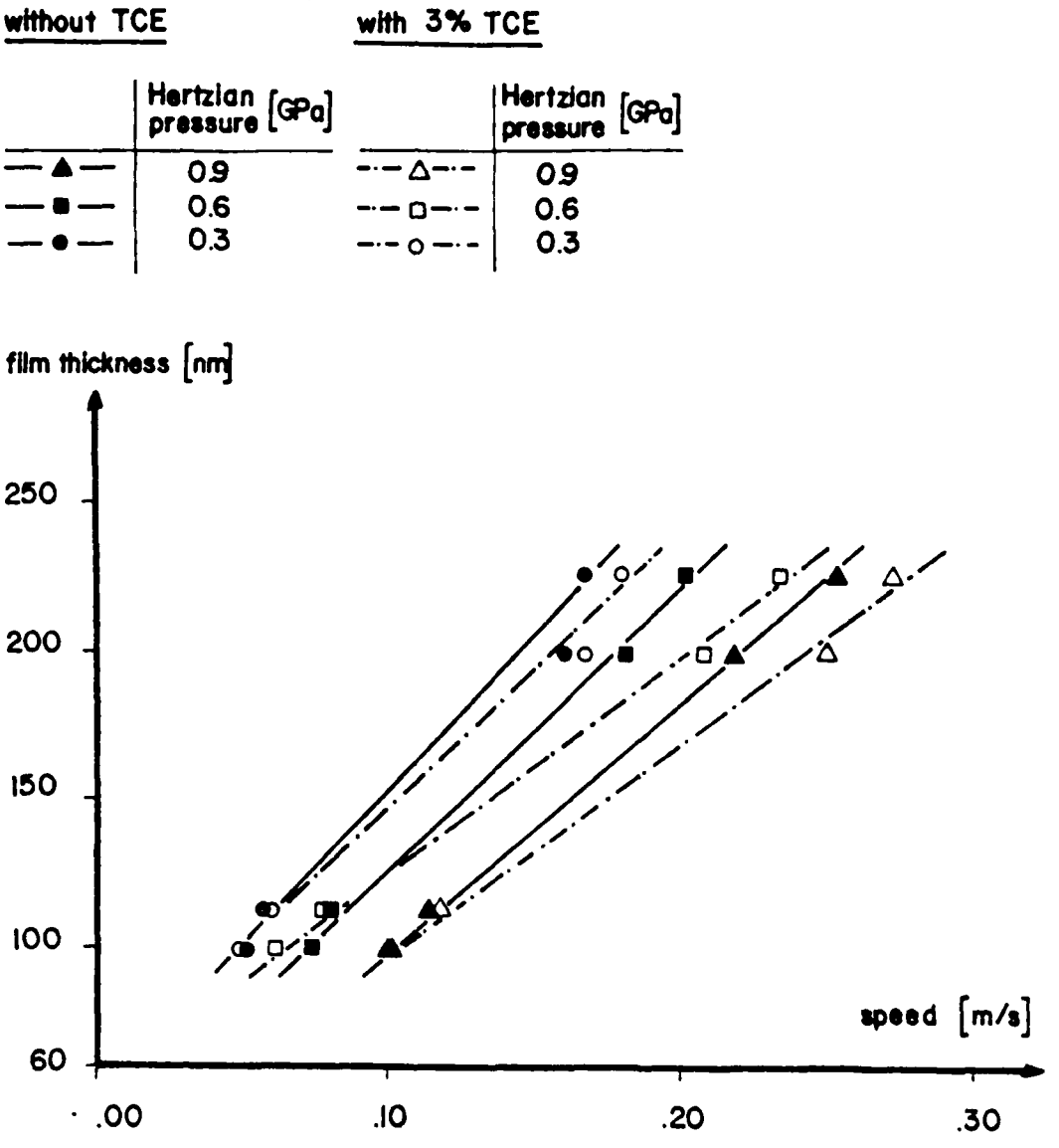

Figure 12 Hertzian contact separations obtained for a polycyclohexyl (traction) fluid with and without trichloroethane (TCE) additive at different average Hertzian pressures as a function of sliding speed.

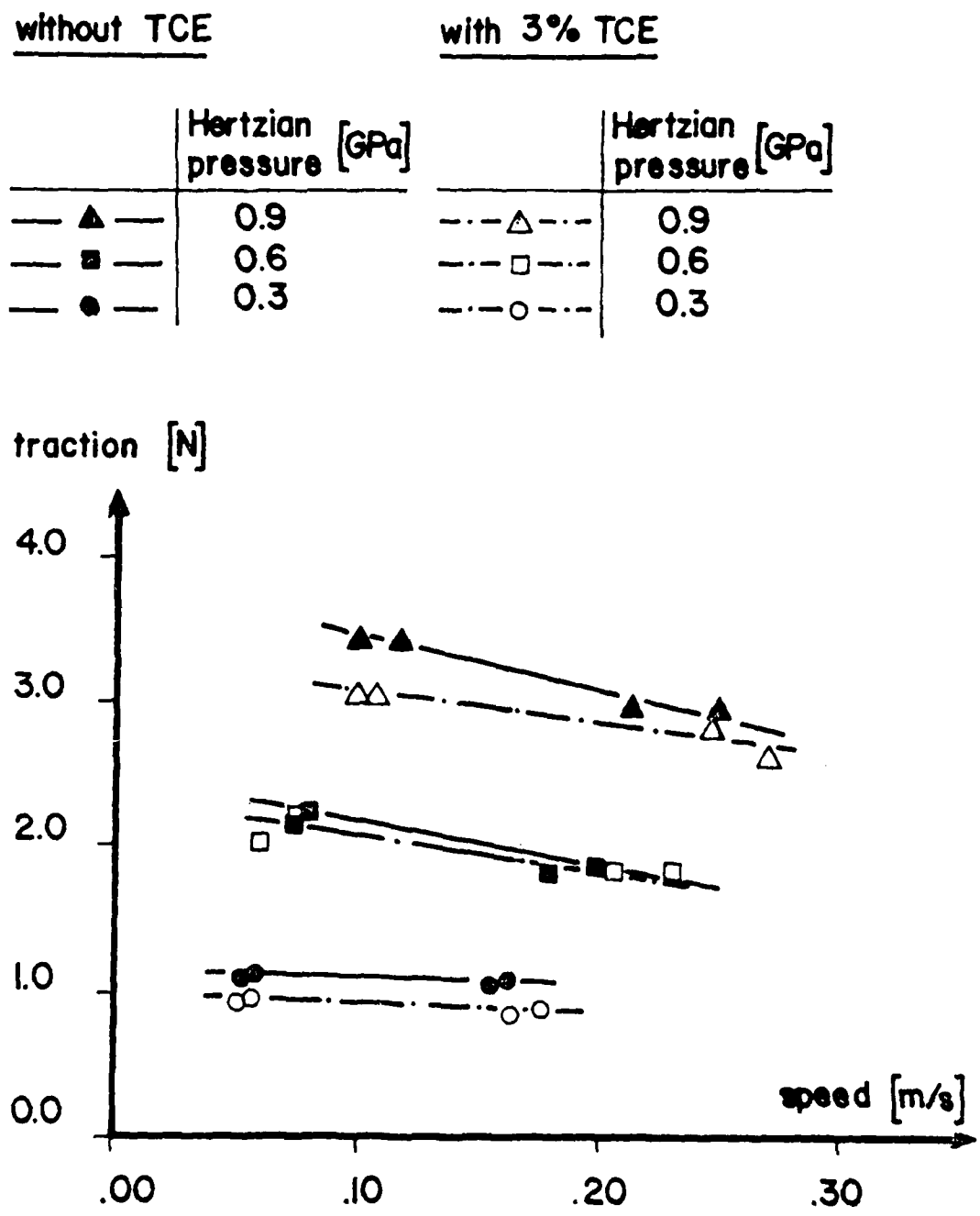

Figure 13 Force of traction for polycyclohexyl (traction) fluid with and without trichloroethane (TCE) additive at different average Hertzian pressures as a function of sliding speed.

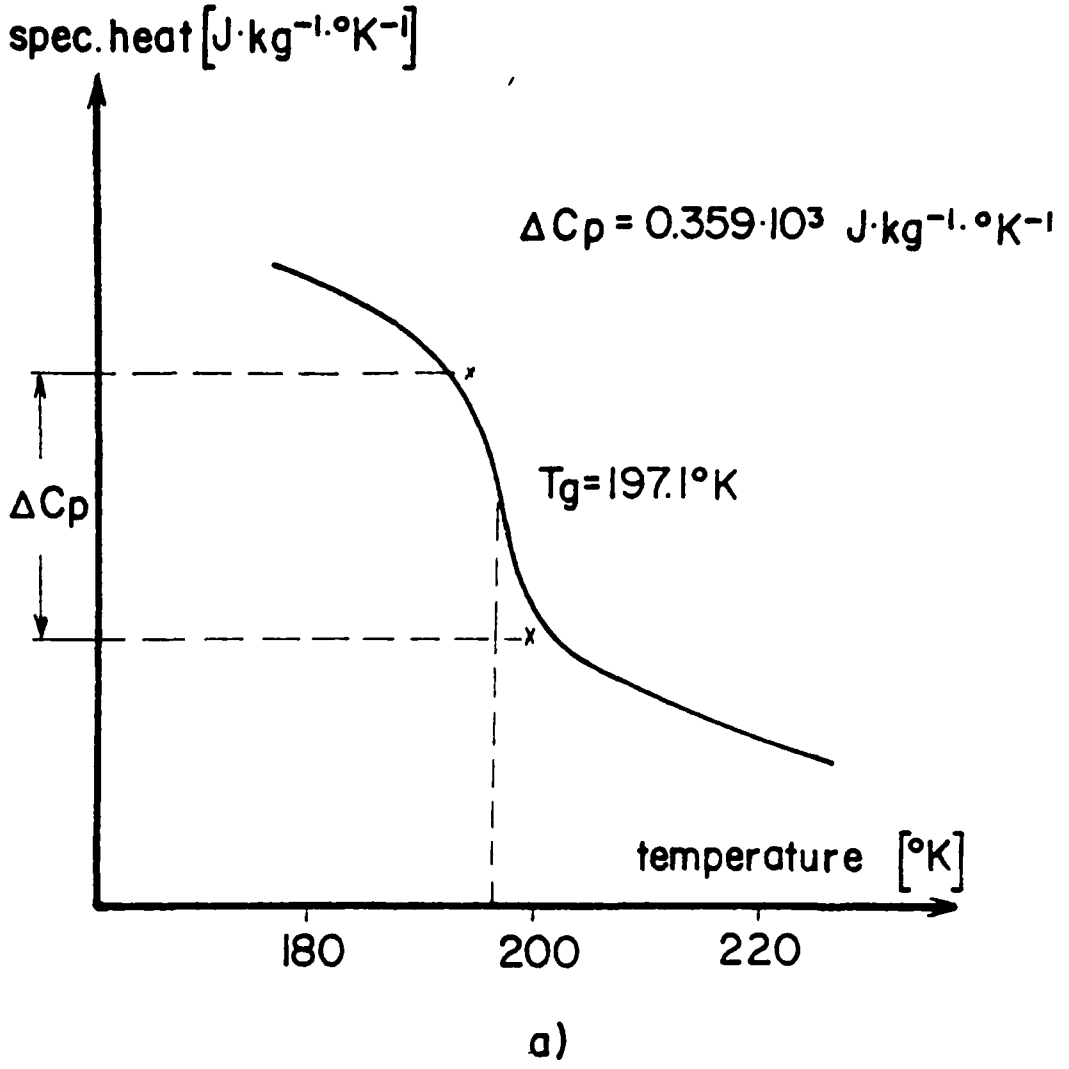

Figure 14 Differential thermal analysis showing glass transitions of polycyclohexyl traction fluid.

no additive

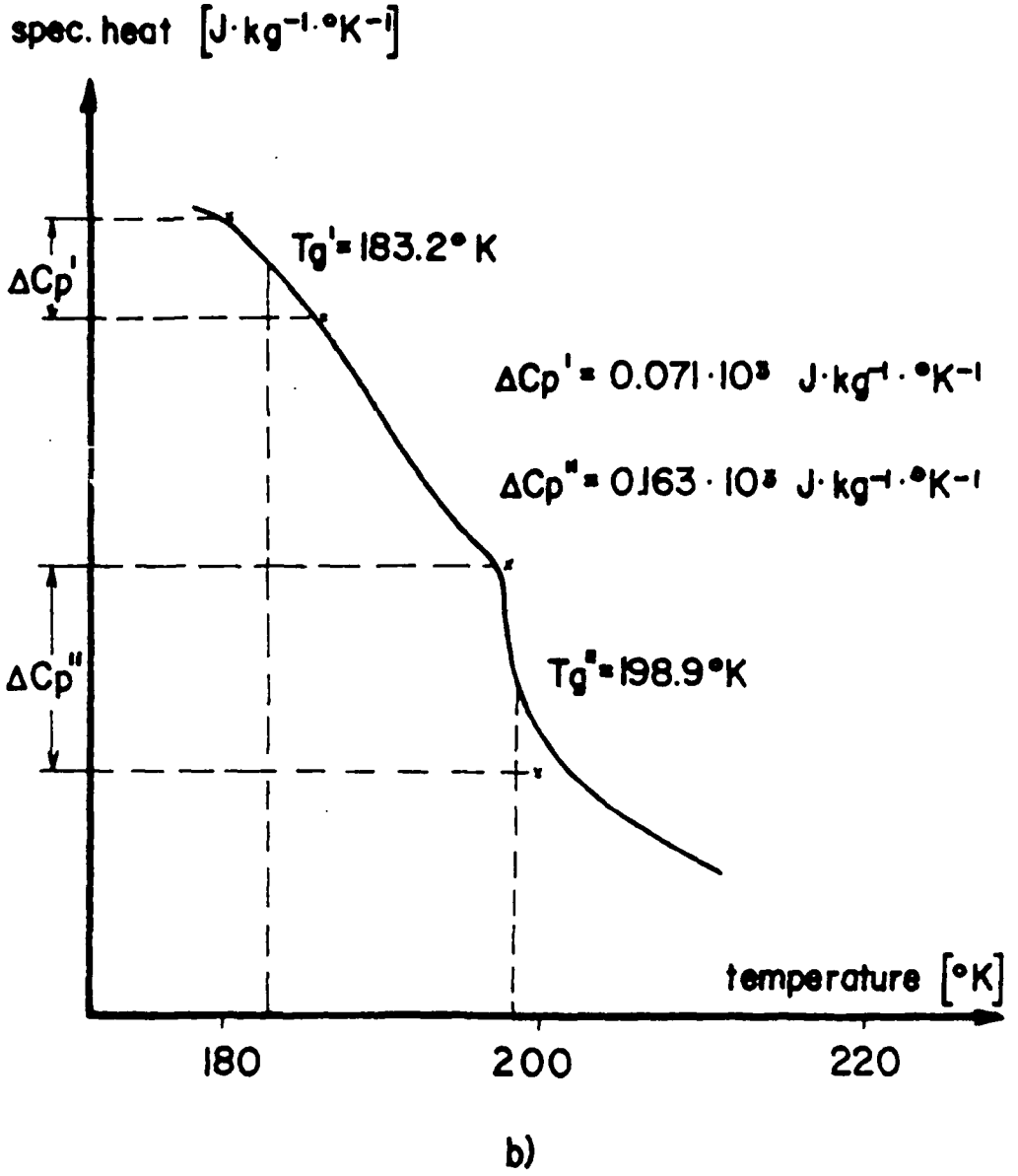

Figure 15 Differential thermal analysis showing glass transitions of polycyclohexyl traction fluid,

with 3% of trichloroethane (TCE)

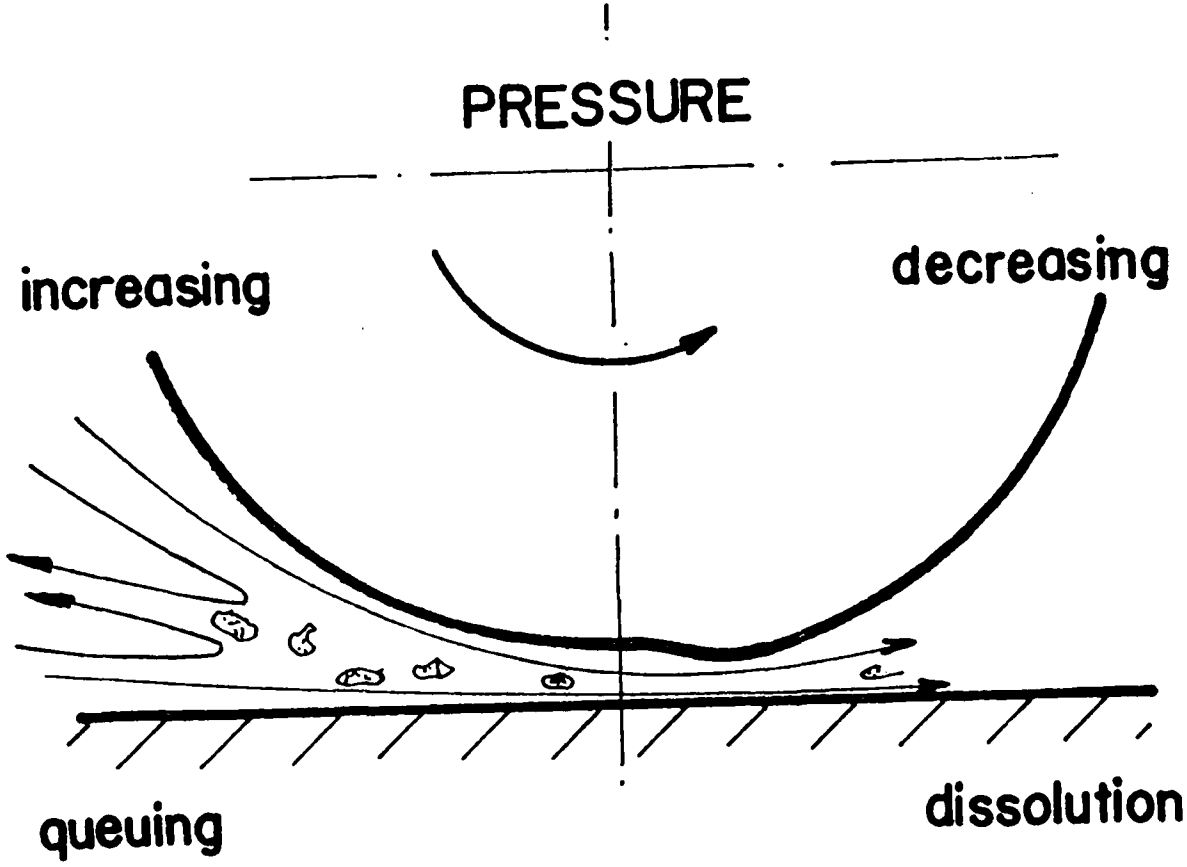

Figure 16 Model to explain the influence of trichloroethane (TCE) additive on flow dichroism.

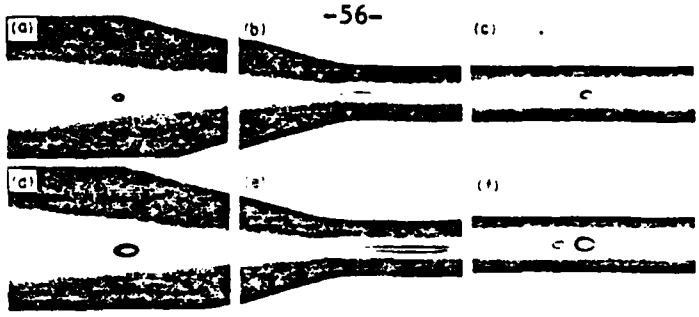

A Photographs of droplets describing the effect of initial droplet size on breakup patterns [11]: (a), (b), and (c) for $a = 0.53$ mm; (d), (e), and (f) for $a = 0.91$ mm. The droplet phase is a 2% PIB solution, the suspending medium is a 2% Separan solution, and the apparent wall shear rate is 39.5 sec^{-1}. The rheological properties of the liquids are given in Figs. 2.2 and 2.3 (see Chapter 2). From H. B. Chin and C. D. Han, *J. Rheol.* 24, 1. Copyright © 1980. Reprinted by permission of John Wiley & Sons, Inc.

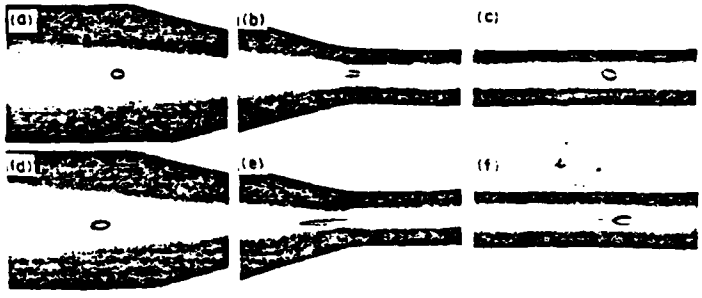

B Photographs of droplets describing the effect of shear rate on breakup patterns [11]: (a), (b), and (c) at $\dot{\gamma} = 13.7$ sec^{-1}; (d), (e), and (f) at $\dot{\gamma} = 102.4$ sec^{-1}. The droplet phase is a 2% PIB solution, the suspending medium is a 2% Separan solution, and the initial droplet size is 0.68 mm. The rheological properties of the liquids are given in Figs. 2.2 and 2.3 (see Chapter 2). From H. B. Chin and C. D. Han, *J. Rheol.* 24, 1. Copyright © 1980. Reprinted by permission of John Wiley & Sons, Inc.

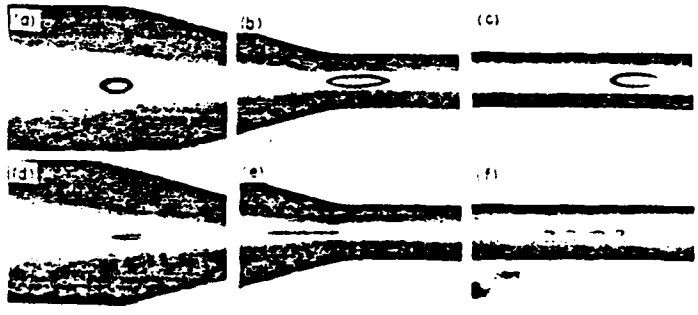

C Photographs of droplets describing the effect of suspending medium viscosity on breakup patterns [11]: (a), (b) and (c) with a 2% Separan solution, $\dot{\gamma} = 102.4$ sec^{-1}, $a = 1.20$ mm; (d), (e), and (f) with a 4% Separan solution, $\dot{\gamma} = 6.6$ sec^{-1}, $a = 0.53$ mm. The droplet phase is a 10% PIB solution. The rheological properties of the liquids are given in Figs. 2.2 and 2.3 (see Chapter 2). From H. B. Chin and C. D. Han, *J. Rheol.* 24, 1. Copyright © 1980. Reprinted by permission of John Wiley & Sons, Inc.

Figure 17

APPENDIX A

Spectroscopic Study of the Effect on an EHD Contact of Trichloroethane Addition to a Traction Fluid

VOLUME 24, 3, 331–339
ASLE TRANSACTIONS

Spectroscopic Study of the Effect on an EHD Contact of Trichloroethane Addition to a Traction Fluid

JAMES L. LAUER and VINCENT W. KING
Rensselaer Polytechnic Institute
Troy, New York 12181

Addition of trichloroethane to a traction fluid was studied in a ball/diamond plate EHD apparatus by infrared emission spectroscopy of the radiation transmitted through the plate. Small concentrations of an organic chloride at first increased infrared radiance, then decreased it. Large concentrations caused a rapid decrease. During running, the infrared spectrum showed an increase of aromatics and olefins. A polymeric deposit formed on the plate. X-ray examination of the ball surface showed the presence of chlorine. Reuse of the same ball with fresh fluid resulted in similar chain of events, indicating that adsorbed chloride could promote fluid deterioration.

INTRODUCTION

The authors have been studying lubricant failure under elastohydrodynamic conditions by infrared emission spectrophotometry for a number of years. For this purpose, a special ball/diamond plate apparatus was built, which allows for the analysis of the infrared radiation generated by friction in the contact and transmitted through the diamond. A highly sensitive infrared Fourier interferometer with a microscope-inlet system was needed for this work since the radiation source is just the thin lubricant film separating ball and plate under high loads. Furthermore, the effective area of the radiating film is limited to the Hertzian contact or, essentially, to the area over which the ball is flattened elastically. Coping with these experimental problems proved to be well worth the effort, however, since it is this small volume ($\sim$3000 μm^3), which must lubricate. Any chemical changes preceding breakdown of the lubricant would be expected to take place in the oil film first and compounds would be more concentrated there than in the entire volume of lubricant. While the authors' previous work was very successful in following temperatures or change of state of the lubricant in the concentrated contact, it was less successful in providing data on lubricant failure, primarily because of the rapidity with which failure would occur.

Trichloroethane allowed the authors to induce failure at a rate convenient for study because it deteriorated the quality of the lubricant. However, the presence of chloride is also of practical concern because chlorinated solvents are used in the field for maintenance. The work reported here shows that failure to remove them entirely before operation can promote lubricant degradation with disastrous consequences. Even when a complete lubricant change removed all the chloride in the bulk fluid, rapid breakdown could still be promoted when the bearing surface was not thoroughly cleaned.

This work concerned only one combination of materials. A stainless-steel ball was used; other materials such as coated metals or nonmetals may behave differently. Only one lubricant system has been explored so far, but it seems likely that others will not be too different.

Only the infrared results are given. They show that chloride promoted olefin formation by molecular breakdown of the lubricant, as well as the formation of some aromatics. The degradation was self-catalyzing since the degraded oil is a poorer lubricant.

APPARATUS

The apparatus was described in detail in a recent paper (*1*). Hence, only a few points are repeated here which are essential for an understanding of the data. Figures 1 and 2 show schematic diagrams. A loaded steel ball (diameter 0.0572 m) is rotated about a horizontal axis through its center in a cup containing the test fluid and made to slide against a diamond window at the bottom. The EHD contact film is formed in the oil between the elastically flattened ball and the diamond surface. Typical film thicknesses are 0.2 μm for the oil used in this study, the precise values depending on loads, linear sliding velocities and temperatures. It is possible to determine these thicknesses from photomicrographs of the interference pattern (distorted Newton's rings). To measure film thickness, an identical apparatus was constructed so that the infrared setup was

Presented at the 35th Annual Meeting
in Anaheim, California,
May 5–8, 1980

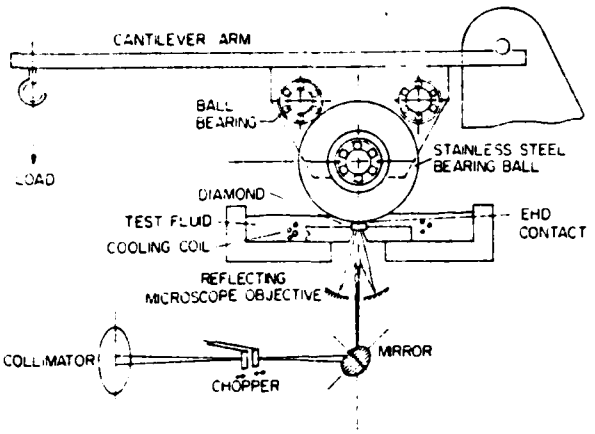

Fig. 1—Schematic of EHD apparatus with provisions for measuring oil film radiation.

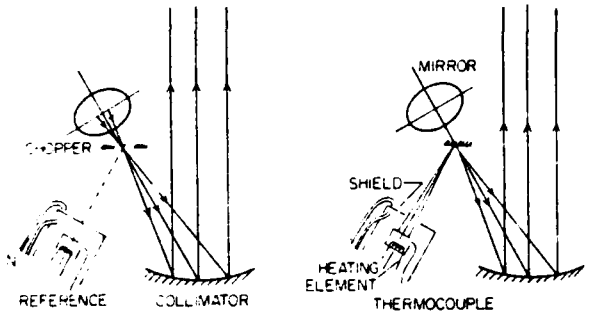

Fig. 2—Infrared light chopper and infrared reference arrangement

not disturbed. The ball was loaded very simply by placing weights on a loading platform resting on rollers on the track perimeter: i.e. rollers, EHD contact and ball center are in the same plane, which is perpendicular to axis of ball rotation. Only the EHD contact friction is significant.

The source of infrared radiation is the thermal energy generated by friction in the EHD contact. The radiation is transmitted through the diamond window, collected by a microscope objective lens made only of curved mirrors, and passed into a Michelson interferometer (Fourier spectrometer) for analysis. The chopper-reference arrangement shown below the lens is very important. By alternatingly passing blackbody reference and source radiation into the interferometer, only the difference between source and reference signals is recorded and a discrete fluid emission spectrum is obtained with only minor continuous background radiation from the solid surfaces. A very sensitive Golay pneumatic cell is the heart of the detector circuitry, which includes phase-locked amplification, analog/digital conversion, a dedicated minicomputer to transform the Michelson mirror-displacement versus signal-amplitude scan into a spectrum of amplitude versus wavenumber. These spectra are plotted by an X-Y recorder responding to computer command.

A coil of aluminum tubing in the cup permitted water cooling and temperature control of the fluid. In most of the work reported here, cooling water temperature was near 10°C, making for an average fluid temperature near the diamond window of about 40°C. Some experiments were conducted at ambient temperature. The lower temperature spectra showed more detail because of narrower band widths. Control was to ∓0.1°C.

An infrared polarizing filter consisting of parallel metal strips deposited on a transparent KRS-5 disk could be placed in the optical path to transmit radiation polarized in the conjunction plane or perpendicular to it. Since the spacing between the strips was only 0.4 μm, the polarizer showed essentially no wavelength discrimination. The purpose of the polarizer is the following: Infrared emission bands correspond to dipole moment oscillations corresponding to vibrational modes of molecules. These dipole moment changes give rise to infrared waves in much the same manner as a radio antenna, or better, an oriented radar aerial to radio waves. If the molecules are not randomly oriented, directional effects will occur for certain vibrational modes and will be observable with a polarizing filter.

MATERIALS

The fluid was a commercial traction fluid, i.e. a fluid transmitting relatively high torques. Previous work by Winer and Sanborn (2), and by Nagaraj, Sanborn and Winer (3) has shown this fluid to produce higher contact temperatures than most of the common high-temperature lubricants. Since it was essentially free of additives, and since the higher temperature was thought to be helpful in a failure study, it was chosen.

The chloride compound was commercial 1,1,2-trichloroethane, boiling at about 115°C. It was separated from the lower-boiling isomer and purified by a simple fractional distillation.

The ball was made of 440C stainless steel, of extra-fine surface finish. The plate was a Type IIA diamond disk, the same as in the authors' previous work. It was specially polished for us to 100 Å smoothness or better.

The traction fluid was a synthetic cycloaliphatic hydrocarbon supplied to the authors without most of the usual additive package. Its viscosity at 37.8°C was 34×10^{-6} m²/s, and at 98.9°C 5.6×10^{-6} m²/s. Pour point was −37°C, density at 37.8°C 889 kg/m³, flash point 163°C, fire point 174°C and specific heat at 37.8°C 2332 J/Kg.K.

The 5P4E referred to in one experiment was a five-ring polyphenyl ether. Its viscosity at 37.8°C was 363×10^{-6} m²/s, and at 98.9°C 13.1×10^{-6} m²/s. The density at 37.8°C was 1190 kg/m³ and the flash and pour points were 288°C and 4.4°C, respectively.

RESULTS

Fluid Flow Pattern and Spectra

Some unusual behavior was noted with the traction fluid only. At low sliding speed and high loads, the mean amplitude of the interferogram showed periodic ups and downs of about three minutes duration (Fig. 3). Since the interferogram is a record of the radiant energy emitted by the contact as a function of interferometer mirror displace-

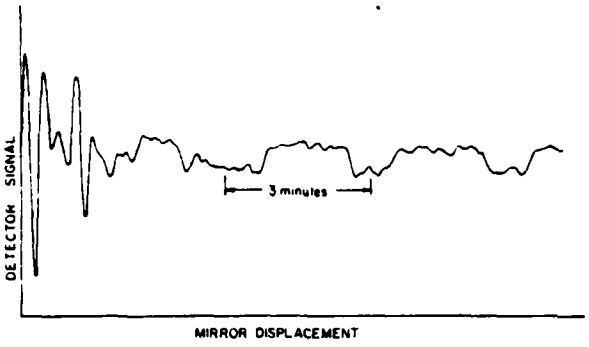

Fig. 3—Interferogram of infrared emission from EHD contact under low load and low speed, showing long-period fluctuations.

ment, these excursions indicate small temperature changes of perhaps 0.5°C. The aperiodic modulations of the interferogram are caused by constructive and destructive interference when the wave fronts of different wavelengths, which are separated by the beamsplitter in the Michelson interferometer, are recombined at different mirror displacements. The mean amplitude of the interferogram is always a constant for a set of operating conditions for the contact; the periodic changes of this mean amplitude, therefore, imply parallel changes in the temperature of the contact. It might be worth mentioning at this point that interferograms are Fourier transforms of spectra, i.e. in the authors' case, records of signal intensity versus infrared frequency. Considerable numerical data processing is required to convert interferograms to spectra, but this effort is necessary when the emitted signal levels are very low.

Spectra thus calculated from the interferograms are shown in Fig. 4. Here it is only important to point out that low-frequency base-line fluctuations in the interferograms did not have any noticeable effect on the spectra. The high-load spectrum is less structured than the low-load spectrum.

The interferogram baseline variations were accompanied by changes of fluid flow pattern about the rotating ball. It will be recalled that the ball/plate contact is at the bottom of the fluid reservoir and that the rotating ball surface carried adhering fluid with it as it emerges from the fluid. At the ball circumference in contact with the diamond, more and more fluid would accumulate, forming a ridge or—looked at from the side—a dromedary-like hump. Then the hump would collapse. After a while, it would start growing again.

Throughout the experiment, the motor speed was kept constant by electronic regulation. When the load on the ball was increased, the periodicity remained essentially the same, but the changes in the interferogram were smaller.

The phenomenon is difficult to ascribe to the usual stick-slip motion of elastomers pressed against a hard surface containing asperities because the hump change or of the interferogram level change was very much longer than the period of ball revolution. However, it could well be related to a "pile up" of lubricant at the EHD inlet, resulting in an unsymmetrical pressure distribution and hysteresis. Hysteresis is a bulk phenomenon implying visco-elastic properties and adhesion of the lubricant.

These phenomena might substantiate Winer's (*4*) and Johnson and Roberts (*5*) models of a visco-elastic traction fluid. The authors' studies were interrupted when the electric motor burnt out because of the high traction.

EHD Spectra of Traction Fluid

Since the traction fluid is not one pure compound but a mixture of various complex hydrocarbons, it is not possible to assign every resonance in the infrared spectrum to a particular mode of vibration or combination of such modes pertaining to molecular structures. However, even without going into details, certain spectral features are clearly seen. For example, the differences between the two spectra of Fig. 4 are quite obvious. The high-load spectrum is much less structured than the low-load spectrum. Both contact temperatures and pressures were higher for the former. Since increased pressures are known to increase spectral contrast, but temperatures to decrease it, the temperature effect is clearly more important than the pressure effect.

Three main emission bands or band groups are seen in the spectra of Fig. 4: (1) the bands below 750 cm^{-1}, which are deformation modes of paraffinic side chains, below 650 cm^{-1} primarily H-C-C- deformations and about 720 cm^{-1} the CH_2 rocking modes; (2) the band peaking near 870–900 cm^{-1}, which are C-C stretching and CH_2 rocking modes of saturated carbocyclic rings, and (3) the bands peaking near 1140 cm^{-1}, which probably relate to similar modes of isoparaffinic groupings. *No bands are visible near* 700 cm^{-1} or near 990 cm^{-1}; if they exist, they are weak and buried in the background. Their absence is indicative of little aromatic or olefinic material in the fluid at the beginning of its use, for Fig. 4 was one of the first spectra obtained from the traction fluid. [For the assignments see Ref. (*6*)]

Another point worth noting in Fig. 4 is the shift of the band contours toward higher frequencies (wavenumbers) with increased load. Close examination of the fine structure of both spectral curves shows, however, that the "shift" is really an increase of intensity of the subbands of higher frequency. There are indications of the presence of most of the low-load peaks in the high-load spectrum, especially between 800 and 1200 cm^{-1}. In spectra of this nature, some of the secondary peaks can be ascribed to different molec-

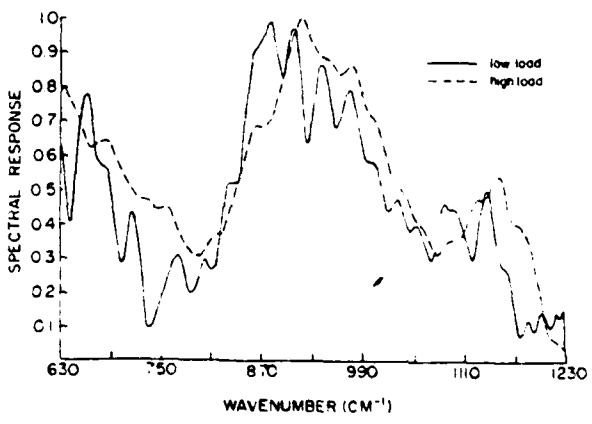

Fig. 4—EHD emission spectra of traction fluid under different load conditions.

ular conformations, i.e. molecular structures differing only in angles between interatomic bonds. Molecules containing saturated carbocyclic rings are especially prone to changes, under pressure or tension, to conformational forms occupying different volumes (*7*), (*8*).

Effect of Trichloroethane Addition on Infrared Emission from EHD Contact

When trichloroethane was added to the EHD apparatus running at high load and constant low speed, immediate changes were noted in the interferogram baseline. (The interferometer mirror was moving normally for scanning. Load and speed were such as to make the long-period oscillations rather small). When 5 ml of trichloroethane were added to the 175 ml of trichloroethane normally in the cup, the baseline would move up gradually, reach a peak, then decline slowly (Fig. 5). The interferogram modulations, shown most prominently near the mirror displacement corresponding to stationary phase for the recombining interferometer beams, become stronger than normal. When 15 ml of trichloroethane were added at once, the baseline also increased, but reached the level corresponding to the maximum after 5 ml of trichloroethane addition much more rapidly, furthermore, the baseline fell back to its normal position quite rapidly and the interferogram modulations were about normal or below normal in amplitude.

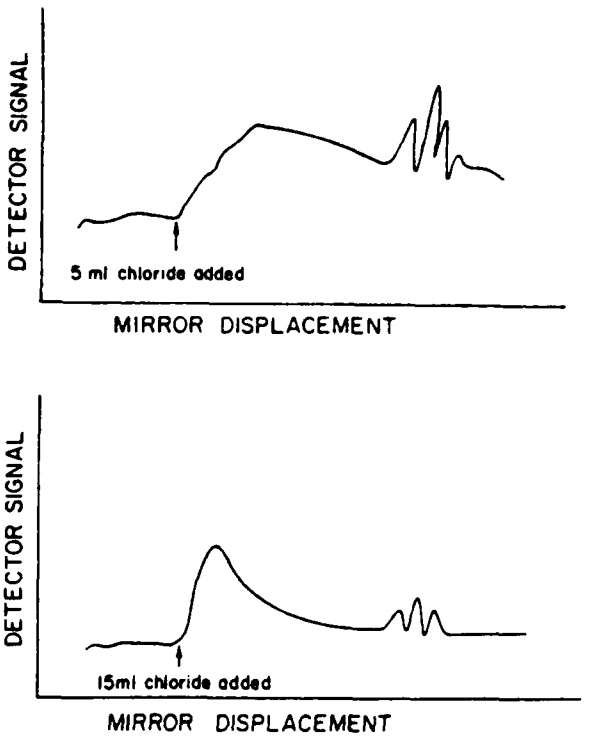

Fig. 5—Changes in interferogram on trichloroethane addition

It should be remembered that the fluid in the cup was mixed rapidly since the ball was turning. These changes of signal level are very similar to the effect on the heat of absorption of the addition of a strongly adsorbed material to a surface covered by a more weakly absorbed material. It is most unlikely, however, that heat of absorption would be noticed by our instrumentation. A change of coefficient of friction is more probable.

These observations are consistent with results published by Rounds (*9*). Rounds measured the change of frictional coefficient as a function of chlorinated wax concentration in a number of base fluids, among them polycyclohexyl derivatives, which are known to be major constituents of traction fluids. He found that for one of the two polycyclohexyls he studied, the coefficient first increased with concentration (Fig. 2 of his paper), reaching maximum near 0.25-percent concentration, and then decreased to a value below that of the base fluid. At the same time, the chlorine content in the surface layer changed similarly, i.e. increased to a maximum, then decreased. Rounds did not emphasize this observation, presumably because it occurred only with one of his traction fluids and not with the other. Overshoots of surface concentration prior to the establishment of equilibrium are often observed in adsorption experiments as a result of initial temperature changes.

Spectra of Traction Fluid Containing Trichloroethane

When various amounts of 1,1,2-trichloroethane were added to the traction fluid, some interesting changes occurred in the spectra of the 630–1230 cm^{-1} wavenumber region (Fig. 6). For comparison of structural detail, all these spectra were drawn on an ordinate scale of 0.0 to 1.0. In order to avoid losing information relating emission band intensities, the "greater unnormalized amplitudes (GUA)" were written next to the spectral traces. Thus, for all the spectra in the first column of Fig. 6, the 930 cm^{-1} band peak had a "spectral response" of unity, but the true measured amplitudes of this peak were 0.62, 0.66, 0.60, and 0.55 for trichloroethane concentrations of 5, 10, 20, and 30 percent respectively. In the absence of trichloroethane, the GUA was 0.58. The occurrence of a maximum GUA with increasing trichloroethane concentration should be noted. In the second column of Fig. 6, the differences between the corresponding spectrum in the first column and the EHD spectrum of the pure traction fluid under the same conditions (high-load spectrum of Fig. 4) were plotted. In calculating the difference spectra the actual amplitudes, i.e. not the normalized (0.0 to 1.0) amplitudes, were used.

The outstanding changes with chloride addition are the new bands shown at the frequencies marked by the arrows in Fig. 1. They are shown more clearly in the difference spectra than in the original spectra and consist of two new bands, one at 700 and one at 990 cm^{-1}. These bands hardly show at 5-percent trichloroethane concentration, but are quite prominent at 10 percent and higher. At 20 percent, the 990 cm^{-1} band is not clearly observed because the peak folded back on itself (peak inversion). Peak emission in a hotter region of the fluid is reabsorbed in colder regions. However, the authors' interest is in occurrence of the new bands. They are not trichloroethane bands, but appear to correlate well with most olefins and aromatics (the strongest trichloroethane bands due to chlorine are at 730 cm^{-1} and below 700 cm^{-1}).

Figure 7 is a comparison of spectra obtained with the

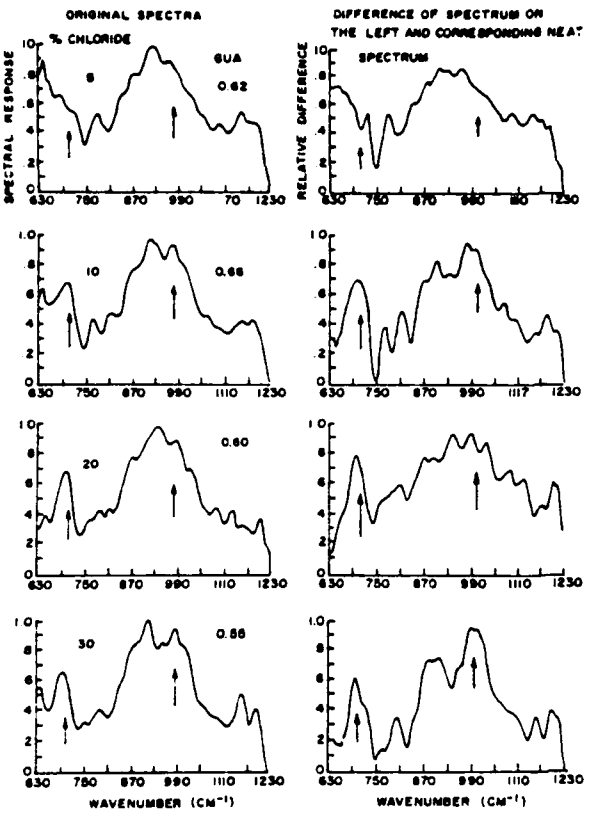

Fig. 6—EHD spectra of traction fluid containing various amounts of chloride.

clear traction fluid and with the fluid containing 15 percent of trichloroethane by volume. The experiments were made in ascending order, i.e. b', a', b, and a. The following observations can be made when comparing the solid line (no trichloroethane) and the broken-line (with trichloroethane) spectra:

(a) The GUA's of the broken-line spectra are equal to or lower than those of the corresponding solid-line spectra. The radiant intensity from the fluid was, therefore, generally less when chloride was present. The GUA is particularly low in the later runs with the chloride, even though the fluid was entirely replaced after every run (new fluid for every run). This observation led us to suspect changes on the ball surface although no scratches were evident.

(b) The bands at 700 cm^{-1} and especially 990 cm^{-1} are more pronounced in the broken-line spectra. Trichloroethane, so-to-speak, "developed" these bands.

(c) The spectrum with the most pronounced peak at 990 cm^{-1} is also the last spectrum of the series and has the lowest GUA.

Spectra of 5P4E (Polyphenyl Ether) for Bearing Ball Run in with a Different Lubricant

Since organic chlorides are used in lubricating oils—as are sulfur-containing additives—as "Extreme Pressure" additives, and since Rounds (9) also reported on interaction between chlorides and aromatic-base fluids, the authors thought it worthwhile to use the ball of the preceding experiments on 5P4E, the polyphenyl ether fluid. A typical

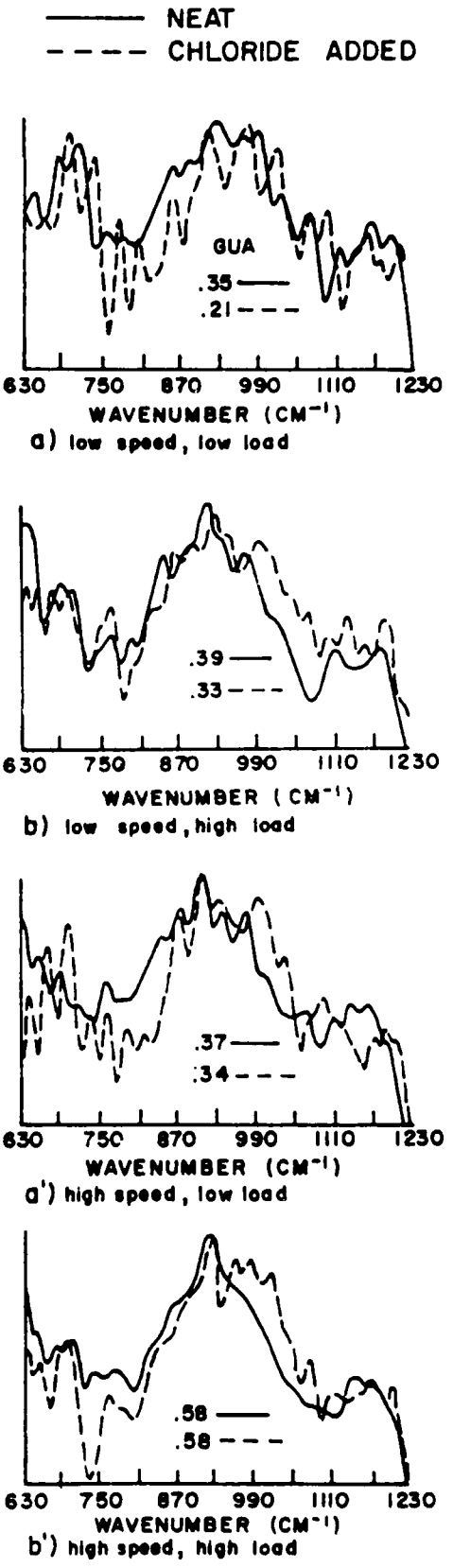

Fig. 7—EHD spectra of traction fluid both near (solid line) and containing 15-percent trichloroethane by volume (broken line). All spectra are normalized to an ordinate (spectral response) scale of unity; however, the greatest unnormalized spectral response (GUA) is given for comparison.

emission spectrum of 5P4E obtained previously under the same high-load/high-speed conditions now used is shown by the solid line of Fig. 8. To the authors' surprise, the emission spectrum now obtained was quite different (broken line). The GUA was much lower than normal, the characteristic 700 cm^{-1} band apparently became a sun of bands now, considerably broader than normal, but—most importantly—the series of bands between 870 and 990 cm^{-1} was not at all characteristic of 5P4E but resembled those of the traction fluid containing trichloroethane which the authors had seen earlier.

Since the system had been cleaned with solvents before the fluid was replaced, the ball surface, having lost some of its polish, seemed to be the responsible agent. Yet, no obvious changes were noted.

In a further experiment, the 5P4E fluid reservoir was maintained at room temperature (all previous experiments referred to were done with the reservoir at ice-water temperature). The EHD spectrum now resembled that of the last traction fluid containing trichloroethane.

After this run, the system was taken apart. The bearing contact had *failed*. The ball was somewhat scored and the fluid contained a suspension of black particles. They were analyzed ferrographically and consisted mostly of metal.

Scanning Electron Microscope and X-ray Analysis of Chloride-Treated Bearing Ball

While some scratch marks were evident on the ball, the ball did not appear to be very different from a new one (440C-stainless). On closer examination, the polish appeared to be somewhat less.

Under the scanning electron microscope (SEM), small scratches were seen at 200X magnification. This instrument also has an integrated X-ray attachment. It is possible to direct an electron beam at any location of the enlarged image visible on the screen and obtain an X-ray diffraction pattern off that spot. When the scratch was thus analyzed, the X-ray pattern showed peaks characteristic of chlorine and some other nonmetals such as phosphorus in trace amounts, but not of any metal. Locations on the ball surface away from the scratches gave rise to X-ray peaks of iron, chromium and nickel, which were very weak compared to those of a fresh ball. From these results, a surface layer thickness of about one micrometer was estimated, based on the assumption of the presence of iron chloride and no other material in the surface layer. This estimate is to be regarded good to an order of magnitude only.

DISCUSSION AND CONCLUSION

The authors believe to have shown a history of lubricant failure. Under high EHD stresses, the traction fluid itself, but more so with *trichloroethane* added, starts to break down by pyrolysis. The standard mechanism is: long chain saturated hydrocarbon → olefins + short chains saturated hydrocarbons and aromatics. The 990 cm^{-1} band has been considered (6) definitive evidence of olefinic structure (out-of-plane C-H). It became more and more prominent in successive runs. It is usually accompanied (6) by another olefin

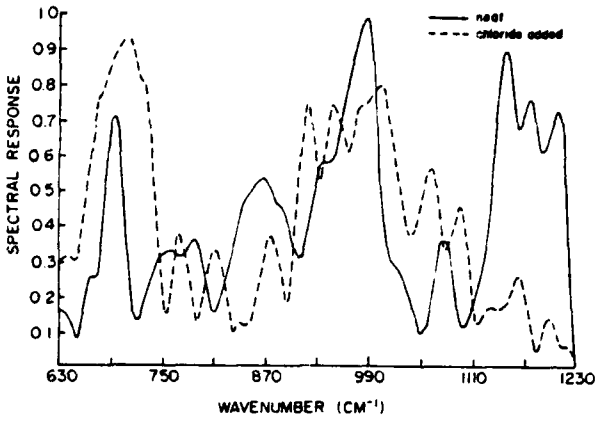

Fig. 8—EHD spectra of 5P4E polyphenyl ether with a clean ball and with a ball containing absorbed chlorine on its surface.

band at 1600 cm^{-1}. While the 1275–1850 cm^{-1} region was run only with the neat traction fluid, where the decomposition was less than when chloride is present, Fig. 9 shows a band at 1600 cm^{-1}, significantly in spectra obtained under the most stress.

The presence of chloride promoted this decomposition, presumably by the formation of a free radical. An aromatic fluid, such as 5P4E, would be particularly susceptible to such attack.

The 1600 cm^{-1} band is more prominent under polarization normal to the conjunction line than under polarization parallel to it (Fig. 9). This could be due to adsorption of the olefin formed on the ball surface.*

The reduction of the GUA's with fluid deterioration is probably caused by a reduced reflectivity of the ball surface and coating of the diamond. Such an effect could seriously alter previous temperature estimates where the ball reflectivity was considered constant. The interferogram changes occurring on trichloroethane addition seem very much related to adsorption on the ball and other surfaces.

As pointed out earlier, Rounds (9) showed that a small concentration of a chlorinated wax in one of his traction fluids increased friction—or traction—and a larger concentration decreased it. Indeed, some of the authors' experiments caused traction to increase when trichloroethane was added. Because of a comment by the referee that chloride additives were known to decrease traction, for which the authors are grateful, the authors recently carried out a series of measurements in a separate but similar apparatus. They found both increases and decreases, but mostly the latter at higher concentrations.

As a result of this investigation, the following picture appears to emerge: Changes of EHD emission spectra observable with the authors' apparatus must either occur very rapidly and repetitively on every rotation of the ball or lead to an adsorbate remaining on the ball surface. An adsorbate of chloride on the ball surface or an adsorbate consisting of reaction products from a reaction catalyzed by chloride in the base fluid could very well reduce traction by changing the wetting characteristics of the surface. As a result of the referee's comment, the authors also measured traction for a 2.5-percent concentration of trichloroethane in the trac-

*Adsorption could reduce free rotation of the C=C bond.

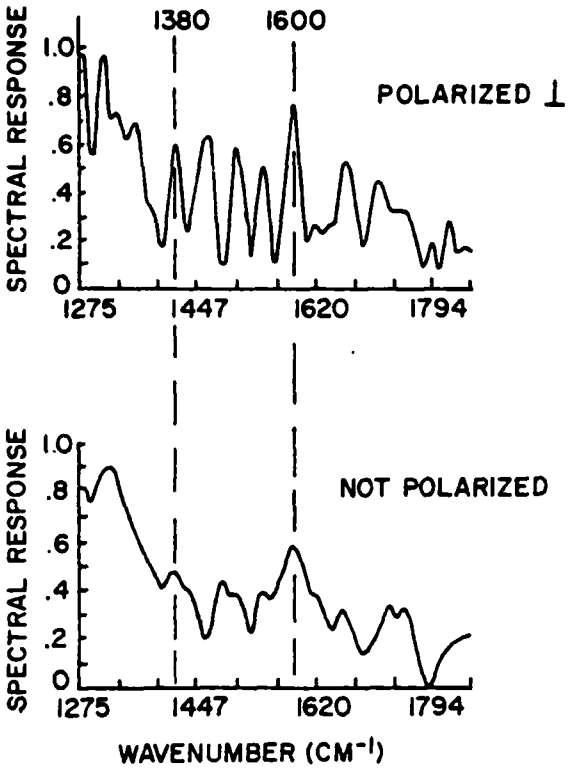

Fig. 9—EHD spectra of traction fluid under high speed and load and with a ball that had much previous use. The upper spectrum was polarized in a plane perpendicular to the conjunction plane.

tion fluid and found it much lower than for the pure traction fluid. Rounds (9) also discussed the possibility of a surface influence on traction and of a competition between a chlorinated hydrocarbon and aromatics for adsorption sites. The authors' polarized spectra seem to be consistent with the presence of adsorbed decomposition products at an early stage of failure. The difference spectra show a maximum of decomposition product peaks for an intermediate trichloroethane concentration in the fluid. Thus, while traction, on the basis of present evidence, is a bulk phenomenon, it is also influenced by the replacement of a high-energy surface (metal) with a low-energy one (of adsorbed chloride and decomposition products). The change of surface by adsorbed chloride and its interaction with aromatic hydrocarbons in particular can lead to lubrication failure.

The reason for the absence in the EHD spectra of a strong emission band due to trichloroethane even when present at relatively high concentrations, was surprising at first. Only characteristic C-Cl bands would be expected to stand out over the hydrocarbon background. The only such band in the spectral region studied is located around 750 cm^{-1}. If, as it seems likely, the C-Cl bond is adsorbed perpendicularly to the metal surface, its change of dipole moment would be mainly directed along the optic axis of the authors' instrumentation and its radiation, by the antenna anology mentioned earlier, would be largely unobservable. For this reason, adsorbed C=O could not be studied by infrared emission until Greenler (*10*) discussed a method of observation at near grazing angles. If this model is true, an increase of the numerical aperture of the authors' objective lens (Fig. 1) would result in the appearance of the C-Cl band. C-Cl contained in the bulk traction fluid of the contact zone is also likely to be oriented similarly by shear and, therefore, about equally invisible.

The absence of a trichloroethane band in the emission spectra is, therefore, consistent with the model of the contact in which the solid surface is altered by adsorption and the traction fluid is highly oriented.

ACKNOWLEDGMENTS

This research was sponsored by the Air Force Office of Scientific Research, Air Force Systems Command, USAF, under Grant No. AFOSR-78-3473 and by NASA-Lewis Research Center, under Grant No. NSG 3170. The United States Government is authorized to reproduce and distribute reprints for Governmental purposes notwithstanding any copyright notation hereon.

REFERENCES

(1) Lauer, J. L. and King, V. W., "Fourier Emission Infrared Microspectrophotometer for Surfaces Analysis—I. Application to Lubrication Problems," *Infrared Physics*, **19**, pp 395–412 (1979).

(2) Turchina, V., Sanborn, D. M. and Winer, W. O., "Temperature Measurements in Sliding Elastohydrodynamic Point Contacts," *Trans. ASME, J. Lubr. Tech., Ser. F.*, **96**, pp 464–71 (1974).

(3) Nagaraj, H. S., Sanborn, D. M. and Winer, W. O., "Direct Surface Temperature Measurements by Infrared Radiation in Elastohydrodynamic Contacts and Correlation with the Blok Flash Temperature Theory," *Wear*, **49**, pp 43–59 (1978).

(4) Bair, S. S. and Winer, W. O., "Surface Temperatures and Glassy State Investigations in Tribology," NASA Contractor Report 3162. NASA Scientific and Technical Information Branch 1979.

(5) Johnson, K. L. and Roberts, A. D., "Observations of Visco-elastic Behavior of an Elastohydrodynamic Lubricant Film," *Proc. of the Royal Soc. of London*, **337A**, pp 217–242 (1974).

(6) Avram M. and Mateescu, GH. D., *Infrared Spectroscopy*, Wiley-Interscience, New York (1972).

(7a) Klaeboe, P., "Vibrational Spectroscopic Studies of Some Trans-1,2-Dihalocyclohexanes," *Acta Chemica Scandinavica*, **25**, pp 695–711 (1972).

(7b) Lauer, J. L., and Peterkin, M. E., "Infrared Spectra of Some Dimethylcyclohexanes at very High Pressures," *Developments in Applied Spectroscopy*, **10**, pp 59–78 (1972).

(8) Eliel, E. L., Allinger, N. L., Angyal, S. J. and Morrison, G. A., *Conformational Analysis*, Wiley-Interscience, New York (1967).

(9) Rounds, F. G., "Effect of Aromatic Hydrocarbons on Friction and Surface Coating Formation with Three Additives," *ASLE Trans.*, **16**, pp 141–149 (1973).

(10) Greenler, R. G., "Infrared Study of Adsorbed Molecules on Metal Surfaces by Reflection Techniques," *J. Chem. Physics*, **44**, pp 310–315 (1966).

DISCUSSION

F. S. CLARK (Member, ASLE)
Monsanto Company
St. Louis, Missouri 63163

In this interesting paper, the authors extend their use of sophisticated spectral techniques to study fluids in an EHD contact. Their new data reveal interesting chemical changes in traction fluids in the contact and show degradative catalysis by organic chloride contamination. Our discussion focuses on the nature of these degradations and how they might occur.

We feel that the contact reactions of the fluids typify ionic rather than radical mechanisms. Radical halogenation of cycloalkanes should give haloalkanes. However, substitution under ionic catalysis and subsequent reactions (elimination, rearrangements) would produce the type of chemical changes seen. In particular, ferric chloride catalyzes such processes. For example, at 70°F it converts 1-methylcyclohexane into a partially aromatic polymer and 3-(2-methylcyclohexyl) toluene (*A1*). The methylcyclohexane serves as an excellent structural model for the traction fluids; unsaturated intermediates would account for the olefin spectra.

Likewise, arylethers would interact with ferric chloride, possibly by initial complexing of the rings or oxygen at ionic sites. One conceivable product from cleavage of the oxygen-carbon bond is tri- or tetra-substituted rings. Alternatively, ferric chloride can induce polymerization and crosslinking (increased substitution) of benzene (*A2*). Do the authors feel the catalyzed changes in the 5P4E spectrum (Fig. 6) could result from crosslinking or highly substituted aryl rings?

Two final questions: Can the authors state how long their rig would survive running on 5P4E without halide contamination? An unformulated polyphenyl ether should not easily lubricate stainless steel. Finally, what loads were used in these experiments?

REFERENCES

(*A1*) Kovacic, P., Morneweck, S. T. and Volz, H. C., "The Nature of the Methylcyclohexane — Ferric Chloride Reaction". *J. Org. Chem.*,**28** (10), pp 2551–4 (1963).

(*A2*) Kovacic, P., "Reactions of Metal Halides with Organic Compounds". Symp. on Aromatic Hydrocarbons, Div. of Petr. Chem., ACS Atlantic City, September 9–14, 1962.

DISCUSSION

BERNARD A. BALDWIN (Member, ASLE)
Phillips Petroleum Co.
Bartlesville, Oklahoma 74004

The authors are to be congratulated on a well-written paper describing experiments on the effects produced in lubricants by surface active molecules.

Couldn't the question of band shifts and GUA shown in Fig. 7 be easily resolved by serially repeating the high-speed, high-load test as a fifth experiment? If the arguments given in the text are correct, the GUA should be much lower than the original value of 0.58 and the spectrum should look more like the low-speed, high-load spectrum than the original high-speed, high-load spectrum.

It would be interesting to see a comparison of band shifts between static high-pressure experiments and the dynamic experiments performed here. Such information could aid in the interpretation and band assignment of the spectra. Probably one of the largest differences would be in the polarization which might establish whether the molecular orientation is due to surface interaction or a dynamic phenomena. Another interesting technique would be the use of perdeuterated solute to help resolve solvent and solute contributions to the emission spectra.

This discusser hopes that this paper represents a beginning of a series of experiments using this spectroscopic technique. There is considerable interest regarding the effect of dispersants, detergents, antiwear additives, and other surface active species on the lubricant and lubricating process.

DISCUSSION

ALAN BEERBOWER (Member, ASLE)
University of California
San Diego, California 92093

The authors are to be complimented on the development of a very elegant technique for probing the events in the tiny but intensive reactor called the "concentrated contact." Since these limited experiments have revealed so much, it is hoped they will proceed to explore other lubricant systems. Some questions arise;

The authors describe the base oil as a "synthetic cycloaliphatic" under MATERIALS, and give some physical properties. Matching these by calculations using previously published methods (*C1*) indicates that the structure probably is several fused rings with about three methyl groups. However, under RESULTS, they attribute the strong bands below 750 cm^{-1} to deformation modes of paraffinic side chains, and near 1140 cm^{-1} to similar modes of insoparaffinic groupings. Then, under DISCUSSION AND CONCLUSION, they describe the "standard mechanism" of pyrolysis as requiring a long saturated chain hydrocarbon. Do the authors have inside information on the presence of such side chains, or do they consider the bands to be unambiguous evidence?

The authors refer to the events which they observed as "adsoption," implying reversible physical or chemical attraction to the surface. However, it is quite evident that strong irreversible chemistry is taking place. Their comments would be appreciated on this hypothetical sequence:

1—The $CH_2Cl\text{-}CHCl_2$ is adsorbed on the metal (as a Lewis acid),

2—It reacts with iron to produce $FeCl_2$ and vinyl chloride,

3—The $FeCl_2$ acts as a catalyst to dehydrogenate naphthenes to cyclo-olefins and aromatics.

Probably the vinyl chloride would contribute to the polymer. Step 3 is analogous to the process by which most unleaded gasoline is produced, where the naphthenes are dehydrogenated using chlorinated platinum catalyst.

The authors state that 5P4E would be "particularly susceptible to such attack" as that described for long chain saturated hydrocarbons. Would they please clarify how this can be relevant, since 5P4E has no saturated atoms? Perhaps the aromatic radical anion theory published by Goldblatt (*C2*) would be more appropriate, since it accounts for the catastrophic failure noted in the final experiment.

REFERENCES

(*B1*) Beerbower, A., "Environmental Capability of Liquid Lubricants," in *Interdisciplinary Approach to Liquid Lubricant Technology*, NASA SP-318.

Superintendent of Documents, U.S. Government Printing Office, Washington, D.C. 20402. Ed. Ku. P. M., pp 365–432 (1973).
(82) Goldblatt, I. L., "A Model for the Lubrication Behavior of Polynuclear Aromatics," *I&EC Prod. Res. Dev.*, **10**, pp 270–278 (1971).

AUTHORS' CLOSURE

The authors thank the discussers for their kind and constructive comments. Since some of the questions occurred to us shortly after this paper was written, we are now in a good position to answer them. Thus we are now in basic agreement with Clark and prefer an ionic mechanism over a free radical one, the reason being our recognition of likely and unavoidable chloride contamination of the supposedly neat traction fluid. The neat fluid (specially supplied to us without the usual additive package) reacted similarly to the chloride-containing fluid, although very much more slowly. We are not sure whether our experiments were carried out as anhydrously as those of Kovacic et al, to which Clark referred. Perhaps the continuous operation on the same recirculating fluid would itself lead to a removal of possible traces of moisture. Our loads corresponded to 400 to 600 MPa average Hertzian pressures.

We should have mentioned in our paper that we have been running infrared spectra on similar materials in a high-pressure diamond anvil cell under static conditions similar to those encountered in our ball/plate apparatus under dynamic conditions. Under static conditions pressure increases will shift most of the bands towards higher frequencies but temperature increases shift them toward lower frequencies. However, temperature effects generally outweigh pressure effects. The other comments by Baldwin are also well taken and we intend to follow up on them. One of the main reasons the experiments suggested by Baldwin were not carried out are the long times required for every experiment and the even longer preparation times. The expected availability of a second interferometer should accelerate our progress in the near future and make it possible to explore Baldwin's suggestions.

Beerbower is correct; we should attribute infrared bands to naphthenic rings and side chains which have similar resonances. The slip occurred because of similar work on paraffins carried out at the time this paper was written. The remainder of his comments are similar to Clark's. Yes, we agree that the aromatic radical anion theory of Goldblatt is a likely explanation.

Our work is continuing and we hope to be able to report results on other lubricant systems in the not too distant future.

APPENDIX B

Alignment of Fluid Molecules in an EHD Contact

PREPRINT NO. 81-LC-5C-1
ASLE PREPRINT

Alignment of Fluid Molecules in an EHD Contact

JAMES L. LAUER, LEONHARD E. KELLER, FRANK H. CHOI, and VINCENT W. KING
Rensselaer Polytechnic Institute
Troy, New York 12181

Dichroic infrared emission spectra have been obtained from an operating elastohydrodynamic contact under conditions showing unequivocally that the molecules of the fluid are aligned under shear flow in the bulk of the fluid and that the extent of the alignment is increased by the presence of an additive in a small concentration. This work applied particularly to polyphenyl ether and to 1,1,2-trichloroethane as the additive, but similar results have been obtained with polycyclohexyls and the same additive. The observation of two separate glass transitions for the polycyclohexyl solution is an indication of the occurrence of a phase separation in the Hertzian inlet zone. A model has been developed to explain the effect of these phenomena and their relation to traction.

INTRODUCTION

The state of the lubricant in an elastohydrodynamic (EHD) contact is still largely unknown and a subject of active research. Is the lubricant a liquid or a glass or a composite of both? What is the special property of torque-transmitting (traction) fluids? Winer (*1*) modeled them as glasses of relatively high yield stress in the Hertzian contact region. He measured these yield stresses in separate experiments and calculated the observed traction coefficients from them—a remarkable achievement. However, he did not attempt to correlate the chemical structure and physical properties of these fluids with their behavior in concentrated contacts. Our own work has shown an almost exact linear relationship between traction coefficient and traction fluid concentration for traction fluid/ester lubricant solutions, yet very sharp decreases of traction for only small concentrations of some additives such as organic chlorides. A large effect by small concentrations of additives would seem to require a mechanism by which these additives are concentrated in the contact region. Adsorption on the bounding surfaces would provide such a mechanism. On the other hand, effects proportional to concentration would seem to be bulk effects. Polyphenyl ether also has torque-transmitting properties and has been studied by many investigators because of its very high temperature stability. This fluid has been variously described as viscoelastic, plastic, as well as glassy.

The behavior of polar additives in lubricants used in the region of boundary lubrication has been generally accounted for by surface adsorption in the Hardy and Bowden-Tabor theories. Similar adsorptive behavior would be expected to prevail under EHD lubrication as well. However, Okabe and Kanno (*2*) were able to show that the adsorption theories for boundary lubrication were oversimplified, for wear prevention continued to improve for solutions of squalane containing polar additives as the additives' concentrations were increased well beyond those required for the formation of monomolecular layers or even a few layers. Furthermore, wear prevention did not correspond to measures of the adsorptivity of the polar groups so that a mysterious "structural property" acquired by the bulk lubricant as a result of the presence of the additives had to be invoked. The modifications described by Rounds (*3*) of the so-called susceptibility toward additives, which was found to result from the presence of certain other additives in particular fluids, are another example of the failure of accounting for concentrations of minor constituents in contacts solely by adsorption on the metal surfaces.

While our Fourier emission microspectrophotometer (*4*) has been shown to be capable of the extremely high sensitivity required for analysis of EHD contact regions, it can hardly be used to analyze a few molecular layers of lubricant additives on surfaces in the presence of bulk fluid. Even the addition of the differential polarization adapter described in this paper proved inadequate for this task. Yet, together with glass transition measurements, it did help us find a bulk fluid effect in the contact region, which would seem to go a long way toward explaining the "mysterious structural property" acquired by the bulk fluid as a result of the presence of additives. Namely, the additives help change the orientation of the bulk fluid molecules, which is produced by the high shear rates prevailing in EHD contacts.

Presented as an American Society of Lubrication Engineers paper at the ASLE/ASME Lubrication Conference in New Orleans, Louisiana, October 5–7, 1981

They may do that by initiating separation under the high contact pressures and cause two-phase shear flow in the contact. The hydrodynamics of the situation would also seem capable of providing an additional mechanism to account for an accumulation of additive in the contact region.

This work has led us to a new model for EHD and boundary lubrication in the presence of polar additives, which includes bulk, i.e. not only boundary surface effects. As a valuable by-product, this work has provided us not only with means of analyzing very thin EHD films in operating bearings but also with means of analyzing very thin organic layers on various surfaces, deposits on heat exchanger tubes, for example. Our new model is also consistent with the observation of drastic reductions of traction coefficients by small concentrations of polar additives.

EXPERIMENTAL

Differential Polarization Infrared Emission Fourier Microspectrophotometer for EHD Contact Spectroscopy

The basic setup of our Michelson interferometer, which we modified from a far infrared absorption instrument to an emission instrument for the 4000 to 50 cm^{-1} wavenumber region, was published before (*4*). However, the emission attachment used to collect the radiation generated in an operating ball/diamond plate sliding EHD contact and passed through the diamond window was substantially modified and requires a brief discussion. Figure 1 shows a schematic diagram of this apparatus. The ball/plate contact is located at the bottom of a cup containing the fluid under study. The (0.057-m diameter) ball is rotated in this cup by a shaft located in a horizontal plane, but since the ball's contact above the diamond is kept constant, the motion is 100 percent sliding under fully flooded conditions. The bulk temperature is kept constant by a coil of tubing through which thermostatted water is circulated. Measures of the temperature at the diamond window and of the fluid in the cup are detected by thermocouples. The infrared radiation produced as a result of the viscous friction in the lubricant is captured by a lens, consisting entirely of reflecting elements. Originally, this lens was of 15× magnification with a numerical aperture of 0.28 and a working distance of 22 mm. The field of view of that lens was of 1.25-mm diameter, thus covering more than the Hertzian area even under our heaviest loads. By replacing this lens by one of 36× (numerical aperture 0.5, but working distance only 8 mm) a substantial gain of radiation-gathering power was achieved (effectively a factor of three) even though—or because of—the diameter of the field of view was reduced to 0.5 mm. The reason is that the temperature in the Hertzian area is not constant, but rapidly varying. Accordingly, the lens with the smaller field of view can be aimed at a portion of the Hertzian region, which radiates more intensely. The smaller working distance of this lens and its smaller depth of field required some mechanical modifications, which were not difficult to accomplish.

The principal change of the optical instrumentation centers around the optional substitution of the radiation chopper by a polarizing disk rotating about the optic axis immediately below the lens. The disk consists of a plate of infrared-transparent TlBr + TlI (KRS − 5) on which parallel bands of aluminum, 0.4 μm apart, were vapor deposited. The disk is driven at constant speed by a stepping motor and a belt/pulley transmission, the angular speed being half that of the chopper frequency. At every quarter turn, therefore, the radiation transmitted by the polarizing disk is alternatingly polarized parallel and perpendicular to the (vertical) reference plane, which may be coincident with the Hertzian conjunction plane (the vertical plane containing the ball/plate conjunction line and the midpoint of the bearing ball) or make an angle φ with it. The angular position of the polarizing disk with respect to the reference plane is determined by a lamp/photocell pickup above a disk attached to the pulley, which is painted with white and black sectors. The angular position of the pickup pointing to these sectors naturally determines the reference plane. The signal from this pickup—or the corresponding reference signal from the tuning fork chopper—provides the reference for the lock-in amplifier so that only differential signals are amplified and recorded.

For example, under Mode 1 operation [Fig. 1(a)], the polarizer is removed and the differential signal $(I - I_b)$ corresponds to the difference of intensity of EHD and standard blackbody radiation, which is alternatingly reflected into the interferometer by the chopper tines. Under Mode 2 operation [Fig. 1(b)], the chopper is removed and the differential signal is the difference of intensities between radiations polarized parallel and perpendicular to the reference plane. This mode of operation provides dichroic spectra. Mode 3 operation is the same as Mode 1 operation except that the polarizer is inserted into the optical path, but without rotation. The orientation of the polarizer can be set to any angle with respect to the reference—or the Hertzian conjunction—plane. In this case, the preferred way is to set the polarization plane parallel or perpendicular to the Hertzian conjunction plane.

Mode 2 operation provides the maximum sensitivity since randomly polarized blackbody or greybody radiation is eliminated. It also provides unequivocal proof of polarization or alignment of the dipolar transition moment causing the observed infrared emission bands and, conversely, permits determination of the orientation of the molecular species of the sample from which these bands originate. In the particular instance of EHD contact radiation, these species must be contained in the bulk fluid since the sensitivity of the method has, so far, not extended to less than about 30 molecular layers. This statement applies to the EHD inlet temperatures of 40° of this paper; the sensitivity at higher temperatures is likely to be better so that fewer molecular layers could be analyzed. Mode 2 operation is limited to polarized bands, i.e. not to the combination frequencies ascribable to a number of transition moments of multitudinous orientations. Since our Mode 2 spectra are dichroic spectra—representing differences of emission intensities polarized parallel and perpendicular to the reference plane—series of spectra are required for interpretation, as will be shown.

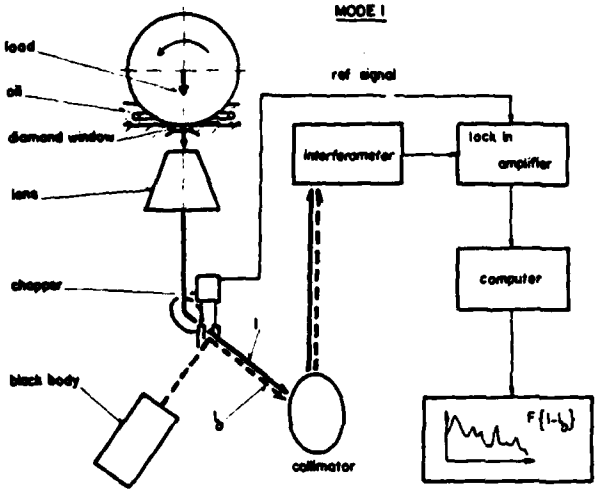

a) NO POLARIZER

(a) Mode 1, no polarizer, blackbody radiation referenced to sample radiation by reflection off chopper blades.

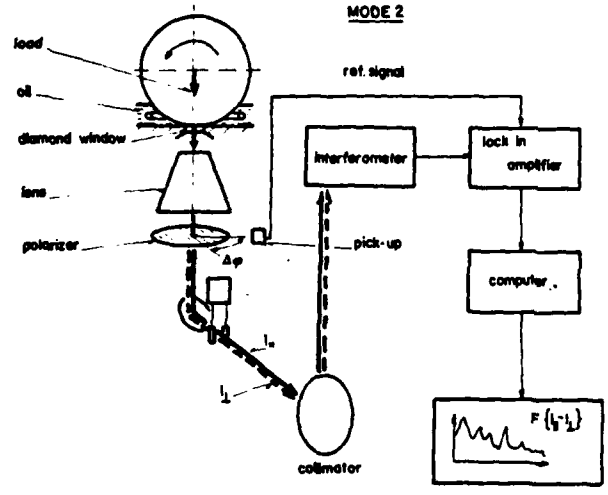

b) ROTATING POLARIZER

(b) Mode 2, rotating polarizer, *mutually perpendicular* planes of polarization referenced against each other, chopper kept open.

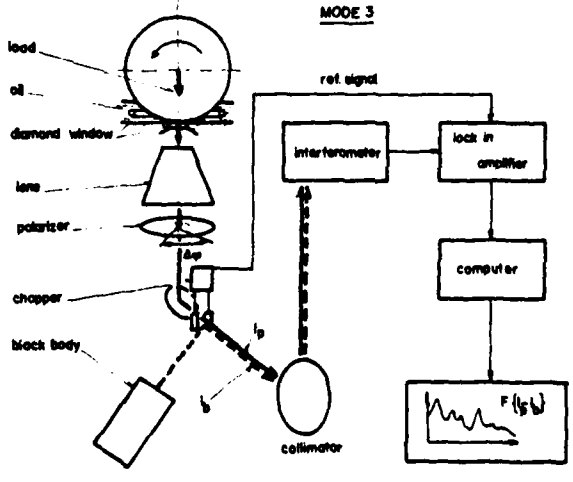

c) STATIONARY POLARIZER

(c) Mode 3, polarizer kept in one position, blackbody radiation referenced to *polarized* sample radiation by reflection off chopper blades.

Fig. 1—Emission spectra recording attachment

Mode 3 operation [Fig. 1(c)], i.e. spectroscopy of radiation polarized in one particular plane and referenced to a stationary blackbody, provides spectra that are more easily interpreted than those of Mode 2, *but requires* at least twice as many experiments for the determination of dichroism and is less sensitive.

The blackbody shown in Fig. 1 is also an advance over our earlier work. It provides an intense output that is highly directional and can be rather quickly varied in terms of both blackbody temperature and magnitude of infrared flux.

Both the details of the three modes of operation and the construction and performance of the instrumental parts will be the subject of a publication in an appropriate journal.

Traction and Film Thickness Measurements

The traction and film thickness measurements relating to our sliding contact, of which those shown in Fig. 2 and 3 are examples, were obtained with the apparatus outlined in Fig. 4. It is similar to those described by Cameron, Winer, and other authors, as it consists of a rotating ball forming a sliding contact with a sapphire window on its upper surface, thus also allowing for convenient EHD film thickness measurements by microscopic observation of Newton rings-type optical interference. In our particular design, the sapphire window is five cm in diameter and twelve mm thick, both to allow easy access to the microscope objective and for heavily loaded contacts. The plate holding the window easily slides on linear bearings whose friction is insignificant compared to that of the EHD contact. The friction at the contact is determined with a strain gauge on the connection between the window plate and the loading platform. The straight lines drawn in Figs. 2 and 3 are the best curves

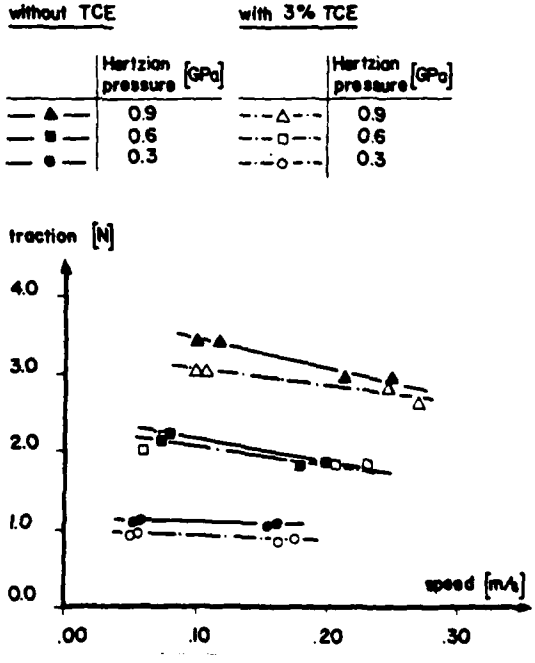

Fig. 2—Force of traction for a polycyclohexyl (traction) fluid with and without trichloroethane (TCE) additive at different average Hertzian pressures as a function of sliding speed.

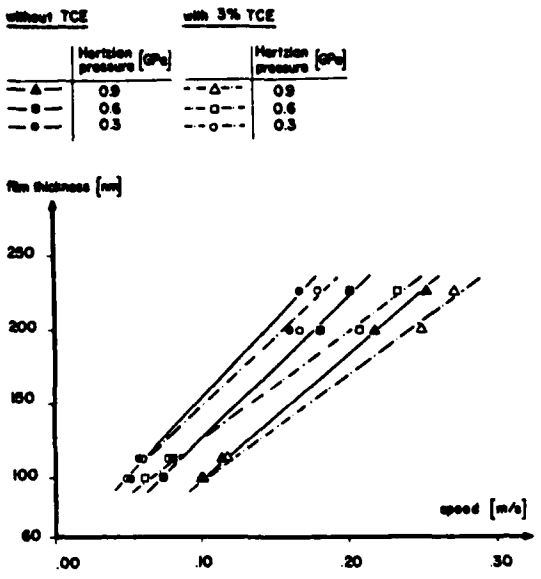

Fig. 3—Hertzian contact separations obtained for a polycyclohexyl (traction) fluid with and without trichloroethane (TCE) additive at different average Hertzian pressures as a function of sliding speed.

representing our data. Data are lacking for low speeds because of experimental limitations.

Since the contact in this apparatus is not identical with that used in the spectrometer—the fluid must be carried up by the ball's rotation, sapphire has different physical properties than diamond—the results are not expected to be identical with the diamond contact. However, we believe them to be sufficiently similar to provide us with relative measurements.

Again the detaiis of this instrumentation will be described elsewhere..

Fluids

Most of the work described here was carried out with polyphenyl ether having the same properties as the fluid used in our earlier investigations and those of other authors, such as Hirst and Moore (5). Measurements were also carried out with a polycyclohexyl traction fluid. The spectral results with the latter turned out to be similar but are not reported here because the latter spectra are much less intense and more difficult to interpret. Polyphenyl ether, being solely aromatic and ether, provides excellent infrared spectra and is a rather pure chemical. It is still a mixture of many isomers, but many of the spectral bands can be assigned to the same transition moments. There are relatively few bands, many of them representing fundamental normal modes of vibration.

The additive used in many of the experiments was 1,1,2-trichloroethane separated from commercial trichloroethane by simple fractional distillation. Its infrared absorption spectrum showed no extraneous features. It was selected because of its relatively high boiling point (115°C), ready availability, and well understood molecular structure as well as because of its similarity to chlorinated solvents and to the chlorides contained in commercial tetraethyl lead, which are frequent contaminants of lubricating oils. In other words, it is a fluid pertinent to field applications, yet well suited to scientific investigations. In the latter respect, it has no strong bands of its own in the spectral region (630-1230 cm^{-1}) of this investigation. Hence, the spectra shown are not altered by its presence or absence, merely as a consequency of mixture. Its strong bands, strong enough to allow detection in concentrations of 1 percent and less, are below 600 cm^{-1} where polyphenyl ether has essentially no infrared modes. Work in that region of the emission presents some difficulty—not an insurmountable one—and will be undertaken at a later date to provide additional confirmation of some of this paper's conclusions.

RESULTS

Figure 5 shows typical EHD emission spectra obtained with the present apparatus. The Mode 1 operation spectrum shows the key bands at 680, 765, 965, and 1180 cm^{-1} representing different fundamental modes of vibration within the polyphenyl ether molecule. The linear sliding speed was 0.6 m/s and the average hertzian pressure about 1.2 GPa. When the chloride was present, the relative band intensities [Fig. 5(b)] changed even though the operating conditions remained the same. Most noticeably, the 680 cm^{-1} band is less intense than the 1180 cm^{-1} band when the chloride is absent [Fig. 5(a)], but stronger when it is present [Fig. 5(b)]. While the average contact surface temperature was basically the same for chloride present and absent, the average EHD film temperature with the chloride present was somewhat lower (estimated at 110°C versus 115°C). This difference would not account for the spectral differences, however. The main reason for the spectral differences is the different molecular orientation—polarization of the bands—produced by the presence and absence of the chloride. Even though no polarizer was used in Mode 1 operation, the emission bands are still influenced by orientation of the transition moment; a transition moment vibrating exactly in the direction of observation cannot give rise to electromagnetic radiation, such as infrared, observable in this direction. The relative intensities of the 680 and

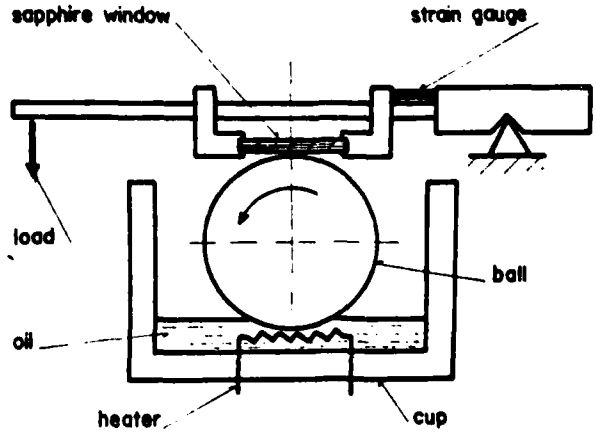

Fig. 4—Apparatus for measuring traction and film thickness

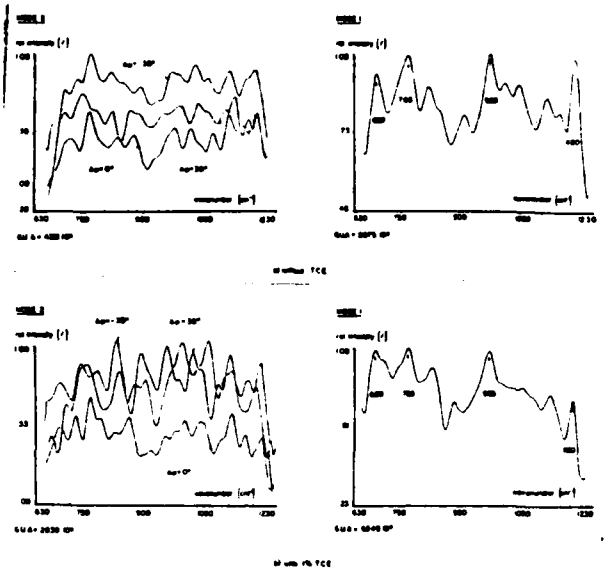

Fig. 5—Infrared emission spectra of polyphenyl ether from an operating EHD contact for both Mode 1 (referenced to a blackbody) and Mode 2 (representing differences between the spectra of mutually perpendicular *planes of polarization*)

The sliding speeds were 0.6 m/s and the average Hertzian pressures 1.2 GPa. The GUA's (greatest unnormalized amplitudes) are relative overall spectral intensities. The Mode 2 spectra are shown for the phase angles (Δφ) shown; they are all on the same scale. Spectral bands referred to in the text are marked by arrows.

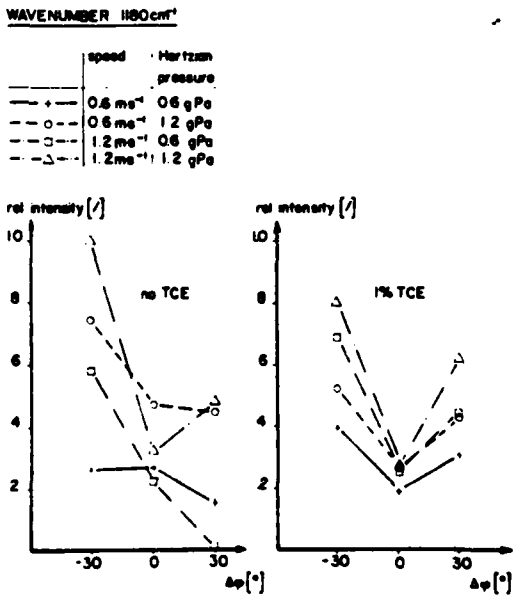

Fig. 6—Dependence of the 1180 cm^{-1} infrared emission band intensity of polyphenyl ether on the phase angle (angle between the Hertzian conjunction plane and the reference plane) with and without trichloroethane (TCE) additive.

765 cm^{-1} bands are particularly sensitive to this effect, since the latter band, representing an out-of-the-phenyl-ring-plane vibration should become unobservable to us when the ring is oriented parallel to the diamond window. It would seem that the presence of chloride is conducive to this orientation (all the spectra are plotted "normalized" so as to fill the ordinate scale available. However, relative band intensities are significant, of course). The reduction of the relative intensity of the 765 cm^{-1} band by pressure and shear was referred to in an earlier publication (*6*).

The mode 2 spectra of Fig. 5 were obtained for three different phase angles φ; i.e., angles between the reference plane and the Hertzian conjunction plane. Since they are a difference spectra—dichroic spectra representing the difference between infrared emissions polarized parallel and perpendicular to the reference plane—they contain rather sharp bands which can point up or down and can only be interpreted by comparison of series of spectra. The very fact that Mode 2 spectra could be recorded from operating contacts is proof of flow polarization and, hence, molecular orientation produced by shear flow. The velocity gradient in the EHD contact helps orient the lubricant molecules along preferred directions. Stationary liquid samples gave no Mode 2 spectra; the difference between the infrared radiation intensities polarized in two mutually perpendicular planes did not depend significantly on frequency. (A small Mode 2 signal, which is nearly independent of frequency, is attributed to apparatus error). In other words, under shear flow, the lubricant molecules are oriented in the plane parallel to the diamond window with respect to the flow direction as well (i.e., in addition to being restricted to motion in this plane as described in the preceding paragraph). The variation of band intensity with phase angle allows deduction of the degree of alignment by the velocity gradient in the EHD contact. Clearly, the presence or absence of the chloride—*one percent only*—has a drastic effect on the degree of orientation.

This effect is more clearly seen by the schematic lines of Fig. 6 for the 1180 cm^{-1} band of polyphenyl ether. Please note that these figures can be compared only relatively—only three experiments were run with and without the chloride (it takes about an hour under fully constant operating conditions to obtain one spectrum). However, there can be no question that the fluid is more shear flow-aligned in the presence of chloride than without, for then the connecting lines are more V-shaped already under less intense operating conditions. Without chloride, only the most drastic operating condition produced the V-shaped intensity plot observed with chloride; with chloride, all of the intensities follow a V-pattern.

The V-pattern is largely a result of the lack of more data points; i.e., more variation in the angle between the (arbitrary) reference plane and the conjunction plane. Many more points were, therefore, obtained for a few selected operating conditions. The plots of Fig. 7 represent such a study. Note that different spectral bands—corresponding to differently directed transition moments—have maxima and minima at different angles, just as expected. Indeed, the precise direction of the molecules as a whole and the proportion so oriented can be calculated from these data—and is in progress. These data were, furthermore, obtained with a titanium nitride-coated bearing ball substituted for the usual uncoated (440C) stainless steel ball. This thin coating made the ball surface about 50 percent harder. (The coating was done in H. Hinterman's Laboratoire Suisse de Recherches Horlogeres at Neuchatel, Switzerland.) There is no apparent difference be-

tween the spectra with and without chloride for coated and uncoated balls! This observation already constitutes a good indication that the polar chloride additive has a bulk, as well as a surface, effect. Very likely, there is a surface effect, however our spectral measurements are not sensitive enough to pick up thin surface layers but are sensitive enough to see differences in the bulk fluid. X-ray surface analysis in conjunction with scanning electron microscopy has shown the presence of adsorbed chloride with both coated and uncoated balls, perhaps more on stainless steel balls (no quantitative analysis has been made). Tractions with titanium nitride-coated balls were not different from tractions with uncoated steel balls.

To show the geometrical relationships more clearly, Fig. 8 has been included. The optical axis of our instrumentation is along the X-direction. The shear plane, or conjunction plane, which is vertical in our experiments, is the X/Y plane. An arbitrary orientation of the transition moment giving rise to an infrared emission band is shown. In general, it would be inclined with respect to the major molecular axis by the angle α as shown. Angle θ and φ represent colatitude and longitude in the usual way.

The model of Fig. 8 has been used to show that the intrinsic molecular dichroism—measured by the angle α—is separable from the flow dichroism under these geometrical conditions (*8*). Since we do observe changes of our dichroic spectra with shear rates, flow dichroism must exist and, furthermore, be affected by the one percent (or less on occasion) of chloride present in the lubricant.

Figure 9 shows glass transitions for the polycyclohexyl (traction) fluid and for a 1 percent solution of trichloroethane in it, which were obtained by differential thermal analysis (DTA). The assumption of a correspondence of temperature decrease with pressure increase is commonly made. The changes in slope of the heat capacity/temperature plots indicate glass transitions. The absolute values of the transitions are less important to us here than the fact that the presence of chloride produced a second glass transition, even though the solution at room temperature was perfectly clear. Somewhere along the line, a phase separation occurred on cooling. When a similar solution was pressurized to very high pressures (up to

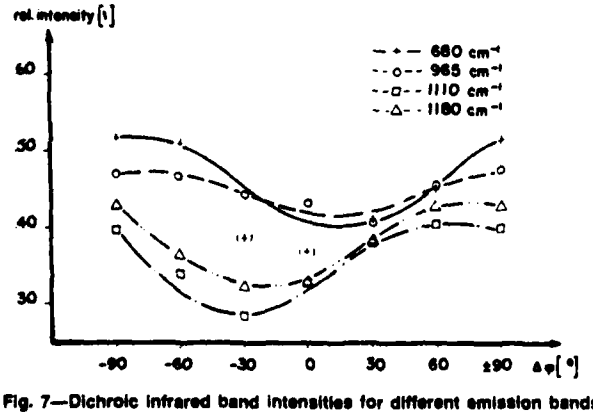

Fig. 7—Dichroic infrared band intensities for different emission bands of polyphenyl ether at different phase angles (angles of the reference plane with the conjunction plane). The sliding speed was 0.6 m/s, the average Hertzian pressure 0.6 GPa. A TiN-coated bearing ball was used.

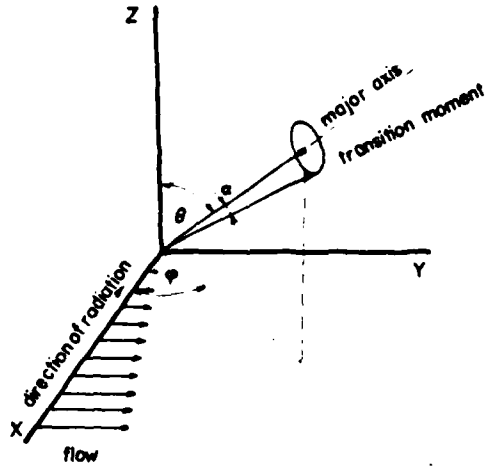

Fig. 8—Coordinate system showing relations for orientation of molecules by shear in a lubricating contact.

12 kbar) in a diamond anvil cell, phase separation (a spider net pattern) was observed to come into focus suddenly under the phase contrast (polarization) microscope. While these experiments were conducted under low shear—or no shear—conditions, there is every reason to believe that the same phenomenon would occur under shear and, theoretically, it would be even more drastic. In other words, it is very likely that the chloride additive—and we made similar observations with lauric acid and other commonly used boundary additives—helps produce a two-phase or multi-phase system (liquid/liquid or liquid/solid) under Hertzian contact pressures.

Analogous phenomena were observed with other materials, such as those used by Rounds (*3*).

DISCUSSION

Already Rounds (*3*) had observed that the addition of small amounts of chlorinated hydrocarbons to polycyclohexyl derivatives (analogous to those used in traction fluids) could reduce traction substantially. Our own measurements (Fig. 2) certainly confirmed these results. He ascribed these results to a surface coating, however. Yes, we, too, noted a chloride layer on our stainless steel ball. However, we also noted similar results when the titanium-nitride coated ball was used and less chloride was adsorbed. Okabe and Kanno (*2*) also came away questioning the surface layer hypothesis. The question remains, of course: if adsorption is not the sole mechanism of additive concentration in the contact region, then what is? A concentration effect must be assumed to account for the unproportionally large influence of small additive concentrations. Furthermore, our present work definitely shows a strong influence of the additive on the flow properties of the bulk lubricant through the Hertzian gap. The fluid molecules are oriented and oriented more easily when the additive is present.

We believe the model of Fig. 10 is consistent with the observations. Additive materials accumulate in the inlet region of the Hertzian contact as another phase is formed under the positive pressure gradient. The flow lines have been shown even to reverse direction at the inlet. The con-

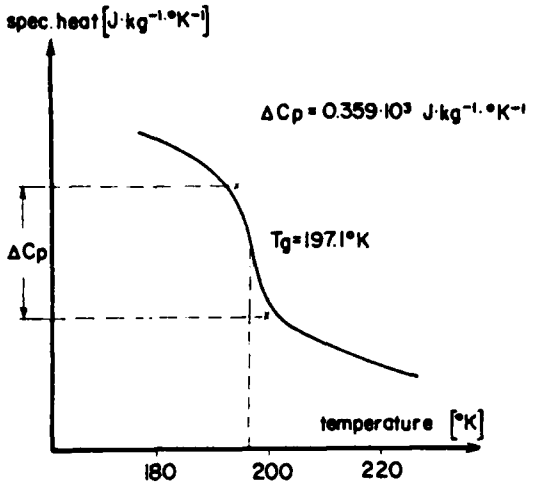

(a) no additive

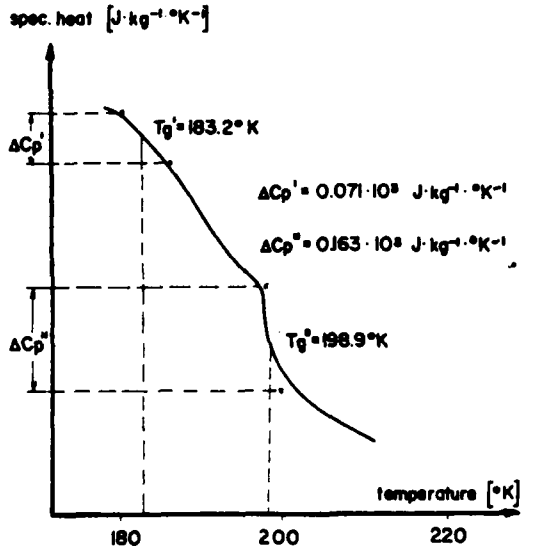

(b) with 3% of trichloroethane (TCE)

Fig. 9—Differential thermal analysis showing glass transitions of polycyclohexyl traction fluid.

ditions in the inlet region determine, as is well known, the film thickness and other properties of the following Hertzian contact region. An appreciable number of additive "blobs" travel through the region in a two-phase flow. This model is consistent with Winer's view of traction in terms of limiting strength of the lubricant, considered as a glass in the Hertzian region. The pressure of the globules or blobs weakens this strength, especially when the material there has become glassy. The idea is similar to the resulting weakening of steel by substantial inclusions of undissolved particles. Hence, the friction, or traction, of a fluid can be substantially reduced by small amounts of impurities or additives and the effect can be independent of the nature of the surfaces.

We do not believe the orientation of the bulk fluid is

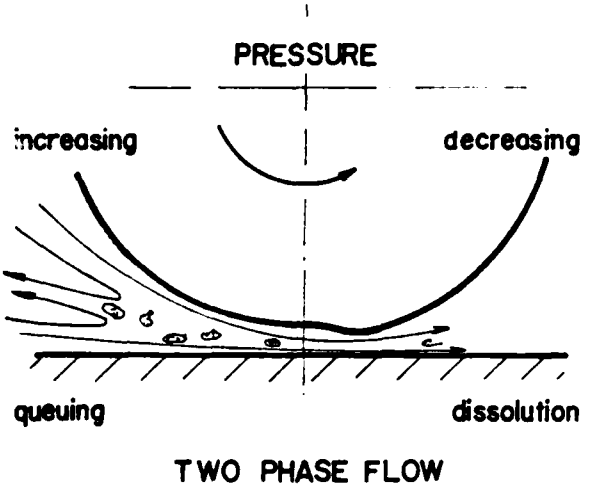

Fig. 10—Model to explain the influence of trichloroethane (TCE) additive on flow dichroism.

produced by "nematic slipping," as conceived by Larsen and Perry (*8*). These authors assumed that adsorbed molecules had a directing effect on the bulk fluid. The explanation could not account for similar results with different surfaces.

The two phases we conceive of originating in the Hertzian inlet region could be liquid/solid as well as liquid/liquid. For example, the traction fluid could be forced into the glassy state under the pressure gradient. As glass particles come out of the liquid phase, the chloride additive would concentrate in the liquid phase, thereby increasing the pressure necessary to solidify the remaining liquid more and more. Since the shear strength of the liquid is less than that of the glass, the traction is reduced. Since the net flow rate of the lubricant under shear is thereby increased, infrared flow polarization is enhanced. Since the lubricant is thus effectively less viscous in the presence of chloride, the Hertzian film thickness is reduced as was observed (Fig. 4). The lower traction also produced a lower film temperature.

This picture is consistent with two observed glass transitions, one for the essentially pure liquid and another for the concentrated solution. However, a change is also conceivable where the glass transition is pushed up to higher and higher pressures. With some fluids, it is possible that the critical pressures are then exceeded and density fluctuation produced. These would not allow the recording of good spectra.

FURTHER WORK IN PROGRESS

Other fluids and additives are under investigation. In some instances, the phase separation has led to increased—rather than decreased traction. An effort is being made to confirm the postulated increased chloride concentration in the inlet zone by our infrared emission microspectrophotometer. Different surface coatings are also being studied.

This is an ongoing investigation. It remains to be seen how general a picture can be drawn.

ACKNOWLEDGMENTS

This research was sponsored by the Air Force Office of

Scientific Research, Air Force Systems Command, USAF, under Grant No. AFOSR-78-3473, and by NASA-Lewis Research Center, under Grant No. NSG-3170.

We also wish to thank SKF-Switzerland for granting us the bearing balls and to H. Hinterman of Laboratoire Suisse de Recherches Horlogères for coating some of them.

We are most grateful to the duPont Company and to Messrs. Brame and McEvoy for the grant of an RIIC-FS-720 Fourier Spectrophotometer.

REFERENCES

(1) Bair, S. S. and Winer, W. O., "Surface Temperatures and Glassy State Investigations in Tribology," Part IV, NASA Contractor Report 3368 on Grant NSG-3106, January 1981.

(2) Okabe, H. and Kanno, T., "Behavior of Polar Compounds in Lubricating Oil Films," ASLE Preprint No. 80-LC-7A-4, presented at the ASME-ASLE Lubrication Conference in San Francisco, CA, August 19–21, 1980.

(3) Rounds, F. G., "Effect of Aromatic Hydrocarbons on Friction and Surface Coating Formation with Three Additives," *ASLE Trans.*, **16**, pp 141–149 (1973).

(4) Lauer, J. L. and King, V. W., "Fourier Emission Infrared Microspectrophotometer for Surface Analysis—I. Application to Lubrication Problems," *Infrared Physics*, **19**, pp 395–412 (1979).

(5) Hirst, W. and Moore, A. J., "The Elastohydrodynamic Behavior of Polyphenyl Ether," *Proc. Royal Soc. London*, **A 344**, pp 403–426 (1975).

(6) King, V. W. and Lauer, J. L., "Temperature Gradients through EHD Films and Molecular Alignment Evidenced by Infrared Spectroscopy," *ASME Trans., J. of Lubr. Tech.*, **103**, pp 65–73 (1981).

(7) Wada, A., "Dichroic Spectra of Biopolymers Oriented by Flow," *Applied Spectroscopy Reviews*, **6**(1), pp 1–30 (1972).

APPENDIX C

Temperature Gradients Through EHD Films and Molecular Alignment Evidenced by Infrared Spectroscopy

Reprinted from January 1981, Vol. 103, Journal of Lubrication Technology

Temperature Gradients Through EHD Films and Molecular Alignment Evidenced By Infrared Spectroscopy

V. W. King

J. L. Lauer[1]

Department of Mechanical Engineering, Aeronautical Engineering & Mechanics, Rensselaer Polytechnic Institute, Troy, N. Y. 12181

Partial and complete emission band reversals have been observed in the infrared emission spectra from portions of operating sliding contacts. An elementary analysis has been carried out to show that partial reversals are due to temperature gradients in the fluid film – the film acts both as a radiation-emitter and absorber, and that total reversals – an emission spectrum appears as an absorption spectrum – are likely to be due to a continuum source, such as hot solid asperities. The total energy radiated under the latter conditions exceeds that under the others. A decrease in gap width with increased load was accompanied by a dramatic spectral change in the case of 5P4E polyphenyl ether, which is indicative of molecular alignment.

Introduction

The temperature of the thin films of lubricant in operating elastohydrodynamic (ehd) bearing contacts has been the object of a number of recent studies, notably by Crook [1], Winer and coworkers [2], and by ourselves [3]. In all these investigations a uniform temperature was assumed across the conjunction region and the lateral temperature distribution – along and across the conjunction line in a ball/plate contact for example – was explored. A uniform temperature across the film appeared to be reasonable because of (i) the very small thickness (0.05 to 1.0 μm, in general) and (ii) the very high linear fluid velocity ($\sim$1 m/s). Most of the heat generated in the contact region by viscous friction in the lubricant would therefore be carried away by convection, while thermal conduction across the lubricant/bearing surface boundaries would play only a minor role.[2] Nevertheless thermal conduction across the boundaries was considered mainly responsible for the increased temperature of the solid surfaces in operating contacts, which could be determined directly by radiation pyrometry. Other possible mechanisms for surface heatings, e.g., elastic deformation and asperity contacts, have been considered – the former was found to have only negligible effect and the latter was thought to be effective primarily when scuffing occurred – but regarded secondary to thermal conduction from the lubricant.

The infrared emission microspectrophotometer, described in an earlier publication [4] was thought to be a logical tool for finding temperature gradients in ehd films since, as will be shown here, reabsorption of thermal emission can occur only when the radiation emitted from a hot source passes a cooler – absorbing – medium. With this instrument the infrared radiation generated in a ball/transparent plate contact and transmitted through the plate (diamond or sapphire flat) was analyzed spectroscopically over a wide frequency region. In contrast to radiation pyrometers, which record the entire thermal flux transmitted, the spectrophotometer permits an examination of infrared band shapes. If some peaks of emission bands are re-absorbed, different lubricant layers must act as radiation emitters and as radiation absorbers; if entire emission spectra appear as absorption spectra, hot asperity contact regions would appear to be the primary heat sources.

To make these measurements possible, the sensitivity of our instrumentation had to be improved. Both types of behavior were found under different operating conditions.

The procedures used in this study will be described and the results discussed for their impact on performance problems.

Apparatus

(i) Spectrometer-Interferometer. Since the main elements of our apparatus were described in earlier publications [3, 4], it will suffice to say that ours is one of the most sensitive instruments available for emission spectroscopy today. However, even more important than sensitivity is discrimination against radiation sources other than the lubricant film, i.e., primarily blackbody radiation from hot boundaries. Phase-locked amplification, digitization of the signal, and mathematical processing in a dedicated minicomputer achieve these goals.

(ii) Emission Optics. Since our objective is the detection of very weak infrared radiation emitted from small areas (Hertzian contacts or parts thereof), the method of in-

Contributed by the Lubrication Division of THE AMERICAN SOCIETY OF MECHANICAL ENGINEERS and presented at the Century 2 ASME-ASLE International Lubrication Conference, San Francisco, Calif., August 18-21, 1980. Manuscript received by the Lubrication Division, February 21, 1980. Paper No. 80-C2/Lub-12.

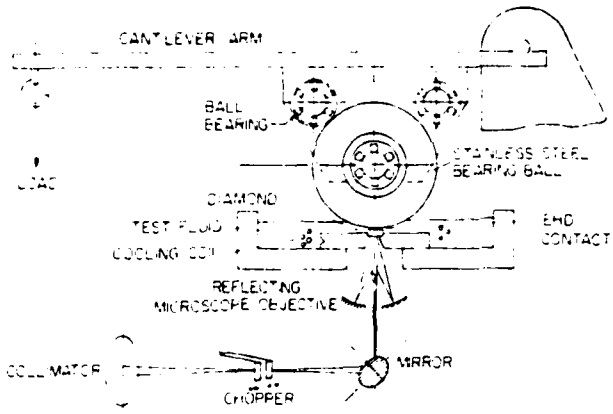

Fig. 1 Mockup bearing assembly

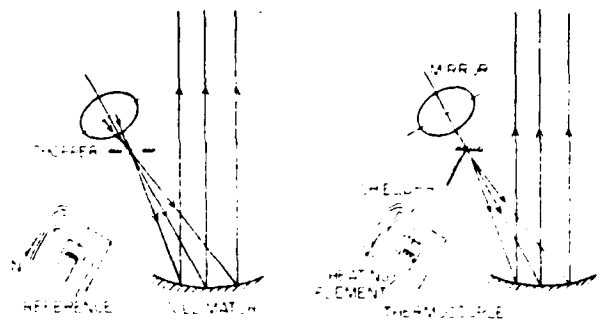

Fig. 2 Chopper and reference assembly

troducing the radiation into the interferometer optics has required careful design and has undergone a number of modifications. Figure 1 shows our present design. The lubricant layer under examination is at the conjunction of the large bearing ball (typically of 0.0286 m diameter) and a diamond window (4 mm diameter). A sliding contact is formed when the ball is rotated by a flexible shaft about an axis perpendicular to the plane of the figure. The electric motor driving the ball is mounted on a table isolated from the optics and the bearing contact. Our present – much improved – results and considerably wider spectral range – are attributable to the almost complete mechanical isolation of the optical instrumentation by an air-floated stone table. The flexible motor-to-ball shaft is the only connection between the optics and the rest of the room; careful tuning of this shaft by clamping it along its length – in the way a cello string is tuned – makes it possible to prevent all the vibrations of interfering frequencies from passing through.

A collecting – all reflecting elements – lens directs the source radiation downward to a 45 deg planar mirror, which brings it into the horizontal plane of incidence of the Michelson interferometer. An enlarged image of the source is formed a short distance downstream of this mirror. This image is in the focal plane of the collimator and constitutes the effective source for the detector. Another image is formed just ahead of the detector, where an iris diaphragm is used to select portions of the contact region for analysis. For most of this work about three-quarters of the central portion of the Hertzian contact area were analyzed.

The radiation from the lubricant layer is invariable superimposed on a background of continuous greybody or blackbody radiation, whose magnitude can exceed that of the discrete lubricant film radiation very considerably. If the total radiation were detected and analyzed simultaneously, the discrete radiation could be lost in the noise level. (The discrete radiation of the lubricant, which gives rise to an emission spectrum equivalent to an absorption spectrum is, of course, our main interest. Discrete emission bands appear at the absorption frequencies for a film of uniform elevated temperature for, effectively, the ball's emissivity is higher at these frequencies than at others. It is as if the ball were coated black there.) Hence it is necessary to oppose the continuous radiation by a blackbody source. This is done by the chopper and reference shown in Fig. 2. The chopper, consisting of a pair of reflecting tuning fork tines vibrating about the collimator focus in a plane oriented at 45 deg with respect to the direction of the source radiation, alternatingly introduces source and reference radiation into the spectrometer. Only the difference of these radiations is detected.

(iii) Polarized Spectra. The interferometer-spectrometer assembly is cylindrically symmetrical about the optic axis with two exceptions: (*a*) the direction of the ball/plate conjunction line and (*b*) the planar germanium-on-salt beam splitter in the Michelson interferometer portion. It was shown by Bell [5] that the beamsplitter polarization effect – asymmetry of signal output when a linearly polarizing plate is rotated about the optic axis – is at most 10%, and that is what we observed. Furthermore, this polarization effect is nearly equal over a wide spectral range for a parallel wire polarizer (we use a wire mesh of 0.4 μm separation deposited on a KRS-5 disk). Hence any polarization effect shown, which is related to individual emission band intensities, must be attributed to processes occurring in the contact itself. (The diamond window is itself subject to uneven stresses and

Nomenclature

F = normal applied load
G = dimensionless material parameter, $\alpha E'$
I = radiation intensity
I^+ = intensity of outgoing radiation
I^- = intensity of ingoing radiation
K = absorption coefficient
L = film thickness
M = metal surface
R_x = effective radius
T = temperature
U = dimensionless speed parameter $U = u\eta_0/E'R_x$
W = Dimensionless load parameter $W = F/E'R_x^2$
g = dimensionless parameter
$g_c = \frac{GW^3}{U^2}$
$g_e = \frac{W^{8/3}}{U^2}$
k = $K/\cos\theta$
n = refractive index
t = transmittance
u = mean surface velocity
y = distance through film from window
α = viscosity/pressure coefficient
β = factor accounting for multiple reflection
ϵ = emissivity
η_0 = fluid viscosity at 1 atmosphere pressure
θ = angle of incidence
θ' = angle of refractive
ρ = reflectivity
τ = optical pathlength

Subscripts

b = refers to blackbody radiation
e = refers to elasticity
0 = window medium
v = refers to viscosity
1 = fluid medium
2 = metal medium
ν = refers to frequency

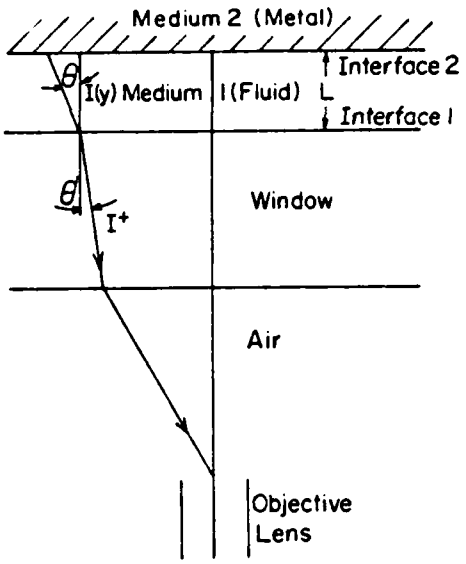

Fig. 3 Schematic diagram of a semi-transparent film sandwiched between a flat metal plate and an infrared transparent window

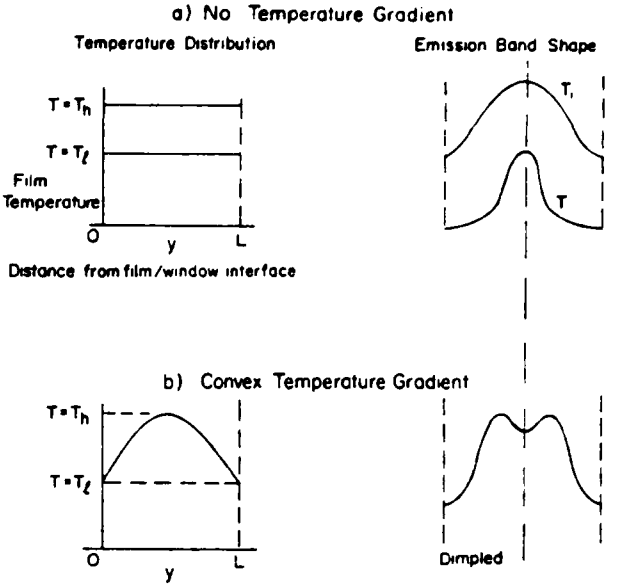

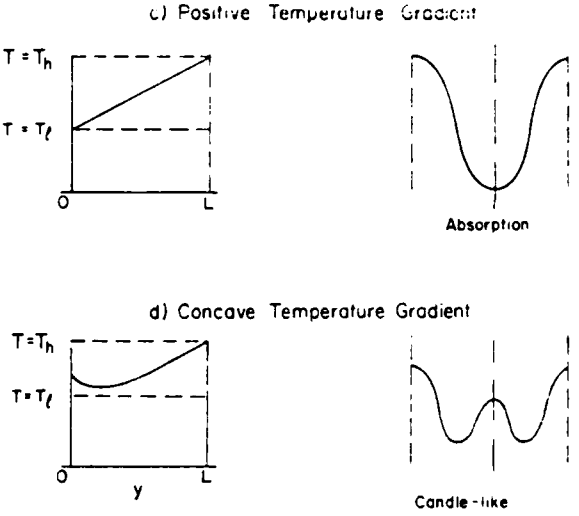

Fig. 4 Effect of temperature distribution through a film on its infrared emission bans shapes

therefore transmitting radiation anisotropically. However, that anisotropy is nearly independent of infrared frequency.)

Such a polarizer was placed at the image location in front of the detector, thus polarizing both source and reference radiations.

(iv) Distribution of Radiance Over the Field of View. Figure 3 gives a schematic diagram of the radiation emitted by a semi-transparent – i.e., transparent over parts of the infrared spectrum, absorbing over other parts – film sandwiched between a flat metal surface and a transparent window. Since the numerical aperture of our most-used objective lens is such that radiation incident on it must lie within a cone of 30 deg half-angle, the rays shown represent the boundaries of the central cone collected. Within the lubricant film the acceptance angle is somewhat greater because the index of refraction of the fluid is less than that of the diamond window.

Since the radiation must, of necessity, be collected over solid angle, the effective optical path within the film is longer than the (normal) film thickness. Furthermore, the field of view used must be adequate to provide a measurable signal. However, since the film thickness rarely exceeds 1 μm, the lateral translation due to inclination of the beam with the optic axis is negligible compared to the typical diameter of the Hertzian area viewed, which is around 100 μm in most of our experiments. (As mentioned earlier, the view area was limited by the iris diaphragm in the image plane ahead of the detector.) For purposes of radiometric accuracy it is necessary that the objective lens and entire spectrometer-interferometer optics attenuate the radiation orginating anywhere within that area equally. This has been shown to be the case.

Theory

(i) Infrared Emission Bandshapes. The building blocks of dielectric materials are molecules consisting of atoms held together by valence forces. These atoms vibrate by thermal energy, giving every molecule a set of resonance vibrations analogous to the resonance modes of mechanical structures. Accordingly, the radiation from a hot continuum source passing through a layer of dielectric material is absorbed only at frequencies corresponding to molecular modes of vibration i.e., a plot of transmitted radiation intensity versus frequency shows absorption bands (absorption spectrum). When the layer of dielectric, e.g., a film of lubricant, is hotter than the detector, it will emit infrared radiation at the resonance frequencies, (the modes of molecular vibration correspond to infrared frequencies) so that a plot of emitted radiation intensity versus frequency shows emission bands (emission spectrum). However, a pure emission spectrum can originate only from a material at uniform temperatures throughout. A temperature distribution through the depth of a lubricant film will lead to partial reabsorption of emission bands, dimpled bands and "candles" sticking out from the bottom of a "depression" (Fig. 4). These phenomena were first observed and analyzed in stellar spectra by astronomers. The well-known Fraunhofer absorption lines in the spectrum of the Sun are indicative of a hot core and a cooler peripheral atmosphere. The theoretical justification is based on the radiation transfer model developed by astrophysicists. However, the schematic drawings of Fig. 4 should be

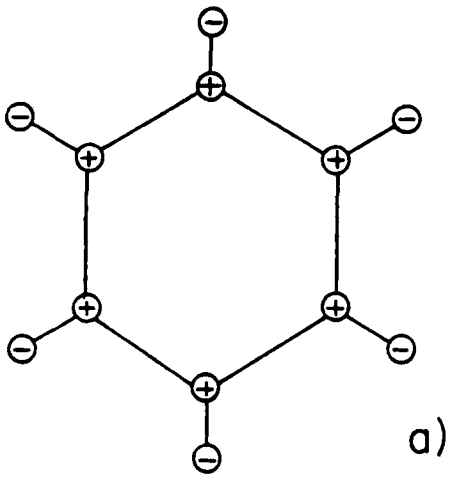

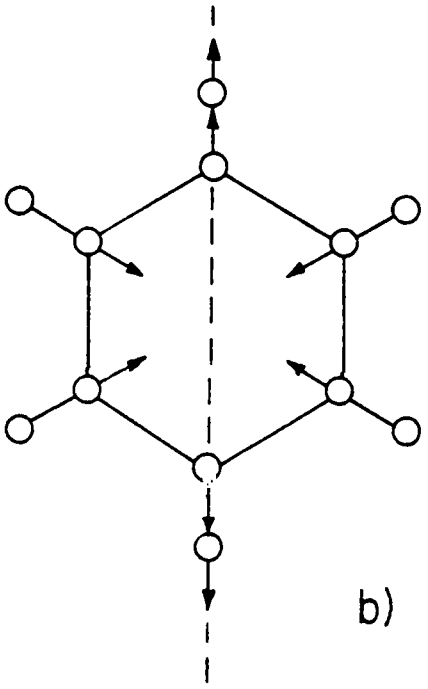

Fig. 5 Normal modes of benzene ring
a. umbrella mode
b. an in-plane mode

adequate for an understanding of the spectroscopic evidence for a temperature distribution through a lubricant film. Appendix A provides a simple mathematical analysis.

(ii) Polarization of Infrared Emission Bands. The polarizing filter inserted into the optical path of the interferometer makes it possible to rotate the plane of polarizaton about the direction of propagation of the radiation. Thus the plane of polarization can be made to contain the ball/plate conjunction line or be perpendicular to it. In order to explain the significance of polarized emission spectra in the context of lubricating contacts, it is necessary to say a few words on how infrared radiation arises. In the previous section the resonances between modes of molecular vibration and infrared radiation frequencies were said to be

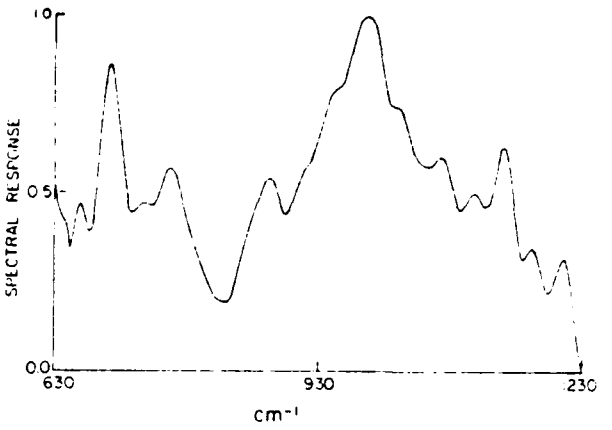

Fig. 6 Ehd emission spectrum in the 630-1230 cm^{-1} range of 5P4E at low speed and high load (800 MPa average pressure)

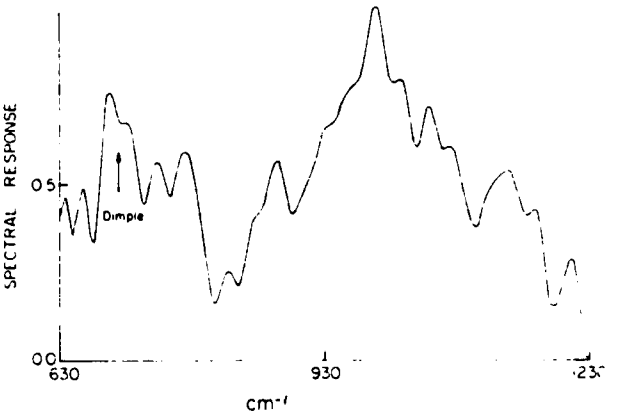

Fig. 7 Ehd emission spectrum in the 630-1230 cm^{-1} range of 5P4E at high speed and low load (600 MPa average pressure)

responsible for emission and absorption spectral bands. But how do these molecular vibrations interact with the infrared electromagnetic radiation? The interaction is explained by a vibrating dipole moment associated with every normal mode of molecular vibration. This transition dipole moment has, as a vector quantity, both magnitude and direction. Just as is the case with a dipole antenna, radiation cannot be propagated in a direction parallel to the dipole moment change but is at maximum in a direction perpendicular to it. The direction of dipole moment change is determined by the molecular geometry. For example, Figure 5(*a*) illustrates the so-called umbrella vibration of the benzene ring, a major constituent of the 5P4E polyphenyl ether lubricant. The inner hexagon is formed by the linkage of six carbon atoms; one hydrogen atom – or other substituent – is attached to every carbon atom. In the umbrella vibrational mode the dipole moment change vector is normal to the plane of the paper. If the plane of the benzene ring, say of 5P4E, is also parallel to the diamond window and perpendicular to the optic axis of the instrumentation, then this vibrational mode is not detectable, because the dipole moment change vector is parallel to the optic axis. On the other hand, the normal mode of the disubstituted benzene ring, shown in Fig. 5(*b*), should be most pronounced with the polarizing filter plane in the direction of the conjunction line (shown) and least pronounced with the polarizing filter plane oriented perpendicularly to it.

A relatively weak emission band at the frequency associated with the vibration illustrated in Fig. 5(*a*) can thus be regarded

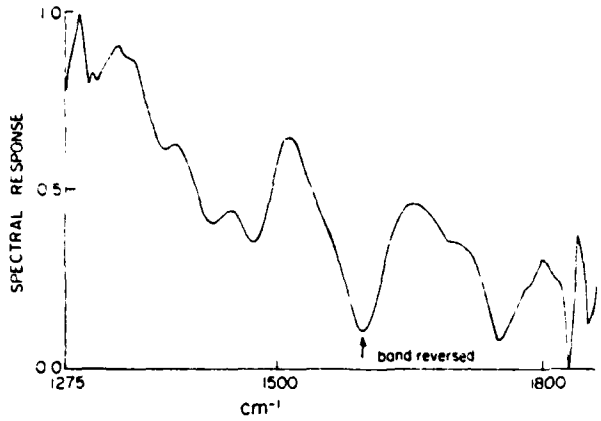

Fig. 8 Ehd emission spectrum in the 1250-1850 cm^{-1} range of 5P4E at low speed and high load (800 MPa average pressure)

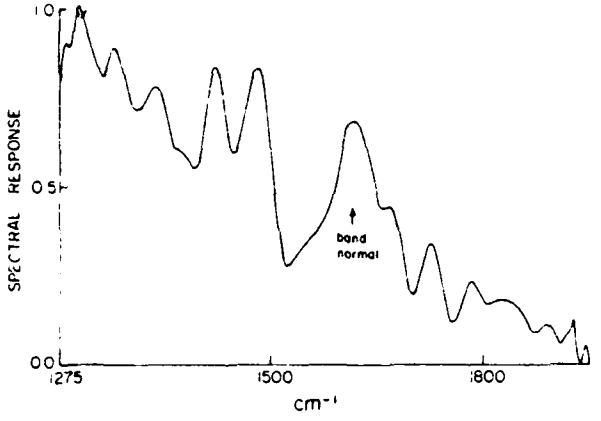

Fig. 9 Ehd emission spectrum in the 1250-1850 cm^{-1} range of 5P4E at high speed and low load (600 MPa average pressure)

as good evidence for alignment of the benzene ring parallel to the contact window (rotation of the polarizer would have little effect on this band) while bands corresponding to the normal mode of Fig. 5(*b*) should be strongly affected by polarizer rotation.

Results

(i) Emission Spectra from ehd Contacts Containing 5P4E Polyether Fluid. All the spectra discussed were *emission* spectra, i.e., the detector source signal always exceeded the – room temperature – reference signal.

Figures 6 and 7 compare low and high load spectra at high speed. Figure 7 shows both a dimple in the 690 cm^{-1} band. The temperature gradient is not easily estimated. At high speed and at low load the film thickness is relatively high, making a temperature gradient a rather likely occurrence.

In a different run at low speed and high load, in which the 1275-1850 cm^{-1} frequency range was studied, the spectrum of Fig. 8 was obtained. When compared with Fig. 9, which shows the corresponding high speed case, complete reversal of all the principal spectral bands is noted. The 1600 cm^{-1} aromatic band is especially outstanding, appearing as absorption in the low speed case. Since all the major bands in this region are reversed in the low speed case, a blackbody radiation at a higher temperature than the lubricant film must have been present. Indeed the total energy in this spectrum was *higher* for the low speed than for the high speed case, the opposite of usual behavior. Examination of the ball after this

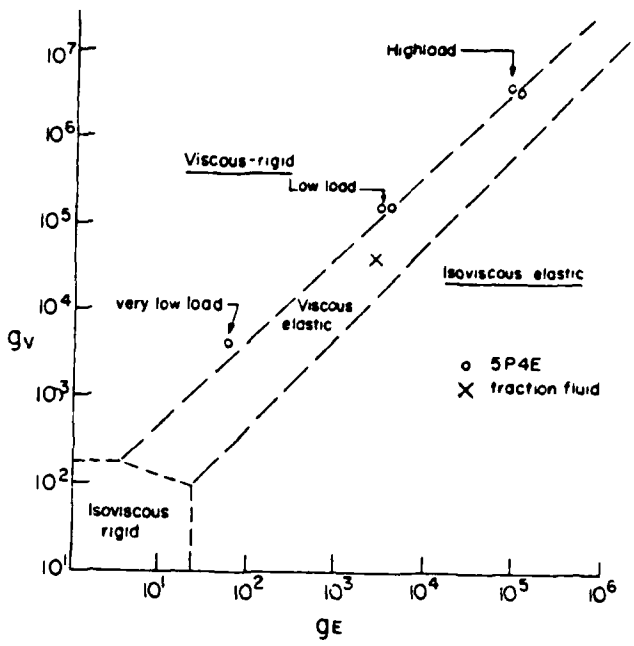

Fig. 10 Lubrication regimes on log-log grid of dimensionless viscosity and elasticity parameters for a circular contact (after Hamrock and Dowson [6])

experiment showed a track mark. In short, the spectral inversion was a result of asperity interaction or solid surfaces contact; this interaction produced hot spots only partly cooled by the fluid.

(ii) Dependence of Molecular Alignment of 5P4E in Concentrated Contacts on Fluid Film Thickness. A recent paper by Hamrock and Dowson [6] makes it easily possible to identify the lubrication regime in elliptical contacts of various eccentricites by means of dimensionless parameters. Our ball/plate contact is circular and characterized by Fig. 10, which has been adapted from this paper, mainly by extension of the coordinate ranges. Since diamond's elastic modulus is very high ($\sim 10^{12}$ S.I. units) the reduced elastic modulus for the steel ball/diamond window combination is also high, ~ 0.30 to 0.35×10^{12}, depending on the nature of the particular diamond, compared to $\sim 0.22 \times 10^{12}$ for a steel ball on a steel plate. The elastic modules does not influence the viscosity parameter g_v at all,[3] but does enter the expression for the elasticity parameter g_e, which it could reduce by a factor of at most $(1/2)^{2/3} = 0.63$ compared to a steel/steel combination. This factor is appreciable but is not enough ever to force our system into the isoviscous-rigid regime. To convince ourselves we operated our apparatus with 5P4E polyphenyl ether cooled to an inlet temperature of 33° (η_0 = 0.881 Pa•s) and at a ball speed of 200 RPM or 0.6 m/s. At this temperature the pressure-viscosity coefficient of 5P4E is 39.3×10^{-9} Pa^{-1}. We used minimum load (3 kg), the weight of the ball and platform alone. Even for these conditions, which should be very conducive to very thick films, we operated at the point marked "very low load" in Fig. 10. It lies near the viscous-rigid and viscous-elastic boundary, but probably in the former regime (average Hertzian pressure 400 MPa). The corresponding infrared emission spectrum was Fig. 11(*a*). Note the relatively strong band at 750 cm^{-1}, almost as strong as the 690 cm^{-1} band to the left. When the load was doubled, the spectrum of Fig. 11(*b*) was obtained.

[3] See Appendix B for definition of mathematical symbols.

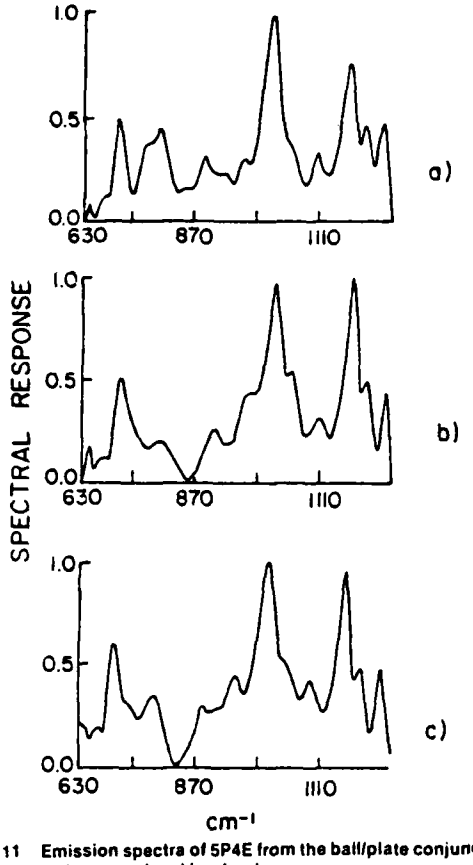

Fig. 11 Emission spectra of 5P4E from the ball/plate conjunction;
a. low speed and low load
b. low speed and high load
c. high speed and high load

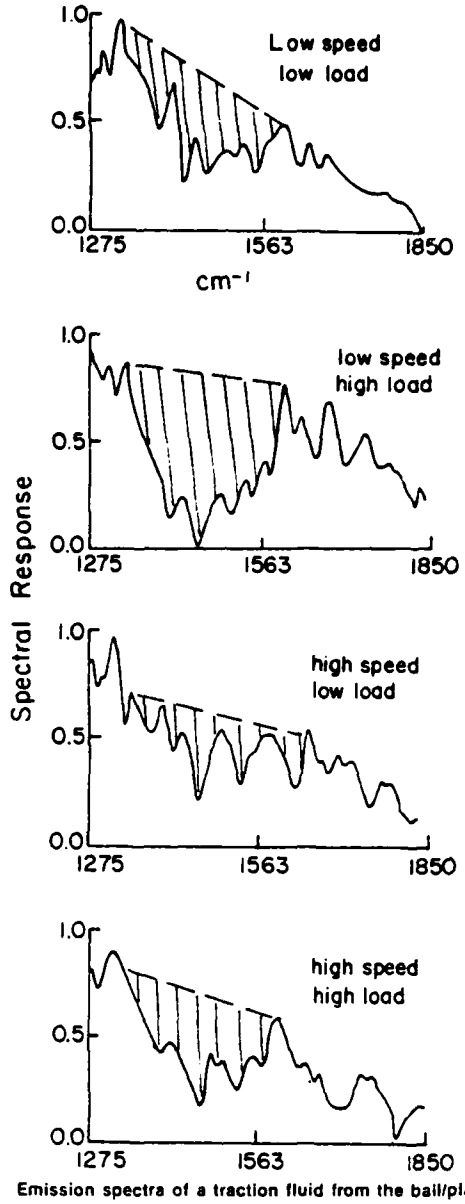

Fig. 12 Emission spectra of a traction fluid from the ball/plate conjunction;
a. low speed and low load
b. low speed and high load
c. high speed and low load
d. high speed and high load

for conditions corresponding to the "low load" operating point just within the viscous elastic regime. Doubling the ball's rotational velocity produced the operating conditions characterized by the operating point just within the viscous-rigid regime are the infrared absorption spectrum of Fig. 11(c). The most interesting result is the almost complete absence of the 750 cm^{-1} emission band in the middle spectrum and a bare indication of it in the bottom spectrum. Since all the other spectral features remained nearly constant and since the 750 cm^{-1} band is well-known to be caused by the "umbrella" mode of vibration of the aromatic ring, in which the change of dipole moment vector is perpendicular to the plane of the ring (Fig. 5), it would seem logical to conclude that the ring is indeed oriented with its plane parallel to the window. Polarization effects would then, as explained in the theoretical section, preclude appearance of the 750 cm^{-1} spectral emission band. Rotation of the polarizing disk referred to earlier about the optic axis of the instrumentation could produce spectral differences only if the plane of the ring was slightly tilted, say preferentially in the plane containing the ball/window conjunction line. Such polarized spectra were obtained and showed differences which, moreover, depended on shear rate. For this reason the 750 cm^{-1} band is also somewhat stronger in the bottom spectrum than in the middle spectrum of Fig. 11.

The disappearance of the 750 cm^{-1} emission band as the gap is narrowed is dramatic evidence of a change of molecular alignment of the fluid as it passes through the contact region. An alignment of the lubricant implies lower effective viscosity compared to random orientation. This spectral change would imply alignment because of flow. A temperature gradient across the gap could also produce partial alignment as some parts of the fluid are held down while others are moved like high grass in a wind storm. It changes the entanglement of separate units as they flow past one another and therefore the effective viscosity.

The change of the 750 cm^{-1} band intensity with respect to intensities of other bands cannot be ascribed to a change of layer thickness alone. It might also be worth pointing out that our emission spectra are consistent with the layer thickness defined by the operating points of Fig. 10.

(iii) Infrared Emission Spectra of a Traction Fluid. Traction fluids transmit torques to a much greater extent than ordinary lubricants. For the same operating conditions they also produce higher temperatures in concentrated contacts than other fluids, which is consistent with their higher traction

(i.e., friction) coefficient. While the composition of these fluids is complex, it is basically a blend of straight chain and carbocyclic hydrocarbons. The rings in the molecules would be expected to provide rigidity of structure. The principal shear might be within the lubricant or between the lubricant and its boundaries and produce a temperature gradient in any case. As mentioned at the end of the preceding section, the gradient could partly align the molecular chains during flow and thereby change the effective viscosity to provide more friction between them.

Figure 12 show a series of spectra under different load and speed conditions, all around the operating point marked in Fig. 10, i.e., within the viscous-elastic regime. Any hydrocarbon contains vibrational modes caused by C-H deformation, which are centered around 1450 cm^{-1}. Even though we obtain emission spectra these bands show up as absorption with respect to a general background. The area of the shaded region in the figure is representative of the absorption. Notice that these areas are greater under high than under low load and that the low speed/high load combination has the greatest area. In view of the previous analysis there must be a temperature gradient through the fluid. At this time the question of asperity contact or a hot zone within the fluid remains unanswered. The thinnest film was produced under low speed/high load conditions, making asperity contact more likely.

Conclusion

Evidence has been produced for (i) molecular alignment and (ii) a temperature gradient within the contact region of a fluid under various operating conditions. There factors could be responsible for effective viscosity changes and provide leads toward the formulation of superior fluids.

Acknowledgments

This research was sponsored by the Air Force Office of Scientific Research, Air Force Systems Command, USAF, under Grant No. AFOSR-78-3473 and by NASA-Lewis Research Center, under Grant No. NGS 3170. The United States Government is authorized to reproduce and distribute reprints for Governmental purposes notwithstanding any copyright notation hereon.

References

1 Crook, A. W., "The Lubrication of Rollers, III, A Theoretical Discussion of Friction and the Temperatures in the Oil Film," *Phil. Trans.*, Vol. A 254, 1961, p. 237.

2 Ausherman, V. K., Nagaraj, H. S., Sanborn, D. M., and Winer, W. O., "Infrared Temperature Mapping in Elastohydrodynamic Lubrication," ASME JOURNAL OF LUBRICATION TECHNOLOGY, Vol. 98, 1976, p. 236.

3 Lauer, J. L., and Peterkin, M. E., "Infrared Emission Spectra of Elastohydrodynamic Contacts," ASME JOURNAL OF LUBRICATION TECHNOLOGY, Vol. 98, 1978, p. 230.

4 Lauer, J. L., "Study of Polyphenyl Ether Fluid (5P4E) in Operating Elastohydrodynamic Contacts by Infrared Emission Spectroscopy," ASME JOURNAL OF LUBRICATION TECHNOLOGY, Vol. 101, 1979, p. 67.

5 Bell, R. J., *Introductory Fourier Transform Spectroscopy*, Academic Press, New York, 1972, Chapter IX.

6 Hamrock, B. J., and Dowson, D., "Minimum Film Thickness in Elliptical Contacts for Different Regimes in Fluid Film Lubrication," NASA Technical Paper 1342, Oct. 1978.

7 Viskanta, R., Hommert, P. J., and Groninger, G. L., "Spectral Remote Sensing of Temperature Distribution in Semitransparent Solids Heated by an External Radiation Source," *Applied Optics*, Vol. 14, 1975, p. 428.

8 Higuchi, S., Tanaka, S., and Kamada, H., *Spectrochim. Acta*, Vol. 28A, 1972, pp. 1721-1730.

APPENDIX A

Mathematical Analysis of Infrared Emission Bandshapes

The following analysis was developed to provide an understanding of the factors underlying our experimental procedures, notably band reversals and partial reabsorption in relation to temperature gradients. It is not intended to be a rigorous theory.

The model for the theoretical discussion is shown in Fig. 3. The analytical method was adopted from that of Viskanta and coworkers [7] and is based on the radiation transfer equation (RTE) developed by the astrophyscists. It provides a general framework applicable to a variety of situations, while the more common ray tracing procedures must be developed separately for every case.

The RTE to be solved for a slab bounded by two parallel surfaces (film sandwiched between the bearing ball flattened over the Hertzian contact area and the diamond window) is

$$\cos\theta \frac{dI_\nu(y,\ \cos\theta)}{\nu - dy} = -k_\nu(y)[n_\nu(y) I_{b\nu}(y) - I_\nu(y,\ \cos\theta)] \quad (1)$$

Azimuthal symmetry is assumed; $I_\nu\ (y,\ \theta)$ is the monochromatic intensity (radiance) at frequency ν and in a direction forming an angle θ with y, the distance from the exit surface of the slab; $K_\nu\ (y)$ is the spectral absorption coefficient, $n_\nu\ (y)$ is the index of refraction of the film and $I_{b\nu}$ (y) is the radiance given by the Planck blackbody function corresponding to the temperature $T(y)$, which is assumed to vary with y in a continuous manner.

Equation (1) merely states that the change in radiance with distance is the difference between the radiation emitted (first term on the right) and the radiation absorbed (second term on the right). It should be remembered that any motion of the semi-transparent film, such as would occur in a lubricating contact, is irrelevant to radiation, which is instantaneous. The energy radiation received by the objective lens represents the total energy emitted over the field of view during the time of observation. In our typical situation (30 minutes of scanning time) it represents a sum over a great many revolutions of the ball.

It has become customary to separate I into an outgoing component I^+ $(\cos\theta > 0)$ and an ingoing component I^- $(\cos\theta < 0)$. The boundary conditions for equation (1) then become

$$I_\nu^-(0,\ \cos\theta) = \zeta_{1\nu} I_\nu^+(0,\ \cos\theta);\ \cos\theta < 0 \quad (2)$$

and

$$I_\nu^+(L,\ \cos\theta) = \epsilon_{2\nu}(\cos\theta) n_\nu^2 I_{b\nu}(L) + \zeta_{2\nu}(\cos\theta) I_\nu^-(L,\ \cos\theta) \quad (3)$$

where $I_{b\nu}\ (L) = I_{b\nu}\ (M)$ is the (blackbody) radiance from the metal surface, $\zeta_\nu\ (\cos\theta)$ is the spectral directional reflectivity of the interface in question, and $\epsilon_{2\nu}\ (\cos\theta) = 1 - \zeta_{2\nu}\ (\cos\theta)$ is the spectral emittance at the metal surface/film interface. Equation (1) is easily solved by an integrating factor. Since Snell's law gives

$$n_\nu \sin\theta = n_{0\nu} \sin\theta'$$

the solution of equation (1) for the spectral intensity emerging outwardly from the film layer into the diamond window can be written as

$$\begin{aligned} I_\nu^+(0,\ \cos\theta') &= [1 - \zeta_{1\nu}(\cos\theta)] (n_{0\nu}/n_1)^2 \beta_\nu(\tau_{L\nu},\ \cos\theta) \\ &\times \{[1 - \zeta_{2\nu}(\cos\theta)] n_\nu^2 I_{b\nu}(M) e^{-\tau_{L\nu}/\cos\theta} \\ &+ \int_0^L n_\nu^2 I_{b\nu}(y) [e^{-\tau_\nu/\cos\theta} \\ &+ \zeta_{2\nu}(\cos\theta) e^{-(2\tau_{L\nu} - \tau_\nu)/\cos\theta}] K_\nu \frac{dy}{\cos\theta} \end{aligned} \quad (5)$$

for $\cos\theta > 0$
where

$$\beta_\nu(\zeta\cos\theta) = [1 - \zeta_{1\nu}(\cos\theta)\zeta_{2\nu}(\cos\theta)e^{-2\tau_{L\nu}\sec\theta}]^{-1} \quad (6)$$

is the factor accounting for multiple reflections between interfaces 1 and 2, $I_{b\nu}(M)$ is the blackbody radiance corresponding to the metal surface, and the optical depth τ_ν and thickness $\tau_{L\nu}$ are defined, respectively as

$$\tau_\nu = \int_0^y K_\nu(y)\,dy \quad (7)$$

and

$$\tau_{L\nu} = \int_0^L K_\nu(y)\,dy \quad (8)$$

Further refraction takes place at the diamond/air interface. It limits the solid angle over which radiation can be introduced into any objective lens, because the critical angle for diamond/air is 36 deg. Hence an objective lens of much larger numerical aperture than our present one (maximum half-angle of 30 deg of the entrance cone) would not increase the radiant flux collected. However, it would provide an effective reduction of the field of view. Multiple reflections within the diamond window need not be considered since their overall effect was estimated to be slight (the diamond window is 2 mm thick; off-axis rays suffer sideways displacement exceeding the limits of the field of view).

The radiant flux of wave number ν entering the instrumentation is the spectral intensity integrated over the solid angle of objective. The first term in the braces of equation (5) is the radiance of the metal surface attenuated by passage through the film and partial reflectance at the boundaries. The second term, the integral, takes into account the emission of radiation by the film itself. It consists of two parts; the first represents the radiant flux emitted by a volume within the film toward the objective lens, the second part represents the radiant flux emitted by the same volume toward the metal surface and reflected back toward the objective.

An advantage of the above formalism is the ease with which the spatial and angular dependence of absorption coefficient, index of refraction, and spectral radiance can be taken into account. Extension from one dimension to three dimensions is also quite straightforward.

Defining $k = K/\cos\theta$, dropping the monochromatic frequency subscript and the angular subscript of reflectivity and radiance yields

$$I^+(0) = (1-\zeta_1)(n_0/n)^2\beta \times \{(1-\zeta_2)n^2 I_b(M)e^{-kL} + \int_0^L n^2 I(y)[e^{-ky} + \zeta_2 e^{-k(2L-y)}]k\,dy\} \quad (9)$$

Since $\tau = ky$ and $\tau_L = kL$. Here $n = n(y)$ and $k = k(y)$.

If this equation is applied to measurements of I^+ at two or three wavenumbers where the absorption coefficient k of the lubricant film is zero, viz.

$$I^+(0) = (1-\zeta_1)n_0^2(1-\zeta_2)I_b(M) \quad (10)$$

the metal surface temperature can be evaluated, since $I_b(M)$ is a known function of temperature (Planck's radiation function). The temperature distribution through the film can then be determined from measurements of $I^+(0)$ at absorption band frequencies by solving for $I(y)$, provided that $k(y)$ and $n(y)$ are known from separate measurements of $k(T)$ and $n(T)$ since $y = y(T)$. Equation (9) then becomes a nonlinear Fredholm integral equation of the first kind for the unknown function $I(Y)$, for which a number of solutions have been worked out, *inter alia,* by Viskanta and coworkers.

Rather than attempting general solutions of equation (9), some pertinent special cases will now be discussed.

(i) Constant reflectivities, indices of refraction, and absorptivities throughout the lubricant film; uniform film temperature.

In this case

$$I^+ = (1-\zeta_1)\beta[(1-\zeta_2)e^{-kL}I_b(M) + I[1 - e^{-kL} + \zeta_2(e^{-kL} - e^{-2kL})] \quad (11)$$

Since the transmittance t can be defined as $t \equiv e^{-kL}$, the above equation can be simplified to

$$I^+ = (1-\zeta_1)\beta[(1-\zeta_2)tI_b(M) + I[1 - t + \zeta_2(t - t^2)] \quad (12)$$

where $\beta = (1-\zeta_1\zeta_2 t^2)^{-1}$ and $I = I_f$ can be identified with the radiance of the film.

Equation (12) can be rewritten in the following form

$$I^+ = (1-\zeta_1)\beta[(1-\zeta_2)tI_b(M) + I(1-t)(1+\zeta_2 t)] \quad (13)$$

It should be remembered that $t = t(\nu)$. Thus, when $I_b(M) >> I$, a plot of I^+ versus wavenumber ν will represent an absorption spectrum. On the other hand, when $I_b(M) << I$, a plot of I^+ versus wavenumber will be an emission spectrum of the film, the factor $(1 - t)$ playing the role of the emissivity. The other factor $(1 + \zeta_2 t)$ provides a small enhancement of the radiation emitted, which is the result of the back-reflection by the metal surface.

When the reflectivity of the ball surface, ζ_2, can be considered as zero, then

$$I^+ (1-\zeta_2)\beta[tI_b(M) + (1-t)I] \quad (14)$$

When, furthermore $I_b(M) = I_f = I$, this equation becomes

$$I^+ = (1-\zeta_1)I_b(M) \quad (15)$$

In this case the emission from the surface is merely a blackbody emission from the lubricant film surface.

Both the emission and the absorption spectra derived in this section, depending on whether the film or the metal surface radiation is stronger, are continuous over the entire frequency region (wavennumber region) covered. In other words, either emission or absorption spectra will be observed.

(ii) Constant reflectivities, indices of refraction and absorptivities throughout the lubricant film; film consists of at least two layers at different temperatures.

This case differs from the preceding one by allowing for the possibility of partial inversion of emission bands in the central region. Figure 4 is an illustration of such a situation, showing inversion "dimples." Since the width as well as the intensity of most infrared emission or absorption bands are greater at higher temperatures, reabsorption of the same band by a cooler layer of the same material will affect mostly the central region of a band, thus growing rise to "dimples." For example, Higuchi and coworkers [8] have shown that the half-band-width of many infrared bands vary with the reciprocal of the viscosity. Since the viscosity of fluids generally decreases exponentially with temperature, band-width increases exponentially. Since the band intensity also increases with temperature, "dimpled" bands can thus appear. These bands are analogous to the well-known self-absorbed atomic arc bands, where the self-absorption takes place near the – cooler – arc envelopes. Often such reabsorbed emission bands were mistaken for real doublets.

A variation of the "dimple" is the "candle," which is also caused by a temperature gradient in the emitting film. It

occurs when the temperature gradient trough the film is small (relatively thick film or relatively weak heat source). An example is shown in Fig. 5. Again the warmest film layer is behind the radiating surface, causing complete or near complete inversion of the emission bands. However, very strong emission bands generated in a thin layer imediately behind the emitting surface will show up as emission bands ("candles") within a trough (the candle holder). They were not re-absorbed. These bands appear at the exact wavenumbers predicted and are usually very sharp. This situation is readily recognized because only the strongest bands stand out as emission and practically all the other bands show up as absorptions over very broad emissions.

The greater bandwidth of infrared vibration bands at higher temperatures has been attributed to greater ease in overcoming the potential barrier for molecular reorientation (Rakov).

Both spectra of type (i) (total emission or absorption) and of type (ii) (reabsorption of some emission bands) have been observed in emission spectra from bearing contacts. To recapitulate: We regard the former caused by a blackbody radiator (metal surface or a lubricant decomposition product) in the contact region, which is giving off stronger radiation than the bulk of the lubricant film.

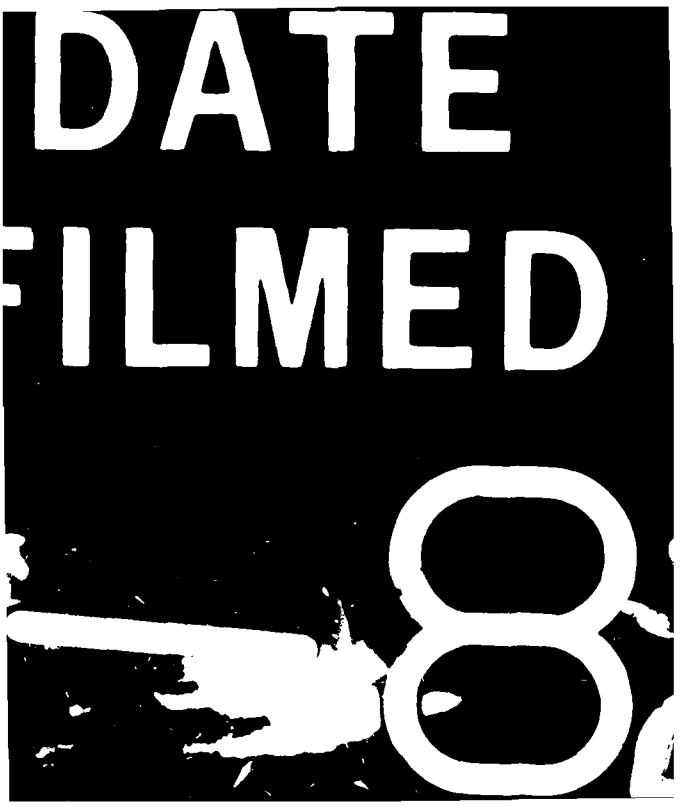
DATE
FILMED
8